JPTM

Molecular Testing for Gastrointestinal Cancer

Aims & Scope

The Journal of Pathology and Translational Medicine is an open venue for the rapid publication of major achievements in various fields of pathology, cytopathology, and biomedical and translational research. The Journal aims to share new insights into the molecular and cellular mechanisms of human diseases and to report major advances in both experimental and clinical medicine, with a particular emphasis on translational research. The investigations of human cells and tissues using high-dimensional biology techniques such as genomics and proteomics will be given a high priority. Articles on stem cell biology are also welcome. The categories of manuscript include original articles, review and perspective articles, case studies, brief case reports, and letters to the editor.

Subscription Information

To subscribe to this journal, please contact the Korean Society of Pathologists/the Korean Society for Cytopathology. Full text PDF files are also available at the official website (http://jpatholtm.org). *Journal of Pathology and Translational Medicine* is indexed by Emerging Sources Citation Index (ESCI), PubMed, PubMed Central, Scopus, KoreaMed, KoMCI, WRPIM, Directory of Open Access Journals (DOAJ), and CrossRef. Circulation number per issue is 700.

CONTENTS

Instructions for Authors for *Journal of Pathology and Translational Medicine* are available at http://jpatholtm.org/authors/authors.php

Molecular Testing for Gastrointestinal Cancer

Hye Seung Lee[1,2] · Woo Ho Kim[2]
Yoonjin Kwak[1,2] · Jiwon Koh[2]
Jeong Mo Bae[3] · Kyoung-Mee Kim[4]
Mee Soo Chang[2,3] · Hye Seung Han[5]
Joon Mee Kim[6] · Hwal Woong Kim[7]
Hee Kyung Chang[8] · Young Hee Choi[9]
Ji Y. Park[10] · Mi Jin Gu[11]
Min Jin Lhee[12] · Jung Yeon Kim[13]
Hee Sung Kim[14] · Mee-Yon Cho[15]

The Gastrointestinal Pathology Study Group of Korean Society of Pathologists · The Molecular Pathology Study Group of Korean Society of Pathologists

Department of Pathology, [1]Seoul National University Bundang Hospital, Seongnam; [2]Seoul National University College of Medicine, Seoul; [3]SMG-SNU Boramae Medical Center, Seoul; [4]Samsung Medical Center, Sungkyunkwan University School of Medicine, Seoul; [5]Konkuk University School of Medicine, Seoul; [6]Inha University School of Medicine, Incheon; [7]Seegene Medical Foundation, Busan; [8]Kosin University Gospel Hospital, Kosin University College of Medicine, Busan; [9]Hallym University Dongtan Sacred Heart Hospital, Hwaseong; [10]Catholic University of Daegu School of Medicine, Daegu; [11]Yeungnam University College of Medicine, Daegu; [12]Seoul Red Cross Hospital, Seoul; [13]Inje University Sanggye Paik Hospital, Seoul; [14]Chung-Ang University College of Medicine, Seoul; [15]Wonju Severance Christian Hospital, Yonsei University Wonju College of Medicine, Wonju, Korea

Corresponding Author
Woo Ho Kim, MD, PhD
Department of Pathology, Seoul National University College of Medicine, 103 Daehak-ro, Jongno-gu, Seoul 03080, Korea
Tel: +82-2-740-8269
Fax: +82-2-765-5600
E-mail: woohokim@snu.ac.kr

With recent advances in molecular diagnostic methods and targeted cancer therapies, several molecular tests have been recommended for gastric cancer (GC) and colorectal cancer (CRC). Microsatellite instability analysis of gastrointestinal cancers is performed to screen for Lynch syndrome, predict favorable prognosis, and screen patients for immunotherapy. The epidermal growth factor receptor (EGFR) tyrosine kinase inhibitor has been approved in metastatic CRCs with wild-type *RAS* (*KRAS* and *NRAS* exon 2–4). A *BRAF* mutation is required for predicting poor prognosis. Additionally, amplification of human epidermal growth factor receptor 2 (*HER2*) and *MET* is also associated with resistance to EGFR inhibitor in metastatic CRC patients. The *BRAF* V600E mutation is found in sporadic microsatellite unstable CRCs, and thus is helpful for ruling out Lynch syndrome. In addition, the *KRAS* mutation is a prognostic biomarker and the *PIK3CA* mutation is a molecular biomarker predicting response to phosphoinositide 3-kinase/AKT/mammalian target of rapamycin inhibitors and response to aspirin therapy in CRC patients. Additionally, HER2 testing should be performed in all recurrent or metastatic GCs. If the results of HER2 immunohistochemistry are equivocal, *HER2* silver or fluorescence *in situ* hybridization testing are essential for confirmative determination of HER2 status. Epstein-Barr virus–positive GCs have distinct characteristics, including heavy lymphoid stroma, hypermethylation phenotype, and high expression of immune modulators. Recent advances in next-generation sequencing technologies enable us to examine various genetic alterations using a single test. Pathologists play a crucial role in ensuring reliable molecular testing and they should also take an integral role between molecular laboratories and clinicians.

Gastric cancer (GC) and colorectal cancer (CRC) are the most common malignancies originating from the gastrointestinal tract.[1] GC is the fourth most commonly diagnosed cancer, and CRC is the third most common cancer in men and the second most common in women worldwide.[2] According to the 2013 nationwide cancer statistics in South Korea, GC and CRC were the third and fourth leading causes of age-standardized cancer mortality,[3] respectively, and 34,331 and 37,986 new cases of GC and CRC, respectively, are expected to occur in 2016.[4]

Major advances in molecular technologies during the past two decades have led to a better understanding of the pathogenesis and management of GCs and CRCs, in particular, adenocarcinomas. The discovery of microsatellite instability (MSI) in gastrointestinal cancers, especially in colorectal adenocarcinomas, has broadened our understanding of carcinogenesis and genetic susceptibility.[5] *RAS* mutation analysis results are critical for predicting resistance to epidermal growth factor receptor (EGFR) inhibitors in metastatic CRC patients, increasing the importance of molecular diagnosis in CRCs.[6] The detection of Epstein-Barr virus (EBV) by *in situ* hybridization (ISH) has enabled the identification of a distinctive subtype of GC,[7] and the efficacy of trastuzumab therapy in GC has proven the clinical relevance of molecular testing in a treatment-related perspective.[8] In addition, trastuzumab therapy is approved in human epidermal growth factor receptor 2 (HER2)–positive advanced esophageal adenocarcinoma,[8] but most genetic alterations reported in esophageal adenocarcinoma do not show significant differences compared to GC.[1] MSI testing is recommended in small intestinal adenocarcinoma,[9] and *KRAS* and *BRAF* mutations are found in a subset of small intestinal adenocarcinoma.[10] However, the incidence of small intestinal adenocarcinoma is too low to review comprehensively.

In this article, we aim to review the current status of various molecular tests for gastrointestinal cancers in Korean patients, specifically gastric adenocarcinoma and colorectal adenocarcinoma considering their national disease burden, and suggest standardized methods and quality control measures. Furthermore, by reviewing the findings from the most recent studies on the molecular features of gastrointestinal cancers, we propose a future next-generation sequencing (NGS) panel for diagnostic, predictive, and prognostic purposes.

MOLECULAR TESTS

Microsatellite instability

Background

Microsatellites are short tandem DNA repeats that are randomly dispersed throughout the human genome, showing significant polymorphism between individuals. MSI is defined as a change in the microsatellite region within a tumor in comparison to that of normal tissue, resulting from either deletion or insertion of repeating units. MSI is caused by a defect in the DNA mismatch repair (MMR) mechanism which normally occurs during DNA replication to correct errors.[11] Since the early 1990s, it has been reported that a subset of CRC is microsatellite unstable (MSI-high frequency [MSI-H]), and that MSI represents a novel mechanism for colorectal carcinogenesis.[12]

MSI is the hallmark genetic aberration of Lynch syndrome.[11] Lynch syndrome is currently diagnosed when a pathogenic germline mutation is identified in one of the DNA MMR genes, *MLH1*, *PMS2*, *MSH2*, *MSH6*, or *MLH3*, and accounts for 2%–4% of all CRCs. Families who meet the Amsterdam criteria for the diagnosis of Lynch syndrome are referred to as having hereditary nonpolyposis CRC.[13] Screening and diagnosis of Lynch syndrome in clinical practice are required in order to reduce various cancer-related risks in the families. Therefore, screening for Lynch syndrome is necessary in newly diagnosed CRC patients, especially in the young or those with family history. Screening is usually done with MSI analysis and immunohistochemistry (IHC) for the four MMR enzymes MLH1, PMS2, MSH2, and MSH6.[14] Additionally, the loss of epithelial cell adhesion molecule (EpCAM) expression has been demonstrated in a small subset of Lynch-syndrome–associated CRCs, which is caused by germline *EpCAM* deletions.[15,16] In Lynch syndrome, the risk of extracolonic lesions is high including gastric, endometrial, renal pelvis/ureter, small bowel, ovarian, brain, hepatobiliary tract, and sebaceous cancers.[1,17]

Sporadic MSI-H is observed in about 15%–20% of sporadic CRCs in Western countries and in about 5%–6% in Eastern countries and is caused by *MLH1* promoter hypermethylation and MLH1 expression loss.[11,18,19] In sporadic CRC patients, MSI status is confirmed as a good prognostic marker.[9,20,21] CRCs with MSI-H frequently show high grade morphology, such as mucin production, signet ring cells, medullary features, and undifferentiated histology, but their biological behavior is less aggressive compared to that of microsatellite stable (MSS) or MSI-low frequency (MSI-L) CRCs.[1] MSI-H is observed in about

10% of sporadic GCs and is associated with older age, antral location, and intestinal type histology.[22,23] The independent prognostic value of MSI status in GC remains controversial; however, a recent meta-analysis showed that MSI-H is associated with better overall and disease-specific survival in GC.[24] Recent advances in genome analysis of CRCs and GCs showed that MSI-H is strongly associated with a distinct subtype characterized by elevated mutation rates ("hypermutated").[25-27] Cristescu *et al*.[27] demonstrated that MSI-H GCs have the best overall and disease-free survival among four molecular subtypes. The new American Joint Committee on Cancer (AJCC) cancer staging manual (8th edition) recommended obtaining the results of MSI testing additionally in both GC and CRC patients for clinical care.[9]

It is generally accepted that a defective MMR system is associated with decreased therapeutic response to fluorouracil-based adjuvant chemotherapy in CRCs and GCs.[28] In contrast, Le *et al*.[29] demonstrated that MSI status in CRCs and non-CRCs (including gastric, endometrial, biliary, and small bowel cancers) is an excellent predictive factor for favorable treatment outcome by immune checkpoint blockade with pembrolizumab. Furthermore, high expression of checkpoint molecules, such as PD-1, PD-L1, CTLA-4, LAG-3, and IDO, is characteristic of gastrointestinal cancers with MSI-H phenotype,[30-32] which suggests that MSI-H tumors are good candidates for immunotherapy.

Indication

Growing evidence has supported the rationale for universal MSI testing in CRC, which showed a higher sensitivity for identifying Lynch syndrome among newly diagnosed CRC.[33] Considering the significant clinical implications of MSI status from both treatment- and prognostic-related perspective, it is recommend that all patients with newly diagnosed GC or CRC be tested for MSI status. MSI testing can be performed in any advanced tumors for immune checkpoint inhibitor treatment.

Methodology

Methods

MSI analysis is performed by polymerase chain reaction (PCR) amplification of DNA extracted from both tumor and corresponding normal tissue, followed by separation of the amplified product by capillary gel electrophoresis. The results are determined by comparison of the peak patterns with a shift in PCR product size of the tumor compared to that of the normal tissue. Currently, the gold standard of MSI testing is the Bethesda panel,[5] which uses PCR for the analysis of the fragment length of five markers: two mononucleotide repeats (BAT25 and BAT26) and three dinucleotide repeats (D5S346, D2S123, and D17S250). Recently developed MSI testing consists of a pentaplex panel of quasimonomorphic mononucleotides markers (NR-27, NR-21, NR-24, BAT-25, and BAT-26), which allows the analysis of MSI in tumors without the need of normal control (reference) DNA.[34] The sensitivity or limit of detection of MSI analysis is approximately 10%, but can vary according to laboratory conditions.

Confirming the loss of MMR proteins (MLH1, PMS2, MSH2, MSH6) by IHC should also be used for the screening of Lynch syndrome. Since PMS2 and MLH1 form a heterodimer, MLH1 loss is related to PMS2 loss observed by IHC. MSH6 forms a heterodimer with MSH2, thus MSH2 loss occurs with concurrent MSH6 loss. However, loss of PMS2 or MSH6 does not lead to loss of MLH1 or MSH2. When compared to PCR-based method, IHC is known to have sufficient sensitivity, specificity, and predictive values.[35] However, the resting expression level of MMR proteins is very low; thus, a reliable diagnosis requires an adequate amount (quantity) of tissue sample and pathologists' experiences in daily practice. For the accurate interpretation of loss of MMR proteins in tumor tissue, internal positive controls such as adjacent non-neoplastic glands, lymphocytes, or stromal cells should show strong nuclear positivity. Longer cold ischemia time or under-fixation can cause false negative results.

Type of specimen

Both fresh frozen and formalin-fixed paraffin embedded (FFPE) tissues are considered suitable for PCR-based methods. Paired PCR results of cancer and matched normal tissues from the same patient are necessary for proper interpretation of the results.

Specimen requirements

Approximately 1 cm^2 of the tumor and normal tissues is required. Needless to state, the most important requirement of the specimen is a sufficient amount of DNA;[36] one of the most common reasons for false-negative MSI results is low tumor cellularity in the sample, for example, conditions such as mucinous carcinoma. Therefore, to ensure a sufficient proportion of the tumor cells, microdissection of the tumor cell area selected by experienced pathologists is generally recommended and widely implemented in many laboratories. Tumor cells should occupy at least 50%–60% of the examined tissue sections.[37]

Reporting

In pathologic reports, patient information, such as patient ID, name, gender, and age, order date, ordering physician, and surgical pathologic diagnosis and number should be included. MSI tumors can be divided into three groups: MSI-H, when ≥ 30% of markers exhibit instability; MSI-L, when < 30% of markers show instability; and MSS, when none of the markers exhibit instability (Fig. 1). According to the Bethesda panel, MSI-H is defined by having instability of two or more makers, MSI-L is defined by having instability of only one marker, and MSS means none of five markers show instability. The results of MSI must be reported as MSS, MSI-L, or MSI-H. Interpretation of the molecular diagnosis and signature of the pathologist are also required for the final diagnosis.

Validation of test

MSI analysis should be validated in each pathology laboratory as laboratory-developed tests. Since the requirements for proper validation of MSI tests are not clearly defined, an external program checklist can be referred to for validation, including that of accuracy, precision, reportable range of the test results, analytic sensitivity and specificity, and positive and negative predictive values. It is recommended to directly compare the results of MSI tests to those of MMR protein IHC or *MLH1* promoter hypermethylation testing.

Quality assurance

Each pathology laboratory should establish internal quality assurance (QA) instructions for MSI analysis and review all performed MSI tests in regular QA meetings. In each MSI test, specialized pathologists should confirm the examined tumor and normal area. Positive and negative controls should be used in each run of PCR and fragmentation analysis. Additionally, we recommend that both MSI tests and IHC for MMR proteins are performed and compared for reliable test results. All pathology laboratories should participate in external QA programs.

Somatic mutation analysis

Background

RAS mutations

The proto-oncogene KRAS encodes a GTPase, which is an early player in the EGFR induced RAS/RAF/mitogen-activated protein kinase (MAPK) signaling pathway. *KRAS* mutations have important roles in various aspects of carcinogenesis, and

KRAS mutations in exon 2 at codons 12 and 13 have been reported to be detected in approximately 35%–45% of CRCs. Negative correlations between *KRAS* mutations and MSI or *BRAF* mutations suggest that these molecular alterations are associated with a distinct subset of CRCs and have prognostic significance.[38] MSI-H status is associated with a favorable prognosis,[20,21] whereas many previous studies supported the association of *KRAS* mutation with a poor prognosis.[39,40] AJCC recommended obtaining the results of *KRAS* mutational testing in CRC patients for predicting patient prognosis,[20] and the poor prognostic effect of *KRAS* mutation is also described in the new AJCC cancer staging manual (8th edition).[9]

Targeted therapies directed against EGFR tyrosine kinase have improved treatment efficacy and patients' survival in various cancers, including CRCs.[41] EGFR blockers cetuximab and panitumumab have proven anti-tumor activity as monotherapies and in combination with chemotherapy and/or radiation in CRC patients,[42,43] and EGFR signaling–associated genes have been studied for their relationship with responsiveness to EGFR inhibitors (Fig. 2). *KRAS* mutations in exon 2 at codons 12 and 13 are associated with resistance to cetuximab and panitumumab, and with poor survival in chemo-refractory metastatic CRC patients.[44] Additionally, oncogenic mutations in *KRAS* codons 59, 61, 117, and 146 and *NRAS* codons 12, 13, and 61 have been reported in approximately 3%–5% of CRC samples.[45,46] Recent clinical trials have demonstrated that extended *RAS* mutation testing, including that for mutations in *KRAS* and
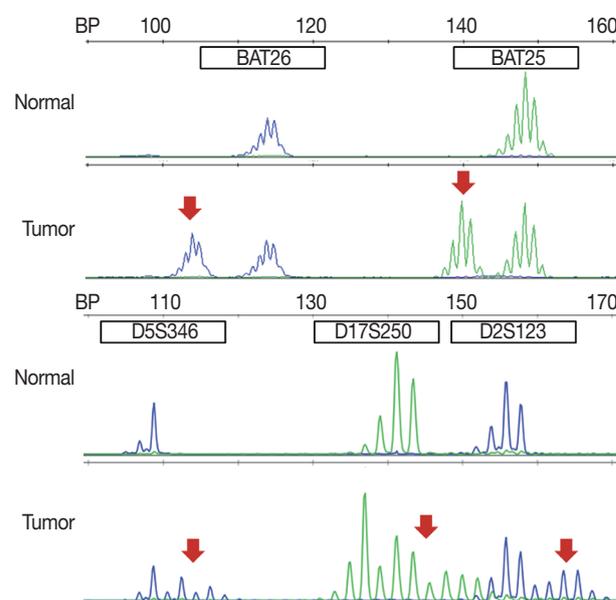
Fig. 1. Fragment pattern of microsatellite instability–high case by GeneScan analysis.

NRAS exons 2 to 4, can be more predictable for lack of responsiveness to EGFR inhibitors than previously proven *KRAS* exon 2 testing in first-line chemotherapy for metastatic CRC patients.[6,47] Recently, *RAS* mutation testing is approved as a companion diagnosis for EGFR inhibitor treatment in metastatic CRC patients.

BRAF mutations

The oncogenic *BRAF* mutation has a role in constitutive activation and downstream signaling along the MAPK signaling pathway. *BRAF* mutations occur in approximately 5%–8% of CRCs and most are the *BRAF* V600E mutation, however, the *BRAF* V600E mutation almost never occurs in GCs.[48,49] The *BRAF* mutation is an early molecular event in the serrated pathway of CRC. Molecular sequencing in serrated pathway CRCs has been reported as *BRAF* mutation/CpG island methylator phenotype (CIMP)/MSI-H or *BRAF* mutation/CIMP/MSS/p16 loss.[50] Many previous studies have confirmed that the *BRAF* mutation is associated with poor prognosis in metastatic CRC patients.[6,47] In addition to metastatic CRCs, earlier-stage

CRC patients with mutated *BRAF* have been reported to show significantly worse overall survival than that of patients with wild-type *BRAF*.[51,52] Especially, this prognostic significance was evident in the MSS CRC group.[9,52]

The *BRAF* V600E mutation is observed in approximately two thirds of microsatellite unstable CRCs caused by MLH1 hypermethylation and protein loss, but it never occurs in microsatellite unstable CRCs associated with Lynch syndrome.[53] Therefore, newly diagnosed CRC cases should be initially examined by MSI analysis with MMR protein IHC, and then Lynch syndrome can be excluded if both MLH1 loss by IHC and *BRAF* V600E mutation or *MLH1* hypermethylation are observed. Further germline mutational analysis for diagnosing Lynch syndrome is commonly performed in patients with MLH1 loss by IHC and *BRAF* wild type or unmethylated *MLH1* (Fig. 3).

For targeted therapies directed against EGFR tyrosine kinase in metastatic CRC patients, oncogenic mutations related to the EGFR signaling pathway are also suggested to be clinically relevant. Theoretically, the *BRAF V600E* mutation is considered a negative predictive marker for response to EGFR tyrosine kinase
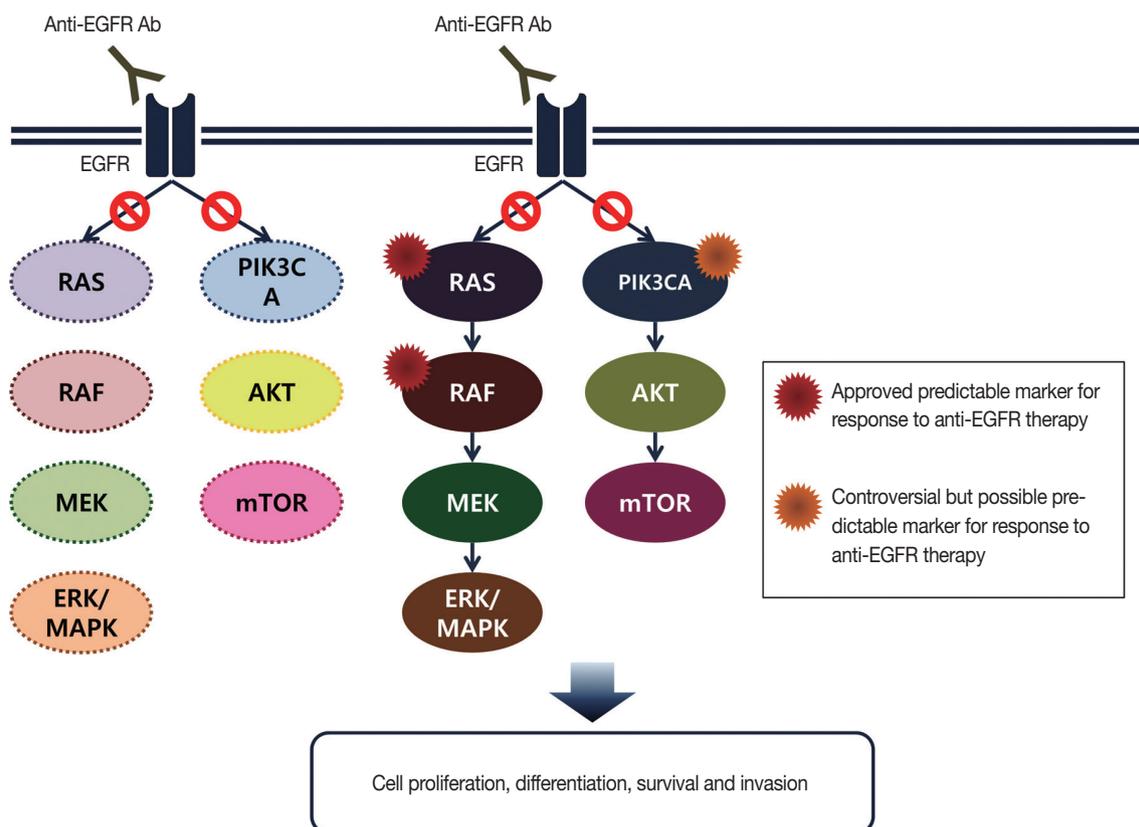
Fig. 2. Epidermal growth factor receptor (EGFR)–related signaling pathway in metastatic colorectal cancer. Anti-EGFR antibodies are able to block downstream signal of EGFR in wild type RAS and RAF (left), but unable to block in mutant RAS or RAF (right). mTOR, mammalian target of rapamycin; MAPK, mitogen-activated protein kinase.
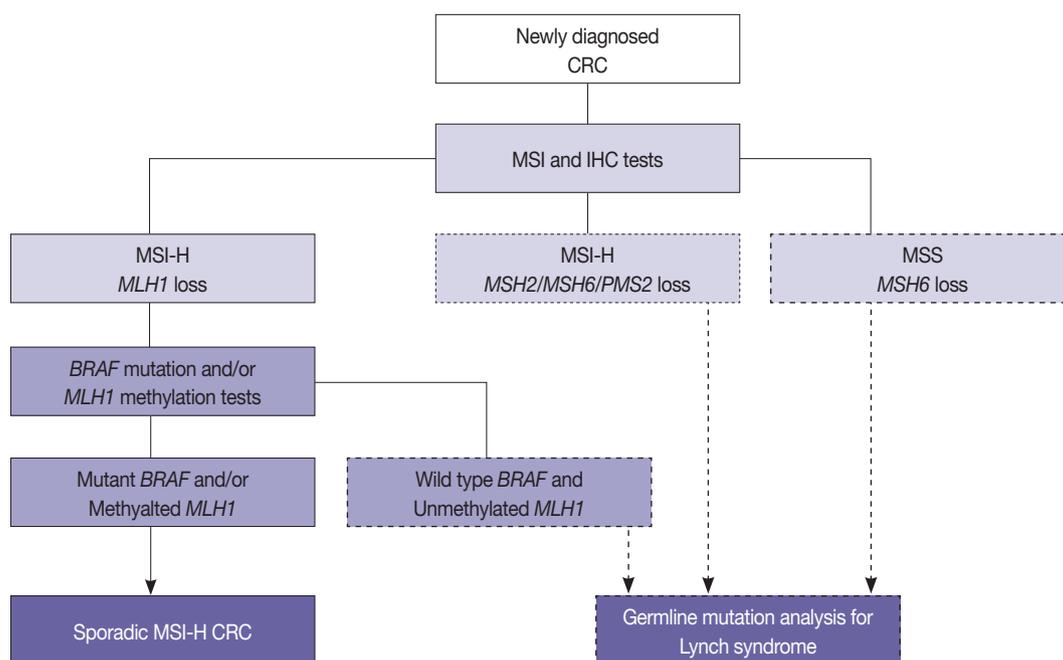
Fig. 3. Algorithm of molecular testing in colorectal cancer (CRC) patients. MSI, microsatellite instability; IHC, immunohistochemistry; MSI-H, microsatellite instability–high; MSS, microsatellite stable.

inhibitors, and several studies have shown that *BRAF* V600E mutations were significantly predictable for resistance to single-agent EGFR inhibitor.[54,55] The predictive role of the *BRAF* V600E mutation remains inconclusive owing to its rare prevalence,[6,47] but the level of evidence for the *BRAF* V600E mutation in CRC is I for blocking the effect of anti-EGFR antibody therapy according to the new AJCC cancer staging manual (8th edition).[9]

In contrast to *BRAF* mutated melanomas, the results of early clinical trials using *BRAF* inhibitors were not successful in treating *BRAF* mutated CRCs.[56,57] However, several clinical trials that combine BRAF and EGFR inhibitors with or without a third agent are currently ongoing or have recently been completed in *BRAF* mutated CRCs.[58]

PIK3CA mutations

In addition to the RAS/RAF/MAPK signaling pathway, activated EGFR can also induce the phosphoinositide 3-kinase (PI3K)/AKT/PTEN pathway. *PIK3CA* mutations in exon 9 and 20 have been studied as effectors of the EGFR downstream signaling pathway, similar to *BRAF* and *RAS*, and they might be related to resistance to EGFR inhibitors.[59] However, *PIK3CA* mutations tend to occur together with *KRAS* mutations.[54,60] Furthermore, confirmative evidence for a role of *PIK3CA* mutations in predicting response to cetuximab has not been shown.[61]

Therefore, the role of *PIK3CA* mutations in routine predictive molecular testing for EGFR inhibitor therapy remains controversial.

The PI3K/AKT/mammalian target of rapamycin (mTOR) pathway is frequently dysregulated in human cancers initiated by various molecular alterations including *PIK3CA* mutations. Janku *et al.*[62] performed early-phase clinical trials in which PI3K/AKT/mTOR inhibitors were administered to the patients with advanced tumors, and demonstrated that *PIK3CA* mutation was independently associated with a better response to PI3K/AKT/mTOR inhibitors.

Many previous studies have reported the prognostic implication of *PIK3CA* mutations in CRC; some studies have shown a significant correlation between *PIK3CA* mutations and patient survival, but other studies have not.[63] Although World Health Organization (WHO) classification suggests that *PIK3CA* mutations are markers for poor prognosis,[1] its practical role for predicting a patient's outcome remains uncertain.

Recently, experimental evidence suggests that cyclooxygenase 2 inhibition of aspirin down-regulates the PI3K signaling pathway. Liao *et al.*[64] reported that regular use of aspirin after cancer diagnosis in *PIK3CA*-mutated CRC patients was associated with a better prognosis,[65] which suggests that *PIK3CA* mutations may serve as molecular biomarkers for predicting response to aspirin therapy.

Indication

Based on confirmative correlation with patient prognosis, *KRAS* mutation testing is recommended in all patients with newly diagnosed CRC. The results of *BRAF* mutation testing are required for predicting a patients' prognosis in both metastatic and earlier stage CRC and for excluding Lynch syndrome in all CRC patients. Especially in metastatic CRC patients, *KRAS* and *NRAS* mutational analysis should be performed for predicting the responses to anti-EGFR antibody therapy, and *BRAF* mutations are essential as poor prognostic biomarkers. Although the prognostic or predictive role of *PIK3CA* mutation is not clear, molecular testing for *PIK3CA* mutation may be necessary for predicting response to PI3K/AKT/mTOR inhibitors and aspirin therapy after CRC diagnosis.

Methodology

Method

Sanger sequencing

Sanger sequencing is a traditional and well-confirmed method which needs ubiquitous instruments and inexpensive reagents, thus Sanger sequencing has been considered the gold standard method in many pathology laboratories for detecting oncogenic gene mutations.[66] In addition, Sanger sequencing has advantages for genetic mutational analysis such as the ability to identify specific mutations and to detect new mutations, and it has high reliability.[66] However, direct sequencing has some disadvantages including lower sensitivity (about 10%–20%), a multistep time-consuming method, subjective data interpretation, and no standardization.[60] Sequencing is not able to detect small amounts of mutated DNA fragments—especially less than 20% of total DNA—in the sample. Accordingly, the tumor samples should be very carefully prepared for to ensure collection of high tumor content.

Pyrosequencing

Compared to Sanger sequencing, pyrosequencing is more sensitive, and it can detect approximately 5% of mutant alleles.[67] It has some advantages compared to Sanger sequencing: (1) it is faster and more convenient; (2) the percentage of mutant allele quantity can be obtained; (3) it can be performed in a closed system in a single well; and (4) it can run multiple samples.[68] Therefore, this technology has provided sufficient analytical sensitivity and specificity for identifying *KRAS*, *NRAS*, and *BRAF* mutations in FFPE samples, even those from tissues with low tumor cell contents.[69] Pyrosequencing also has some disadvantages: (1) it requires additional costly instruments as compared to Sanger sequencer, as well as expensive reagents and consumables; (2) its data analysis is complex and challenging; (3) it can only sequence a short length of nucleotide sequence; and (4) it cannot detect new mutations.[70] However, the read length is sufficient for *KRAS*, *NRAS*, and *BRAF* sequencing because hot spots of these mutations are located within short length sequences.

Real-time PCR–based mutation detection methods

The detection of *KRAS* mutations using real-time PCR-based commercial kits has been suggested to be more reliable and sensitive than sequencing methods. The merits of commercial kits using real-time PCR systems are high sensitivity (approximately 1%), fast turn-around time, straightforward data interpretation, a closed-tube with a one-step process, small intra- and inter-lot deviations, and good concordance among the different real-time PCR systems. The disadvantages are that they have a relatively high cost per sample and high DNA input requirements.[71] In addition, they cannot detect all mutations or identify specific mutations.

The currently used commercial kits for detecting *KRAS* mutations are as follows: Asuragen, DxS TheraScreen *KRAS* mutation detection kit, EntroGen, Roche COBAS, TrimGen Mutector II *KRAS* kit, and ViennaLab.[71] Kim *et al.*[72] reported that *KRAS* mutational status was discordant between primary and metastatic sites in 17.5% of samples, using the Sanger sequencing method. In contrast, Miglio *et al.*[73] demonstrated concordant *KRAS* mutation status and type of mutation between primary and metastatic tumors and successful amplification in fine needle aspiration biopsy specimens with low tumor cell numbers, using the TheraScreen test. The TheraScreen *KRAS* RGQ PCR Kit uses Scorpions and ARMS technologies and detects six mutations in codon 12 and one in codon 13 of *KRAS*. The COBAS *KRAS* mutation test kit (Roche Molecular Systems, Inc., Branchburg, NJ, USA) is a TaqMelt PCR assay and can detect 19 *KRAS* mutations in codons 12, 13, and 61. The COBAS test was also reported to have higher sensitivity than Sanger sequencing and can detect minor mutations including G13C, G13R, and Q61H, which are detected in less than 1% of CRCs.[60,74]

Another real-time PCR–based method, the peptide nucleic acid (PNA)–clamp assay, has recently been approved in Korea. The PNA-clamp assay utilizes PNAs that are modified DNA that recognize and bind to their complementary nucleic acid sequences with greater stability and specificity and cannot function as primers for DNA polymerases. PNA-clamp PCR is a low cost

and highly sensitive method (0.1% of sensitivity) for detecting mutated genes, and is useful in clinical practice.[75] The PNA-clamp mutation detection kit cannot identify specific mutations.

For improving detection sensitivity, high-resolution melting analysis, mutant-enriched PCR (enriched PCR–restriction fragment length polymorphism assay), and co-amplification at lower denaturation temperature–PCR methods can be applied in clinical mutation tests.[71]

Next-generation sequencing

As mentioned above, mutations in the genes related to the EGFR signaling network may be responsible for resistance to EGFR inhibitors or worse overall survival in CRC patients, but it is difficult and less practical to test all related gene mutations including *KRAS* exon 2–4, *NRAS* exon 2–4, *BRAF* V600E, and *PIK3CA* in each individual metastatic CRC patient using conventional methods. Therefore, a high-throughput method is more practical or recommended for sequencing multiple EGFR signaling-related genes in a single test to detect various mutations. Recently, several studies have demonstrated the advantages of NGS including high sensitivity and specificity compared to those of PCR-based commercial kits and sequencing methods.[70,76] The above testing methods are summarized in Table 1.

Type of specimen

The sample can be fresh, frozen, or FFPE. Surgical resection, endoscopic or needle biopsies, and cytology specimens are all acceptable sample types for mutation tests. If possible, the resection specimen is recommended for molecular analysis. However, biopsies are more commonly provided in inoperable advanced and metastatic CRC patients, and moreover, only cytology specimens may be available. Therefore, in such cases, the detection method should be successful with low total DNA quantity and highly sensitive for samples with a low tumor to total DNA ratio.

Specimen requirements

The tissue specimen should contain cancer cells and a pathologist needs to estimate the content of tumor cells. Tumor cell enrichment by micro- or macro-dissection is required to increase the sensitivity of mutation tests. FFPE blocks are commonly available for mutation tests, but formalin fixation induces DNA denaturation and degradation.[77] Prolonged formalin fixation, decalcification, and prolonged storage of the paraffin blocks negatively affect the integrity of DNA,[78] and the specimen quality is important for successful test results. The pathologist has the responsibility of selecting the most appropriate tissue block and tumor area to be tested.

Reporting

With patient and clinical information, the absence or presence of a gene mutation should be reported in the pathologic records. If possible, the affected codon and specific change should be indicated. Appropriate nomenclature should be used and ambiguous terms are not recommended in reports. The reports should also include specimen type and test method used.

Validation of test

The analytical performance of both sequencing and commercial kits should be validated in each laboratory. It is recommended at least 40 samples be tested with many days and runs.[79] Both samples with known and unknown mutational status are recommended for validation. Additional comparative methods may be done with each testing method. The results of the vali-

Table 1. Comparison among various detection methods for gene mutation analysis

	Sanger sequencing	Pyrosequencing	Real-time PCR	PNA-clamp assay	Next generation sequencing
Advantage	Gold standard	More rapid and sensitive than Sanger sequencing	Simple and fast	Simple and fast	High-throughput
Instrument	Ubiquitous	Not ubiquitous	Depending on kit	Ubiquitous	Costly equipment
Sensitivity (%)	10–20	5	1	0.1	1
Method	Labor-intensive, time-consuming	Convenient, closed system	Closed system, one-step process	Closed system, one-step process	Time-consuming
Mutant allele quantity (%)	Unmeasurable	Measurable	Unmeasurable	Unmeasurable	Measurable
Detect all or new mutation	Yes	No	No	No	Yes
Detect specific mutation	Yes	Yes	No	No	Yes
Data interpretation	Subjective	Less subjective, but complex	Simple and easy	Simple and easy	Complicated (need statistics)

PCR, polymerase chain reaction; PNA, peptide nucleic acid.

dation should be analyzed by assessing accuracy, precision, analytical sensitivity and specificity, reportable range, and reference range.[79]

Quality assurance

Each pathology laboratory should establish internal QA instructions for using each mutation analysis method and review all performed mutation analysis in regular QA meetings. The sequence information of wild- and mutant-types and their clinical significance should be determined. Each PCR test should include positive and negative controls. The laboratory must compare test positivity rate to its reported range, and maintain testing trends including clinical implications of gene mutation, concordance between methods, and positivity rates. All pathology laboratories should participate in external QA programs.

Gene amplification and rearrangements

Background

Targeting of oncogenic drivers has been increasingly applied clinically in several advanced human malignancies resulting in improvement of overall survival. At this moment, a few receptor tyrosine kinase inhibitors, such as trastuzumab, ramucirumab, and cetuximab, have been approved for targeted therapy. In addition, EGFR family (HER1–4), fibroblast growth factor receptor 2 (FGFR2), and MET are being explored as potential therapeutics and some have been successful in early-stage trials.

HER2

HER2 has important oncogenic roles including modulation of cell growth, differentiation, and survival. Protein overexpres-
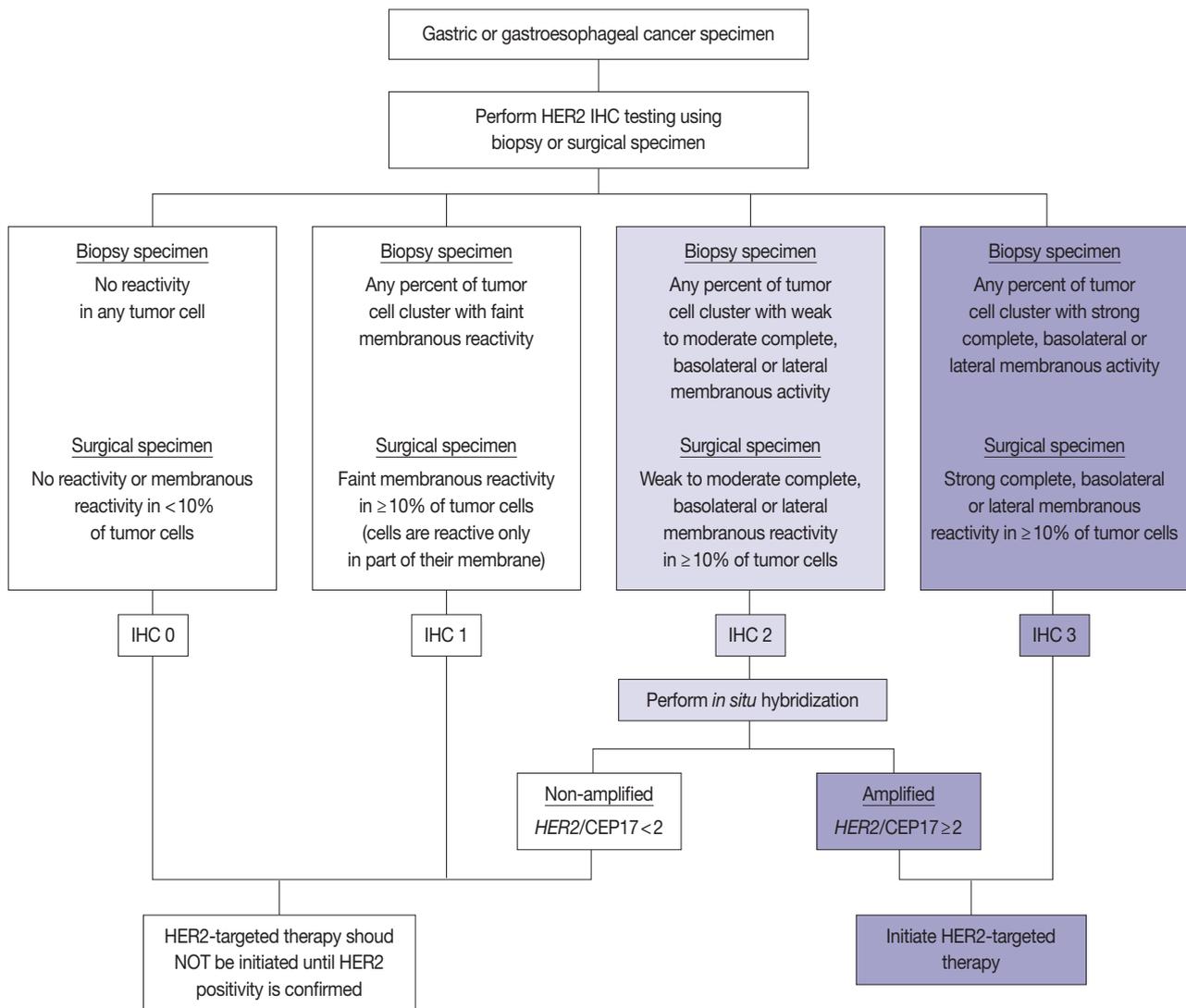
Fig. 4. Recommended gastric human epidermal growth factor receptor 2 (HER2) testing algorithm. IHC, immunohistochemistry.

sion of HER2 mainly occurs through *HER2* gene amplification, resulting in subsequent activation of abnormal cell signaling.[80] After the successful results of the Trastuzumab for Gastric Cancer (ToGA) trial,[8] trastuzumab against *HER2* has been approved for the treatment of HER2-positive advanced GC. HER2 testing is necessary in daily practice for treatment of advanced GC patients and the recommended HER2 testing algorithm is presented in Fig. 4.

Following the success of the ToGA trial, HER2 blockade has been of great clinical interest in CRC.[81-83] Somatic *HER2* amplification occurs in approximately 2%–7% of metastatic colorectal adenocarcinomas,[81-83] and HER2-positivity (IHC3+ or IHC2+/amplification) is observed in about 5% of advanced CRCs.[83] *HER2* gene amplification has been reported to be more frequent in rectal cancer than in right or left colon cancer.[82] *KRAS* mutation and *HER2* amplification were suggested to be mutually exclusive,[84] but our previous study demonstrated that *HER2* amplification might occur in *KRAS*-mutated CRCs.[60] A few clinical trials with trastuzumab-based combinations have been performed.[83,85,86] Although earlier studies reported controversial results,[85] recent trials suggest the possibility of HER2 blockade as a targeted therapy in advanced CRC patients.[84] Together, the HERACLES and MyPathway trials supported preclinical results that targeting HER2 with trastuzumab plus either lapatinib or pertuzumab is more effective than standard combination chemotherapy in HER2-positive CRC patients.[83,86]

For predicting response to EGFR inhibitors such as cetuximab, *RAS* mutation has been approved as a companion diagnosis. In addition to *RAS* mutation, gene amplification of the receptor tyrosine kinases *HER2* has been shown to bypass EGFR signaling and activate the MEK-ERK cascade, suggesting predictive roles of this gene. This has been supported by a previous study that identified *HER2* amplification in samples from metastatic CRC patients who did not benefit from EGFR inhibitor treatment.[87]

FGFR2

Clinical trials using antibodies against FGFR2b are now being conducted in GC patients. Oncogenic activation of FGFR2 via gene amplification occurs in a subset of common cancers, especially diffuse type GC.[88,89] *FGFR2* amplification has been detected in about 8% of gastroesophageal cancers.[88] AZD4547 is a selective FGFR1–3 inhibitor with activity in *FGFR2* amplified cancer models. In the SHINE trial in advanced GC patients with *FGFR2* amplification or polysomy, AZD4547 was well-tolerated, but there was no progression-free survival benefit in the AZD-treated group.[90] However, in a recent translational clinical trial, GCs with high-level clonal *FGFR2* amplification have a high response rate to the selective FGFR2 inhibitor AZD4547.[91]

MET and others

In addition to *HER2* amplification, *MET* amplification was also found in a small subset of *RAS* and *BRAF* wild-type metastatic patients and is suggested to be associated with resistance to cetuximab treatment.[92] *MET* exon 14 deletion has been postulated to be one potential mechanism for MET protein overexpression.[93] A recent study suggested *MET* amplification as a novel mechanism of the resistance to EGFR and BRAF combination blockade in *BRAF*-mutated CRCs; furthermore, the study showed that switching from EGFR to MET inhibition resulted in clinical response of the disease.[94]

KRAS gene amplification is observed in a minor subset of CRC cases (1%–2%) and has been reported to be nearly always mutually exclusive with *KRAS* mutations.[45] The database by the The Cancer Genome Atlas (TCGA) network has shown that *NRAS*, *BRAF*, and *CRAF* gene amplification can also be observed in a very low prevalence (< 1%), but their clinical implication is not clear.[26]

ROS1 gene rearrangement

ATP-binding sites in the kinase domains of anaplastic lymphoma kinase (ALK) and ROS1 share 77% amino acid identity.[95] *In vitro* evidence suggests that *ROS1* may be a more sensitive target than *ALK* to inhibition by crizotinib.[96] The incidence of *ROS1* rearrangement in gastric adenocarcinomas has been reported to be between 0.5% and 1%.[95,97]

NTRK gene rearrangements

Neurotrophic tropomyosin receptor kinase (*NTRK*) gene rearrangements have oncogenic and transforming potential, and recently have emerged as targets for cancer therapy with developing selective inhibitors.[98] *NTRK1*, *2*, and *3* gene rearrangements occur in several human cancers and they have been reported to have a 0.5% prevalence including *TPM3-NTRK1* in CRCs.[98] A novel *LMNA-NTRK1* rearrangement was reported in a metastatic CRC patient, who showed response to the pan-TRK inhibitor entrectinib.[99]

Indication

HER2 IHC should be routinely performed in all inoperable, locally advanced, recurrent, and metastatic GCs and gastroesophageal junction (GEJ) cancers at the initial diagnosis and in the diagnosis of recurred or metastatic GCs. If the HER2 IHC results

is equivocal of any cause, *HER2* genetic testing by fluorescence *in situ* hybridization (FISH) or silver *in situ* hybridization (SISH) should be performed. Given that the majority of metastatic GCs are inoperable and need immediate first-line chemotherapy and they are predicted to progress very rapidly, HER2 IHC with or without SISH/FISH should be performed as quickly as possible.[100] Additionally, HER2 testing should be performed at relapse in patients with previously c-erbB2–negative tumors.

Other gene analyses such as *FGFR2*, *HER2*, *ROS1*, and *NTRK* are necessary in patients with pretreated metastatic GCs or CRCs for selecting targeted therapy. *HER2* and *MET* amplification status would be helpful for predicting resistance to EGFR inhibitors.

Methodology

Method

Dual color FISH is recommended for gene amplification analysis. If possible, dual color SISH is also favored. Although both FISH and SISH, even if single-probe, showed good agreement for *HER2* copy number testing in previous studies,[101] it is widely accepted that SISH is a more preferred methodology than FISH because SISH is a bright-field methodology and enables pathologists to identify tumor area and HER2-positive area more rapidly, considering marked intratumoral HER2 heterogeneity.[100,102] Moreover, SISH slides can be stored for a longer period of time without bleaching than FISH slides.

ISH testing should be rejected and repeated if: (1) controls are not as expected, (2) the observer cannot find and count at least 20 invasive tumor cells, (3) > 25% of signals are unscorable owing to weak signals, (4) > 10% of signals occur over cytoplasm, (5) the nuclear resolution is poor, and (6) auto-fluorescence is strong.[103]

Gene amplification status can also be examined by quantitative real-time PCR and digital PCR for target and reference gene fragments. Previous studies have demonstrated a close correlation between ISH results and quantitative PCR results using tissue or plasma samples, but with weak-to-moderate correlation.[104] This may be due to intratumoral heterogeneity and normal cell contamination. Therefore, ISH in cancer tissue samples is the gold standard method for gene amplification testing. PCR-based methods are not acceptable for confirmatory molecular diagnosis.

Type of specimen

Both surgical resection and biopsy can be used for ISH analysis. However, biopsies are more commonly available because advanced and metastatic gastrointestinal cancers are usually inoperable. Intratumoral heterogeneity of oncogenic gene amplification has been demonstrated by many researchers. Especially, heterogeneous HER2 expression is very common in GC and GEJ cancer, where upwards of 30% of HER2-positive GCs have been reported, and *HER2* genetic status is closely correlated with HER2 expression status. Therefore, considering intratumoral HER2 heterogeneity, at least four to six biopsies by endoscopy are needed for sufficient and acceptable tests and to avoid false-negative results. The tissue microarray method is not recommended in routine clinical practice in pathology laboratories owing to HER2 heterogeneity.[100,102]

Specimen requirements

In order to obtain acceptable ISH results, specimen quality is important which relies on excellent sample fixation and preparation procedures. Regarding the cold ischemia time, it is recommended to transfer the endoscopic biopsy specimens into fixatives within 20 minutes of excision and the surgical excision specimens into fixatives within 1 hour of resection. However, most of the surgical specimens cannot be subject to fixation within less than 1 hour of resection in daily practice; thus, the cold ischemia time should be as short as possible in each pathology laboratory. The Task Force for gastric HER2 testing recommended that laboratories have their own validation results of optimal cold ischemia time for biopsies and surgical specimens for appropriate tissue handling protocols.[100] The fixation should be done using a sufficient amount of 10% neutral buffered formalin and the duration of fixation should be 8–72 hours. Although it may be influenced by primary fixation or storage conditions, sections should not be used if cut > 6 weeks earlier.[103] During the preparation, insufficient deparaffinization can result in nuclear bubbles in ISH slides, and over-digestion may result in nuclear holes.[102]

Reporting

In metastatic GC patients, treatment must be planned with full knowledge of a patient's HER2 status. When ISH signals are counted, it is recommended for the pathologists to use HER2 IHC slides as screening results and to count signals in the HER2 IHC-positive area in order to overcome heterogeneous HER2 reactivity.[104] At least 20 evaluable and non-overlapping cells from IHC 2+ areas should be counted initially. If ISH results indicate borderline amplification (*HER2*:CEP17 ratio 1.8–2.2), another 20 cells should be counted to reconfirm the *HER2*:CEP17 ratio. Only cells with at least one ISH signal for each probe should be counted if dual probes are used. The final diag-

nosis is defined as "ISH positive" if the *HER2*:CEP17 ratio is ≥ 2.0 and "ISH negative" if the *HER2*:CEP17 ratio is < 2.0. The reports of HER2 testing should provide a confirmative HER2 status, and an "equivocal" result, which is defined in the recommendations of HER2 testing in breast cancer, should not be accepted in GC patients.[100] Testing must be reported as 'indeterminate' if the interpretation of the *HER2* ISH result is precluded owing to technical issues such as poor specimen handling, significant tissue crushing artifact, and edge artifact.[105]

Usually, the diagnostic criteria of gene amplification, including *FGFR2* and *MET* in GC and *HER2* and *MET* in CRC, have been defined as a target gene:reference gene ratio > 2,[91] and the positivity criteria have been adopted from the recommendations of the gastric HER2 test. However, the HERACLES trial in metastatic CRC patients defined HER2-positivity criteria as tumors with a HER2 IHC 3+ score in more than 50% of cells or with HER2 IHC 2+ and a *HER2*:CEP17 > 2 in more than 50% of cells by FISH.[83] The final molecular diagnosis should be determined using the validated criteria for each target gene and in each organ.

Validation of test

In initial performing HER2 testing in GC, 25–50 GC cases should be analyzed in parallel, using IHC and ISH, and the concordance rate of IHC and ISH should be > 90% if equivocal IHC 2+ cases are excluded. Since HER2 testing and diagnosis in GC have unique features compared to that of breast cancer, initial set-up and validation must be independent of breast cancer protocols, performed by specifically trained persons in gastric HER2 testing, and documented in GC HER2 testing protocols.[100,102] Other gene amplification tests need to be validated for each gene and organ with full consideration of the differences among genes and organs.

Quality assurance

Each pathology laboratory should establish internal QA instructions for the ISH method and review all performed ISH analysis in regular QA meetings. It is recommended that all SISH slides and several representative images for FISH are stored. If possible, performing parallel analysis such as IHC is also recommended. The laboratory must maintain testing trends including positivity rates and scoring distributions, and record the possible reasons for their variation. All pathology laboratories should participate in external QA programs.

Epstein-Barr virus

Background

The EBV is a ubiquitous human herpes virus having a 172-kb DNA genome implicated in the etiology of many human malignancies.[106] The previous studies have demonstrated the presence of EBV in 2%–16% of conventional gastric adenocarcinomas worldwide, but the number of patients with EBV-associated GC is high because of the high incidence of GC, especially in Korea.[7] By TCGA results, EBV-positive GCs have a tendency of CIMP, but do not show a MSI-H phenotype or hMLH1 hypermethylation.[25] EBV-positive GCs were strongly associated with *CDKN2A* (*p16INK4A*) promoter hypermethylation and *PIK3CA* mutation.[25] The *PIK3CA* mutations were more dispersed in EBV-positive GCs, but localized in the kinase domain (exon 20) in EBV-negative cancers.

Morphologically, EBV-positive GC has characteristic abundant lymphoid stroma. By WHO classification, gastric carcinoma with lymphoid stroma is an uncommon subtype and is closely associated with the presence of EBV.[1] The high throughput study by the TCGA network revealed that IL-12 mediated immune cell signaling signatures were activated and *PD-L1/2* mRNA was overexpressed in EBV-positive GCs.[25] Recent studies supported the relationship between the presence of EBV and aberrant immune checkpoint protein expression by demonstrating high PD-L1 protein expression in EBV-positive GCs.[107,108] Therefore, EBV-positive GCs are suggested to be good candidates for immune checkpoint inhibitor therapy.

Indication

EBV-associated gastric carcinoma has a characteristic heavy lymphoid stroma, but the extent and degree of lymphoid stroma is variable and EBV status cannot be predicted by histologic features only. Furthermore, although EBV and MSI are mutually exclusive in GCs, microsatellite unstable GCs are also associated with lymphocyte-rich histology.[109] Therefore, to determine the EBV status of GC patients, laboratory detection of EBV is necessary in the newly diagnosed GC patients.

Methodology

Method

Laboratory detection of EBV may be performed by several published methods:[110] (1) ISH identification of EBV-encoded small RNAs (EBER) directly in tumor cells; (2) EBV clonality assay by Southern blot analysis to distinguish latent form repli-

cative infections; (3) EBV DNA amplification to detect viral DNA in patient tissues; (4) EBV viral load assays to quantitate EBV DNA in blood or body fluids to monitor disease status over time; (5) IHC for LMP1, EBNA1, EBNA2, LMP2A (latent state proteins of EBV), and BZLF1 (lytic state protein; so-called switch protein from lytic to latent state) to detect EBV-producing proteins and distinguish latent from replicative infections; (6) viral culture, which is possible but impractical for clinical use; (7) electron microscopy, which is also impractical; and (8) serology using VCA, EBNA, EA, and heterophile antibodies to monitor disease-association, -regression or -progression over time.

The presence or absence of EBV is examined by EBER ISH, and it is considered the gold standard for detecting and localizing latent EBV in tissue samples.[111] EBER transcripts are amplified, which represent a reliable target for determining the presence or absence of EBV in tissue sections by ISH. Commercially available EBER probes are labeled with biotin, digoxigenin, or fluorescein (Dako, Glostrup, Denmark; Enzo Diagnostics, Farmingdale, NY, USA; Kreatech Diagnostics, Amsterdam, The Netherlands; Novocastra Laboratories Ltd., Newcastle, UK; Shandon Lipshaw, Pittsburgh, PA, USA; Innogenex, San Ramon, CA; Ventana Medical Systems, Tucson, AZ, USA).[110] The IHC method has some merits in that it is fast, convenient, and widely used compared with the ISH method. However, LMP1 is undetectable in EBV-associated carcinomas, and BZLF1 is the only characteristic of lytic viral replication.[110]

Type of specimen

EBER ISH can be accomplished on paraffin sections from biopsy or surgical excision or on cytology preparations.

Specimen requirements

For EBER ISH, specimen quality is also important, which is dependent on good sample fixation and preparation procedures. The recommendations for specimen quality are the same as the other ISH analyses described above. The pathologists should select tumor sections with sufficient tumor cells to be included.

Reporting

EBER is usually detected uniformly in all of the tumor cells comprising an EBV-associated malignancy, but only focal EBER expression may be observed in tumors occasionally. EBER ISH signals are interpreted by microscopic examination and only the nuclear EBER positivity in tumor cells is defined as EBV-positive. Microscopic examination has additional advantages including evaluation of cell type and distribution of EBER signals.

Validation of test

The initial validation of EBER ISH is not different from that of the other ISH methods. It should be noted that nonspecific positivity in the cytoplasm of scattered normal epithelial cell is sometimes observed, and EBER-positive memory B cells are rarely found in some of the GC specimens.

Quality assurance

QA of EBER ISH is also similar to that of the other ISH methods. The internal and external QA programs are mandatory.

NEXT-GENERATION SEQUENCING CANCER PANEL

GC and CRC are genetically heterogeneous disorders driven by various genetic alterations.[112,113] Recently, the development of NGS has allowed a sharply increased sequencing capacity and rapid analysis of multiplexed samples.[114] NGS has cast a light on the comprehensive genetic aberration of the disease[115] and enabled the discovery of candidate genes as potential targets in cancer therapy.[116] Through the recent development of molecular genomics, molecular profiling of gastrointestinal carcinoma by large-scale cancer genomics projects has also been performed.[25,26] The TCGA research network completed the genomic sequencing of CRC and classified it based on the molecular feature.[25,26]

In the TCGA report, GCs are divided into two classes: the hypermutated and nonhypermutated tumor. The non-hypermutated tumor includes genomically stable and chromosomally unstable subtypes. EBV-positive and MSI-H subtypes represent the hypermutated tumor and have frequent mutations in *PIK3CA* and *ARID1A*. Other studies have discovered that *RHOA* and *CDH1* are possible driver genes in diffuse-type GC.[117,118] The gene mutations that contribute to gastric carcinoma, which have been revealed in previous large-scale studies, are listed in Table 2. CRC was also categorized into the hypermutated and the non-hypermutated tumor. The hypermutated tumors are characterized by elevated levels of MSI and defects in DNA MMR mechanisms. An activating mutation of *BRAF* is frequently presented in the hypermutated tumor.[119,120] Recurrent mutation of *TP53*, *KRAS*, *APC*, and *PIK3CA* has been consistently reported in previous studies and it is notable that the significantly frequent *KRAS* mutation is identified in non-hypermutated tumors (Table 3).[114,119,121]

In the era of precision medicine, the clinical implication of NGS for multiple biomarker tests has been consistently required. With the aid of TCGA data which highlighted relevant genetic

alterations and driver mutations linked to its biological pathway, various panels for multi-gene profile of carcinoma have been suggested. Multi-gene panels should identify a clinically action-able genetic aberration including variants linked to molecular classification, prediction of treatment response, and current/

future target of therapy.[122] For instance, the Ion AmpliSeq Colon and Lung Cancer Research Panel includes more than 20 genes, such as RTK genes, RTK signaling genes, and other well-known cancer-related genes. However, these panels have not been fully validated using clinical samples and their inter-laboratory repro-

Table 2. Recurrent somatic genetic alteration in gastric cancer analyzed using next-generation sequencing

Gene	Classification	Core pathway	Process	Mutational rate (%)			Reference
				Previous study	Hypermutated tumor[a]	Nonhypermutated tumor[a]	
TP53	TSG	Cell cycle/apoptosis, DNA damage control	Cell survival	14–59	35	50	27,116–118,123–127
PIK3CA[b]	Oncogene	PI3K-AKT	Cell survival	7–36	40	12	27,116–118,123–127
CDH1[c]	TSG	APC	Cell fate	4–36	-	11	27,116–118,124–126
ARID1A[b]	TSG	Chromatin modification	Cell fate	8–27	44	14	27,116,118,123–126
PTEN	TSG	PI3K-AKT	Cell survival	0–27	13	-	27,116,123,125,127
KRAS	Oncogene	RAS/RAF	Cell survival	0–27	19	6	27,116,118,125,127
RHOA[c]	Oncogene	RHO/ROCK	Cell survival	0–23	-	6	27,116,118
APC	TSG	APC	Cell fate	3–14	-	7	27,116,118,123,124
ERBB3	Oncogene	RTK	Cell survival	0–10	25	-	27,116
ERBB2	Oncogene	RTK	Cell survival	2–9	-	3	27,116,118,126,127
CTNNB1	Oncogene	APC	Cell fate	2–9	-	4	27,116,118,124
MET	Oncogene	RTK	Cell survival	0–9		-	116,127
FBXW7	TSG	NOTCH	Cell fate	2–6	24	-	27,118,127
SMAD4	TSG	TGF-β	Cell survival	4–6	-	8	27,118
EGFR	Oncogene	RTK	Cell survival	0–6	-	-	27,116,127
NRAS	Oncogene	RAS/RAF	Cell survival	0–5	-	-	116,125,127

TSG, tumour suppressor gene; PI3K, phosphoinositide 3-kinase; RTK, receptor tyrosine kinase; TGF-β, transforming growth factor β.
[a]Data of mutation rates are from The Cancer Genome Atlas database;[25] [b]More frequently mutated gene in gastric cancer with microsatellite instability–high frequency feature or Epstein-Barr virus positivity; [c]More frequently mutated gene in gastric cancer with diffuse type of Lauren classification.

Table 3. Recurrent somatic genetic alteration in colorectal cancer analyzed using next-generation sequencing

Gene	Classification	Core pathway	Process	Mutational rate (%)			Reference
				Previous study	Hypermutated tumor[a]	Nonhypermutated tumor[a]	
TP53[b]	TSG	Cell cycle/apoptosis, DNA damage control	Cell survival	27–65	20	60	119–121,128,129
KRAS[b]	Oncogene	RAS/RAF	Cell survival	33–58	30	43	119–121,128–131
APC[b,c]	TSG	APC	Cell fate	40–56	51	81	121,129
PIK3CA[b]	Oncogene	PI3K-AKT	Cell survival	14–20	-	18	119,120,128,129,131
BRAF[c]	Oncogene	RAS/RAF	Cell survival	5–14	46	-	119,120,128–131
PTEN	TSG	PI3K-AKT	Cell survival	2–13	-	-	119,128,129
EGFR	Oncogene	RTK	Cell survival	0–11	-	-	128,129,131
SMAD4[b]	TSG	TGF-β	Cell survival	2–11	-	10	119,121,128,129
FBXW7[b]	TSG	NOTCH	Cell fate	4–10	-	11	119,120,128,129
NRAS	Oncogene	RAS	Cell survival	2–7	-	9	119,120,128–131
MET	Oncogene	RTK	Cell survival	2–4	-	-	119,120
CTNNB1	Oncogene	APC	Cell fate	1–4	-	5	121,128,129
AKT1	Oncogene	PI3K	Cell survival	1–4	-	-	119,128,129
ERBB2	Oncogene	RTK	Cell survival	1–3	-	-	128,129
ALK	Oncogene	RTK	Cell survival	1–2	-	-	120,128,129
MAP2K1	Oncogene	RAS/RAF	Cell survival	0–2	-	-	119–121,128

TSG, tumour suppressor gene; PI3K, phosphoinositide 3-kinase; RTK, receptor tyrosine kinase; TGF-β, transforming growth factor β.
[a]Data of mutation rates are from The Cancer Genome Atlas database;[26] [b]More frequently mutated gene in nonhypermutated colorectal cancer; [c]More frequently mutated gene in hypermutated colorectal cancer.

ducibility has not been shown. Hence, the search for an ideal cancer marker panel and its validation by multi-centered and large-scale studies is still needed.

CONCLUSION

Remarkable developments in molecular and genomic techniques have increased the importance of molecular classification or grading in gastrointestinal cancers. Molecular testing is necessary for screening hereditary disease, predicting patient prognosis, and predicting the responses to targeted therapy. Standardization and quality control of the pre-analytic, analytic, and post-analytic steps of each molecular test are essential for reliable diagnostic results. In particular, the pathologists are responsible for the selection of appropriate specimen, with sufficient tumor cell quantity and well-preserved nucleic acids, authorizing the test results, and providing reliable molecular and genomic information to the clinician. Because the validation of the test, diagnostic criteria, and interpretation are not the same for each gene or each tumor, pathologists with subspecialty expertise are necessary. Therefore, the pathologists must obtain recent and integrated knowledge, and accumulate their experience in molecular testing.

REFERENCES

1. Bosman FT, Carneiro F, Hruban RH, Theise ND. WHO classification of tumours of the digestive system. Lyon: IARC Press, 2010; 13-177.

2. Jemal A, Center MM, DeSantis C, Ward EM. Global patterns of cancer incidence and mortality rates and trends. Cancer Epidemiol Biomarkers Prev 2010; 19: 1893-907.

3. Oh CM, Won YJ, Jung KW, et al. Cancer statistics in Korea: incidence, mortality, survival, and prevalence in 2013. Cancer Res Treat 2016; 48: 436-50.

4. Jung KW, Won YJ, Oh CM, et al. Prediction of cancer incidence and mortality in Korea, 2016. Cancer Res Treat 2016; 48: 451-7.

5. Boland CR, Thibodeau SN, Hamilton SR, et al. A National Cancer Institute Workshop on Microsatellite Instability for cancer detection and familial predisposition: development of international criteria for the determination of microsatellite instability in colorectal cancer. Cancer Res 1998; 58: 5248-57.

6. Douillard JY, Oliner KS, Siena S, et al. Panitumumab-FOLFOX4 treatment and RAS mutations in colorectal cancer. N Engl J Med 2013; 369: 1023-34.

7. Lee HS, Chang MS, Yang HK, Lee BL, Kim WH. Epstein-barr virus-positive gastric carcinoma has a distinct protein expression profile in comparison with epstein-barr virus-negative carcinoma. Clin Cancer Res 2004; 10: 1698-705.

8. Bang YJ, Van Cutsem E, Feyereislova A, et al. Trastuzumab in combination with chemotherapy versus chemotherapy alone for treatment of HER2-positive advanced gastric or gastro-oesophageal junction cancer (ToGA): a phase 3, open-label, randomised controlled trial. Lancet 2010; 376: 687-97.

9. Amin MB, Edge S, Greene F, et al. AJCC cancer staging manual. 8th ed. New York: Spinger, 2017; 203-74.

10. Jun SY, Kim M, Gu MJ, et al. Clinicopathologic and prognostic associations of KRAS and BRAF mutations in small intestinal adenocarcinoma. Mod Pathol 2016; 29: 402-15.

11. Peltomaki P. Role of DNA mismatch repair defects in the pathogenesis of human cancer. J Clin Oncol 2003; 21: 1174-9.

12. Ionov Y, Peinado MA, Malkhosyan S, Shibata D, Perucho M. Ubiquitous somatic mutations in simple repeated sequences reveal a new mechanism for colonic carcinogenesis. Nature 1993; 363: 558-61.

13. Boland CR. Evolution of the nomenclature for the hereditary colorectal cancer syndromes. Fam Cancer 2005; 4: 211-8.

14. Hampel H. Point: justification for Lynch syndrome screening among all patients with newly diagnosed colorectal cancer. J Natl Compr Canc Netw 2010; 8: 597-601.

15. Kloor M, Voigt AY, Schackert HK, Schirmacher P, von Knebel Doeberitz M, Bläker H. Analysis of EPCAM protein expression in diagnostics of Lynch syndrome. J Clin Oncol 2011; 29: 223-7.

16. Huth C, Kloor M, Voigt AY, et al. The molecular basis of EPCAM expression loss in Lynch syndrome-associated tumors. Mod Pathol 2012; 25: 911-6.

17. Watson P, Vasen HF, Mecklin JP, et al. The risk of extra-colonic, extra-endometrial cancer in the Lynch syndrome. Int J Cancer 2008; 123: 444-9.

18. Kim JH, Shin SH, Kwon HJ, Cho NY, Kang GH. Prognostic implications of CpG island hypermethylator phenotype in colorectal cancers. Virchows Arch 2009; 455: 485-94.

19. Thibodeau SN, French AJ, Cunningham JM, et al. Microsatellite in-

stability in colorectal cancer: different mutator phenotypes and the principal involvement of hMLH1. Cancer Res 1998; 58: 1713-8.

20. Edge SB, Byrd DR, Compton CC, Fritz AG, Greene FL, Trotti A. AJCC cancer staging manual. 7th ed. New York: Springer, 2010; 241-9.

21. Sinicrope FA, Rego RL, Halling KC, *et al*. Prognostic impact of microsatellite instability and DNA ploidy in human colon carcinoma patients. Gastroenterology 2006; 131: 729-37.

22. Kim JY, Shin NR, Kim A, *et al*. Microsatellite instability status in gastric cancer: a reappraisal of its clinical significance and relationship with mucin phenotypes. Korean J Pathol 2013; 47: 28-35.

23. Lee HS, Choi SI, Lee HK, *et al*. Distinct clinical features and outcomes of gastric cancers with microsatellite instability. Mod Pathol 2002; 15: 632-40.

24. Choi YY, Bae JM, An JY, *et al*. Is microsatellite instability a prognostic marker in gastric cancer? A systematic review with meta-analysis. J Surg Oncol 2014; 110: 129-35.

25. Cancer Genome Atlas Research Network. Comprehensive molecular characterization of gastric adenocarcinoma. Nature 2014; 513: 202-9.

26. Cancer Genome Atlas Research Network. Comprehensive molecular characterization of human colon and rectal cancer. Nature 2012; 487: 330-7.

27. Cristescu R, Lee J, Nebozhyn M, *et al*. Molecular analysis of gastric cancer identifies subtypes associated with distinct clinical outcomes. Nat Med 2015; 21: 449-56.

28. Sargent DJ, Marsoni S, Monges G, *et al*. Defective mismatch repair as a predictive marker for lack of efficacy of fluorouracil-based adjuvant therapy in colon cancer. J Clin Oncol 2010; 28: 3219-26.

29. Le DT, Uram JN, Wang H, *et al*. PD-1 blockade in tumors with mismatch-repair deficiency. N Engl J Med 2015; 372: 2509-20.

30. Rosenbaum MW, Bledsoe JR, Morales-Oyarvide V, Huynh TG, Mino-Kenudson M. PD-L1 expression in colorectal cancer is associated with microsatellite instability, *BRAF* mutation, medullary morphology and cytotoxic tumor-infiltrating lymphocytes. Mod Pathol 2016; 29: 1104-12.

31. Xiao Y, Freeman GJ. The microsatellite instable subset of colorectal cancer is a particularly good candidate for checkpoint blockade immunotherapy. Cancer Discov 2015; 5: 16-8.

32. Boger C, Behrens HM, Mathiak M, Krüger S, Kalthoff H, Röcken C. PD-L1 is an independent prognostic predictor in gastric cancer of Western patients. Oncotarget 2016; 7: 24269-83.

33. Moreira L, Balaguer F, Lindor N, *et al*. Identification of Lynch syndrome among patients with colorectal cancer. JAMA 2012; 308: 1555-65.

34. Buhard O, Suraweera N, Lectard A, Duval A, Hamelin R. Qua-

35. Lindor NM, Burgart LJ, Leontovich O, *et al*. Immunohistochemistry versus microsatellite instability testing in phenotyping colorectal tumors. J Clin Oncol 2002; 20: 1043-8.

36. de la Chapelle A, Hampel H. Clinical relevance of microsatellite instability in colorectal cancer. J Clin Oncol 2010; 28: 3380-7.

37. Oh JR, Kim DW, Lee HS, *et al*. Microsatellite instability testing in Korean patients with colorectal cancer. Fam Cancer 2012; 11: 459-66.

38. Lin EI, Tseng LH, Gocke CD, *et al*. Mutational profiling of colorectal cancers with microsatellite instability. Oncotarget 2015; 6: 42334-44.

39. Richman SD, Seymour MT, Chambers P, *et al*. *KRAS* and *BRAF* mutations in advanced colorectal cancer are associated with poor prognosis but do not preclude benefit from oxaliplatin or irinotecan: results from the MRC FOCUS trial. J Clin Oncol 2009; 27: 5931-7.

40. Phipps AI, Buchanan DD, Makar KW, *et al*. *KRAS*-mutation status in relation to colorectal cancer survival: the joint impact of correlated tumour markers. Br J Cancer 2013; 108: 1757-64.

41. Spano JP, Fagard R, Soria JC, Rixe O, Khayat D, Milano G. Epidermal growth factor receptor signaling in colorectal cancer: preclinical data and therapeutic perspectives. Ann Oncol 2005; 16: 189-94.

42. Karapetis CS, Khambata-Ford S, Jonker DJ, *et al*. K-ras mutations and benefit from cetuximab in advanced colorectal cancer. N Engl J Med 2008; 359: 1757-65.

43. Van Cutsem E, Kohne CH, Hitre E, *et al*. Cetuximab and chemotherapy as initial treatment for metastatic colorectal cancer. N Engl J Med 2009; 360: 1408-17.

44. Lievre A, Bachet JB, Boige V, *et al*. *KRAS* mutations as an independent prognostic factor in patients with advanced colorectal cancer treated with cetuximab. J Clin Oncol 2008; 26: 374-9.

45. Smith G, Bounds R, Wolf H, Steele RJ, Carey FA, Wolf CR. Activating K-Ras mutations outwith 'hotspot' codons in sporadic colorectal tumours: implications for personalised cancer medicine. Br J Cancer 2010; 102: 693-703.

46. Vaughn CP, Zobell SD, Furtado LV, Baker CL, Samowitz WS. Frequency of *KRAS*, *BRAF*, and *NRAS* mutations in colorectal cancer. Genes Chromosomes Cancer 2011; 50: 307-12.

47. Heinemann V, von Weikersthal LF, Decker T, *et al*. FOLFIRI plus cetuximab versus FOLFIRI plus bevacizumab as first-line treatment for patients with metastatic colorectal cancer (FIRE-3): a randomised, open-label, phase 3 trial. Lancet Oncol 2014; 15: 1065-75.

48. van Grieken NC, Aoyama T, Chambers PA, *et al*. *KRAS* and *BRAF* mutations are rare and related to DNA mismatch repair deficiency in gastric cancer from the East and the West: results from a large

international multicentre study. Br J Cancer 2013; 108: 1495-501.

49. Lee SH, Lee JW, Soung YH, *et al*. *BRAF* and *KRAS* mutations in stomach cancer. Oncogene 2003; 22: 6942-5.

50. Bettington M, Walker N, Clouston A, Brown I, Leggett B, Whitehall V. The serrated pathway to colorectal carcinoma: current concepts and challenges. Histopathology 2013; 62: 367-86.

51. Roth AD, Tejpar S, Delorenzi M, *et al*. Prognostic role of KRAS and BRAF in stage II and III resected colon cancer: results of the translational study on the PETACC-3, EORTC 40993, SAKK 60-00 trial. J Clin Oncol 2010; 28: 466-74.

52. Sinicrope FA, Shi Q, Smyrk TC, *et al*. Molecular markers identify subtypes of stage III colon cancer associated with patient outcomes. Gastroenterology 2015; 148: 88-99.

53. Palomaki GE, McClain MR, Melillo S, Hampel HL, Thibodeau SN. EGAPP supplementary evidence review: DNA testing strategies aimed at reducing morbidity and mortality from Lynch syndrome. Genet Med 2009; 11: 42-65.

54. De Roock W, Claes B, Bernasconi D, *et al*. Effects of *KRAS*, *BRAF*, *NRAS*, and *PIK3CA* mutations on the efficacy of cetuximab plus chemotherapy in chemotherapy-refractory metastatic colorectal cancer: a retrospective consortium analysis. Lancet Oncol 2010; 11: 753-62.

55. Di Nicolantonio F, Martini M, Molinari F, *et al*. Wild-type BRAF is required for response to panitumumab or cetuximab in metastatic colorectal cancer. J Clin Oncol 2008; 26: 5705-12.

56. Kopetz S, Desai J, Chan E, *et al*. Phase II pilot study of vemurafenib in patients with metastatic *BRAF*-mutated colorectal cancer. J Clin Oncol 2015; 33: 4032-8.

57. Corcoran RB, Atreya CE, Falchook GS, *et al*. Combined BRAF and MEK inhibition with dabrafenib and trametinib in *BRAF* V600-mutant colorectal cancer. J Clin Oncol 2015; 33: 4023-31.

58. Hyman DM, Puzanov I, Subbiah V, *et al*. Vemurafenib in multiple nonmelanoma cancers with *BRAF* V600 mutations. N Engl J Med 2015; 373: 726-36.

59. Perrone F, Lampis A, Orsenigo M, *et al*. PI3KCA/PTEN deregulation contributes to impaired responses to cetuximab in metastatic colorectal cancer patients. Ann Oncol 2009; 20: 84-90.

60. Nam SK, Yun S, Koh J, *et al*. BRAF, PIK3CA, and HER2 oncogenic alterations according to *KRAS* mutation status in advanced colorectal cancers with distant metastasis. PLoS One 2016; 11: e0151865.

61. Prenen H, De Schutter J, Jacobs B, *et al*. *PIK3CA* mutations are not a major determinant of resistance to the epidermal growth factor receptor inhibitor cetuximab in metastatic colorectal cancer. Clin Cancer Res 2009; 15: 3184-8.

62. Janku F, Wheler JJ, Naing A, *et al*. *PIK3CA* mutation H1047R is as-

sociated with response to PI3K/AKT/mTOR signaling pathway inhibitors in early-phase clinical trials. Cancer Res 2013; 73: 276-84.

63. Mei ZB, Duan CY, Li CB, Cui L, Ogino S. Prognostic role of tumor *PIK3CA* mutation in colorectal cancer: a systematic review and meta-analysis. Ann Oncol 2016; 27: 1836-48.

64. Liao X, Lochhead P, Nishihara R, *et al*. Aspirin use, tumor *PIK3CA* mutation, and colorectal-cancer survival. N Engl J Med 2012; 367: 1596-606.

65. Ogino S, Lochhead P, Giovannucci E, Meyerhardt JA, Fuchs CS, Chan AT. Discovery of colorectal cancer *PIK3CA* mutation as potential predictive biomarker: power and promise of molecular pathological epidemiology. Oncogene 2014; 33: 2949-55.

66. Franca LT, Carrilho E, Kist TB. A review of DNA sequencing techniques. Q Rev Biophys 2002; 35: 169-200.

67. Ogino S, Kawasaki T, Brahmandam M, *et al*. Sensitive sequencing method for *KRAS* mutation detection by pyrosequencing. J Mol Diagn 2005; 7: 413-21.

68. Ahmadian A, Ehn M, Hober S. Pyrosequencing: history, biochemistry and future. Clin Chim Acta 2006; 363: 83-94.

69. Sundstrom M, Edlund K, Lindell M, *et al*. KRAS analysis in colorectal carcinoma: analytical aspects of pyrosequencing and allele-specific PCR in clinical practice. BMC Cancer 2010; 10: 660.

70. Altimari A, de Biase D, De Maglio G, *et al*. 454 next generation-sequencing outperforms allele-specific PCR, Sanger sequencing, and pyrosequencing for routine *KRAS* mutation analysis of formalin-fixed, paraffin-embedded samples. Onco Targets Ther 2013; 6: 1057-64.

71. Herreros-Villanueva M, Chen CC, Yuan SS, Liu TC, Er TK. *KRAS* mutations: analytical considerations. Clin Chim Acta 2014; 431: 211-20.

72. Kim MJ, Lee HS, Kim JH, *et al*. Different metastatic pattern according to the *KRAS* mutational status and site-specific discordance of KRAS status in patients with colorectal cancer. BMC Cancer 2012; 12: 347.

73. Miglio U, Mezzapelle R, Paganotti A, *et al*. Mutation analysis of *KRAS* in primary colorectal cancer and matched metastases by means of highly sensitivity molecular assay. Pathol Res Pract 2013; 209: 233-6.

74. Gonzalez de Castro D, Angulo B, Gomez B, *et al*. A comparison of three methods for detecting *KRAS* mutations in formalin-fixed colorectal cancer specimens. Br J Cancer 2012; 107: 345-51.

75. Oh JE, Lim HS, An CH, *et al*. Detection of low-level *KRAS* mutations using PNA-mediated asymmetric PCR clamping and melting curve analysis with unlabeled probes. J Mol Diagn 2010; 12: 418-24.

76. Peeters M, Oliner KS, Parker A, *et al*. Massively parallel tumor

multigene sequencing to evaluate response to panitumumab in a randomized phase III study of metastatic colorectal cancer. Clin Cancer Res 2013; 19: 1902-12.

77. Srinivasan M, Sedmak D, Jewell S. Effect of fixatives and tissue processing on the content and integrity of nucleic acids. Am J Pathol 2002; 161: 1961-71.

78. Nam SK, Im J, Kwak Y, *et al*. Effects of fixation and storage of human tissue samples on nucleic Acid preservation. Korean J Pathol 2014; 48: 36-42.

79. Kamel-Reid S, Zhang T, Persons DL, Nikiforova MN, Halling KC. Validation of KRAS testing for anti-EGFR therapeutic decisions for patients with metastatic colorectal carcinoma. Arch Pathol Lab Med 2012; 136: 26-32.

80. Yarden Y, Sliwkowski MX. Untangling the ErbB signalling network. Nat Rev Mol Cell Biol 2001; 2: 127-37.

81. Conradi LC, Styczen H, Sprenger T, *et al*. Frequency of HER-2 positivity in rectal cancer and prognosis. Am J Surg Pathol 2013; 37: 522-31.

82. Seo AN, Kwak Y, Kim DW, *et al*. HER2 status in colorectal cancer: its clinical significance and the relationship between *HER2* gene amplification and expression. PLoS One 2014; 9: e98528.

83. Sartore-Bianchi A, Trusolino L, Martino C, *et al*. Dual-targeted therapy with trastuzumab and lapatinib in treatment-refractory, *KRAS* codon 12/13 wild-type, HER2-positive metastatic colorectal cancer (HERACLES): a proof-of-concept, multicentre, open-label, phase 2 trial. Lancet Oncol 2016; 17: 738-46.

84. Schmoll HJ. Targeting HER2: precision oncology for colorectal cancer. Lancet Oncol 2016; 17: 685-6.

85. Ramanathan RK, Hwang JJ, Zamboni WC, *et al*. Low overexpression of HER-2/neu in advanced colorectal cancer limits the usefulness of trastuzumab (Herceptin) and irinotecan as therapy: a phase II trial. Cancer Invest 2004; 22: 858-65.

86. Hurwitz H, Hainsworth JD, Swanton C, *et al*. Targeted therapy for gastrointestinaI (GI) tumors based on molecular profiles: early results from MyPathway, an open-label phase IIa basket study in patients with advanced solid tumors. J Clin Oncol 2016; 34 Suppl: 653.

87. Bertotti A, Migliardi G, Galimi F, *et al*. A molecularly annotated platform of patient-derived xenografts ("xenopatients") identifies HER2 as an effective therapeutic target in cetuximab-resistant colorectal cancer. Cancer Discov 2011; 1: 508-23.

88. Turner N, Grose R. Fibroblast growth factor signalling: from development to cancer. Nat Rev Cancer 2010; 10: 116-29.

89. Dieci MV, Arnedos M, Andre F, Soria JC. Fibroblast growth factor receptor inhibitors as a cancer treatment: from a biologic rationale to medical perspectives. Cancer Discov 2013; 3: 264-79.

90. Bang YJ, Van Cutsem E, Mansoor W, *et al*. A randomized, open-label phase II study of AZD4547 (AZD) versus Paclitaxel (P) in previously treated patients with advanced gastric cancer (AGC) with fibroblast growth factor receptor 2 (FGFR2) polysomy or gene amplification (amp): SHINE study. J Clin Oncol 2015; 33 Suppl: 4014.

91. Pearson A, Smyth E, Babina IS, *et al*. High-level clonal *FGFR* amplification and response to FGFR inhibition in a translational clinical trial. Cancer Discov 2016; 6: 838-51.

92. Bardelli A, Corso S, Bertotti A, *et al*. Amplification of the MET receptor drives resistance to anti-EGFR therapies in colorectal cancer. Cancer Discov 2013; 3: 658-73.

93. Lee J, Ou SH, Lee JM, *et al*. Gastrointestinal malignancies harbor actionable *MET* exon 14 deletions. Oncotarget 2015; 6: 28211-22.

94. Pietrantonio F, Oddo D, Gloghini A, *et al*. MET-driven resistance to dual EGFR and BRAF blockade may be overcome by switching from EGFR to MET inhibition in *BRAF*-mutated colorectal cancer. Cancer Discov 2016; 6: 963-71.

95. Davies KD, Doebele RC. Molecular pathways: ROS1 fusion proteins in cancer. Clin Cancer Res 2013; 19: 4040-5.

96. Shaw AT, Ou SH, Bang YJ, *et al*. Crizotinib in ROS1-rearranged non-small-cell lung cancer. N Engl J Med 2014; 371: 1963-71.

97. Lee J, Lee SE, Kang SY, *et al*. Identification of ROS1 rearrangement in gastric adenocarcinoma. Cancer 2013; 119: 1627-35.

98. Amatu A, Sartore-Bianchi A, Siena S. *NTRK* gene fusions as novel targets of cancer therapy across multiple tumour types. ESMO Open 2016; 1: e000023.

99. Sartore-Bianchi A, Ardini E, Bosotti R, *et al*. Sensitivity to entrectinib associated with a novel *LMNA-NTRK1* gene fusion in metastatic colorectal cancer. J Natl Cancer Inst 2016; 108: djv306.

100. Kim KM, Bilous M, Chu KM, *et al*. Human epidermal growth factor receptor 2 testing in gastric cancer: recommendations of an Asia-Pacific task force. Asia Pac J Clin Oncol 2014; 10: 297-307.

101. Fox SB, Kumarasinghe MP, Armes JE, *et al*. Gastric HER2 Testing Study (GaTHER): an evaluation of gastric/gastroesophageal junction cancer testing accuracy in Australia. Am J Surg Pathol 2012; 36: 577-82.

102. Ruschoff J, Hanna W, Bilous M, *et al*. HER2 testing in gastric cancer: a practical approach. Mod Pathol 2012; 25: 637-50.

103. Wolff AC, Hammond ME, Hicks DG, *et al*. Recommendations for human epidermal growth factor receptor 2 testing in breast cancer: American Society of Clinical Oncology/College of American Pathologists clinical practice guideline update. J Clin Oncol 2013; 31: 3997-4013.

104. Lee HE, Park KU, Yoo SB, *et al*. Clinical significance of intratumoral *HER2* heterogeneity in gastric cancer. Eur J Cancer 2013; 49: 1448-57.

105. Koudelakova V, Berkovcova J, Trojanec R, *et al*. Evaluation of *HER2* gene status in breast cancer samples with indeterminate fluorescence *in situ* hybridization by quantitative real-time PCR. J Mol Diagn 2015; 17: 446-55.

106. Longnecker RM, Kieff E, Cohen JI. Epstein-Barr virus. In: Knipe DM, Howley PM, Cohen JI, *et al.*, eds. Fields virology. 6th ed. Philadelphia: Lippincott-Williams and Wilkins, 2013; 1898-959.

107. Ma C, Patel K, Singhi AD, *et al*. Programmed death-ligand 1 expression is common in gastric cancer associated with Epstein-Barr virus or microsatellite instability. Am J Surg Pathol 2016; 40: 1496-506.

108. Kawazoe A, Kuwata T, Kuboki Y, *et al*. Clinicopathological features of programmed death ligand 1 expression with tumor-infiltrating lymphocyte, mismatch repair, and Epstein-Barr virus status in a large cohort of gastric cancer patients. Gastric Cancer 2016 Sep 14 [Epub]. https://doi.org/ 10.1007/s10120-016-0631-3.

109. Chetty R. Gastrointestinal cancers accompanied by a dense lymphoid component: an overview with special reference to gastric and colonic medullary and lymphoepithelioma-like carcinomas. J Clin Pathol 2012; 65: 1062-5.

110. Gulley ML. Molecular diagnosis of Epstein-Barr virus-related diseases. J Mol Diagn 2001; 3: 1-10.

111. Ambinder RF, Mann RB. Epstein-Barr-encoded RNA *in situ* hybridization: diagnostic applications. Hum Pathol 1994; 25: 602-5.

112. Carethers JM, Jung BH. Genetics and genetic biomarkers in sporadic colorectal cancer. Gastroenterology 2015; 149: 1177-90.e3.

113. Chia NY, Tan P. Molecular classification of gastric cancer. Ann Oncol 2016; 27: 763-9.

114. Chevrier S, Arnould L, Ghiringhelli F, Coudert B, Fumoleau P, Boidot R. Next-generation sequencing analysis of lung and colon carcinomas reveals a variety of genetic alterations. Int J Oncol 2014; 45: 1167-74.

115. Lin Y, Wu Z, Guo W, Li J. Gene mutations in gastric cancer: a review of recent next-generation sequencing studies. Tumour Biol 2015; 36: 7385-94.

116. Cerami E, Gao J, Dogrusoz U, *et al*. The cBio cancer genomics portal: an open platform for exploring multidimensional cancer genomics data. Cancer Discov 2012; 2: 401-4.

117. Lee YS, Cho YS, Lee GK, *et al*. Genomic profile analysis of diffuse-type gastric cancers. Genome Biol 2014; 15: R55.

118. Li X, Wu WK, Xing R, *et al*. Distinct subtypes of gastric cancer defined by molecular characterization include novel mutational signatures with prognostic capability. Cancer Res 2016; 76: 1724-32.

119. D'Haene N, Le Mercier M, De Nève N, *et al*. Clinical validation of targeted next generation sequencing for colon and lung cancers. PLoS One 2015; 10: e0138245.

120. Mukherjee S, Ma Z, Wheeler S, *et al*. Chromosomal microarray provides enhanced targetable gene aberration detection when paired with next generation sequencing panel in profiling lung and colorectal tumors. Cancer Genet 2016; 209: 119-29.

121. Yu J, Wu WK, Li X, *et al*. Novel recurrently mutated genes and a prognostic mutation signature in colorectal cancer. Gut 2015; 64: 636-45.

122. Marrone M, Filipski KK, Gillanders EM, Schully SD, Freedman AN. Multi-marker solid tumor panels using next-generation sequencing to direct molecularly targeted therapies. PLoS Curr 2014; 6: ecurrents.eogt.aa5415d435fc886145bd7137a280a971.

123. Wang K, Kan J, Yuen ST, *et al*. Exome sequencing identifies frequent mutation of ARID1A in molecular subtypes of gastric cancer. Nat Genet 2011; 43: 1219-23.

124. Wong SS, Kim KM, Ting JC, *et al*. Genomic landscape and genetic heterogeneity in gastric adenocarcinoma revealed by whole-genome sequencing. Nat Commun 2014; 5: 5477.

125. Ali SM, Sanford EM, Klempner SJ, *et al*. Prospective comprehensive genomic profiling of advanced gastric carcinoma cases reveals frequent clinically relevant genomic alterations and new routes for targeted therapies. Oncologist 2015; 20: 499-507.

126. Kuboki Y, Yamashita S, Niwa T, *et al*. Comprehensive analyses using next-generation sequencing and immunohistochemistry enable precise treatment in advanced gastric cancer. Ann Oncol 2016; 27: 127-33.

127. Bria E, Pilotto S, Simbolo M, *et al*. Comprehensive molecular portrait using next generation sequencing of resected intestinal-type gastric cancer patients dichotomized according to prognosis. Sci Rep 2016; 6: 22982.

128. Malapelle U, Pisapia P, Sgariglia R, *et al*. Less frequently mutated genes in colorectal cancer: evidences from next-generation sequencing of 653 routine cases. J Clin Pathol 2016; 69: 767-71.

129. Dallol A, Buhmeida A, Al-Ahwal MS, *et al*. Clinical significance of frequent somatic mutations detected by high-throughput targeted sequencing in archived colorectal cancer samples. J Transl Med 2016; 14: 118.

130. Sakai K, Tsurutani J, Yamanaka T, *et al*. Extended *RAS* and *BRAF* mutation snalysis using next-generation sequencing. PLoS One 2015; 10: e0121891.

131. Magliacane G, Grassini G, Bartocci P, *et al*. Rapid targeted somatic mutation analysis of solid tumors in routine clinical diagnostics. Oncotarget 2015; 6: 30592-603.

Mesothelin Expression in Gastric Adenocarcinoma and Its Relation to Clinical Outcomes

Song-Hee Han · Mee Joo
Hanseong Kim · Sunhee Chang

Department of Pathology, Inje University Ilsan
Paik Hospital, Goyang, Korea

Corresponding Author
Sunhee Chang, MD, PhD
Department of Pathology, Inje University Ilsan Paik
Hospital, 170 Juhwa-ro, Ilsanseo-gu, Goyang
10380, Korea
Tel: +82-31-910-7142
Fax: +82-31-910-7139
E-mail: pathate714@gmail.com

Background: Although surgical resection with chemotherapy is considered effective for patients with advanced gastric cancer, it remains the third leading cause of cancer-related death in South Korea. Several studies have reported that mesothelial markers including mesothelin, calretinin, and Wilms tumor protein 1 (WT1) were positive in variable carcinomas, associated with prognosis, and were evaluated as potential markers for targeted therapy. The aim of this study was to assess the immunohistochemical expression of mesothelial markers (mesothelin, calretinin, and WT1) in gastric adenocarcinoma and their relations to clinocopathological features and prognosis. **Methods:** We evaluated calretinin, WT1, and mesothelin expression by immunohistochemical staining in 117 gastric adenocarcinomas. **Results:** Mesothelin was positively stained in 30 cases (25.6%). Mesothelin expression was related to increased depth of invasion (p = .002), lymph node metastasis (p = .013), and presence of lymphovascular (p = .015) and perineural invasion (p = .004). Patients with mesothelin expression had significantly worse disease-free survival rate compared with that of nonmesothelin expression group (p = .024). Univariate analysis showed that mesothelin expression is related to short-term survival. None of the 117 gastric adenocarcinomas stained for calretinin or WT1. **Conclusions:** Mesothelin expression was associated with poor prognosis. Our results suggest that mesothelin-targeted therapy should be considered as an important therapeutic alternative for gastric adenocarcinoma patients with mesothelin expression.

Key Words: Mesothelin; Gastric adenocarcinoma; Prognosis

Gastric cancer is a major health problem worldwide, causing approximately one million deaths every year.[1] In South Korea, gastric cancer is the third leading cause of cancer-related death.[2] With improved screening methods such as endoscopy and the development of new techniques such as endoscopic submucosal dissection, patients can be diagnosed with gastric cancer at an early stage and are expected to have increased long-term survival rate and higher quality of life.[3] Although surgical resection with chemotherapy is considered effective for patients with recurrent, metastatic, or advanced gastric cancer (AGC), the 5-year survival rate for patients with AGC is only 20%–30%.[4] Chemotherapy increases survival rate, enhances quality of life, and can achieve symptomatic control; however, it is associated with increased drug toxicity.[5] In recent years, the identification of druggable oncogenic alterations such as human epidermal growth factor receptor 2 (HER2) overexpression and the development of drugs that specifically target HER2 have led to substantial improvement in the prognosis of patients with AGC.[6] However, oncogenic alterations are detected in only 6.0%–29.5% of gastric adenocarcinomas.[7] Thus, development of novel effective targeted

therapy is essential for the management of AGC.

Mesothelin, calretinin, and Wilms tumor protein 1 (WT1) are immunohistochemical markers for mesothelial differentiation. These markers are positive in various carcinomas and have been associated with prognosis. Mesothelin has been found to be expressed in some carcinomas, particularly those arising in the ovary, pancreas, and stomach, and has prognostic value.[8-12] Calretinin expression has been reported in carcinomas of various tissues including the ovary, testis, adrenal cortex, colon, breast, sinonasal tract, thymus, skin, and even soft tissues.[13] Previous studies have reported the prognostic implications of calretinin expression in breast cancer and malignant mesothelioma.[14,15] Qi et al.[16] reported that WT1-positive expression was associated with unfavorable clinical outcomes in patients with ovarian cancer, endometrial cancer, and noncarcinoma malignancies.

A few studies have investigated the expression of these mesothelial markers in gastric adenocarcinoma. Mesothelin expression percentages ranged from 15.4% to 59.4%; however, conflicting results were reported on the relationship between prognosis of patients with gastric adenocarcinoma and positive

mesothelin expression.[11,12] Several studies have examined the importance of WT1 and calretinin expression in gastric adenocarcinoma. However, mesothelial marker expression in gastric adenocarcinoma and the prognostic value of such expression remain unclear.

To investigate the prognostic significance of mesothelial markers in gastric adenocarcinoma, we evaluated the expression of mesothelial markers (mesothelin, calretinin, and WT1) in gastric adenocarcinoma and the association between positive mesothelial markers and clinicopathological variables and disease-free survival (DFS).

MATERIALS AND METHODS

Patients and tissue samples

Subjects in this study totaled 117 patients who had histologically confirmed gastric adenocarcinoma and who underwent radical resection at Inje University Ilsan Hospital from January 2005 to December 2011. These specimens were composed of 86 early gastric cancer and 31 AGC cases. The patients enrolled in this study had not received neoadjuvant chemotherapy or radiation therapy prior to surgery. Patients were followed for 1–10 years. The clinicopathological features including patient age, gender, and other factors are shown in Table 1. Hematoxylin and eosin (H&E)–stained slides for all cases were reviewed to confirm the diagnosis. The study was approved by the Institutional Review Board of Inje University Ilsan Hospital (ISPAIK 2015-10-017).

Tissue microarray construction

Paraffin blocks containing representative samples of the tumors were selected by reviewing all of the H&E-stained slides. For the tissue microarray (TMA), two tissue cores with a diameter of 3 mm were extracted from a representative tumor area and were sequentially placed in recipient tissue array blocks using a tissue arraying instrument (Labro, Seoul, Korea). Sections from TMA blocks were prepared (4 μm thickness) for routine H&E staining. Other sections were prepared on charged slides for immunohistochemical staining.

Immunohistochemical evaluation

Immunohistochemistry was performed using standard methods. Formalin-fixed, 4 μm-thick, paraffin-embedded tissue sections were deparaffinized and subjected to antigen retrieval (im-

Table 1. Clinicopathological correlation of mesothelin expression in gastric adenocarcinoma

Parameter	Mesothelin positive (n=30, 25.6%)	Mesothelin negative (n=87, 74.4%)	p-value
Age, mean (range, yr)	66 (41–89)	66 (35–91)	
Gender			.110
Female	8 (20.0)	32 (80.0)	
Male	22 (28.6)	55 (71.4)	
Stage			.001
EGC	16 (18.6)	70 (81.4)	
AGC	14 (45.2)	17 (54.8)	
Lymph node metastasis			.013
Present	16 (38.1)	26 (61.9)	
Absent	14 (18.7)	61 (81.3)	
Lauren classification			.113
Intestinal	17 (18.6)	74 (81.4)	
Diffuse	13 (50.0)	13 (50.0)	
Recurrence			.120
Present			
Local recurrence	2 (15.4)	2 (15.4)	
Distant metastasis	6 (46.2)	3 (23.0)	
Absent	22 (21.2)	82 (78.8)	
Lymphovascular invasion			.015
Present	18 (36.0)	32 (64.0)	
Absent	12 (17.9)	55 (82.1)	
Perineural invasion			.004
Present	13 (46.4)	15 (53.6)	
Absent	17 (19.1)	72 (80.9)	

Values are presented as number (%).
EGC, early gastric cancer; AGC, advanced gastric cancer.

mersed in 10 mmol/L citrate buffer [pH 6.0] and microwaved for 25 minutes). Slides were stained using an automatic staining device: Bond-X autoimmunostainer (Leica Microsystems, Wetzlar, Germany) with Bond Polymer Refine Detection System (Leica Microsystems). The following monoclonal mouse antibodies were used: anti-calretinin (1:50, Novocastra, Newcastle upon Tyne, UK), anti-WT1 (1:100, DAKO, Carpinteria, CA, USA), and anti-mesothelin (1:20; Leica). All slides were subsequently counterstained with hematoxylin. The mesothelial hyperplasia of pleura was used as a positive control. For a negative control, nonimmune mouse serum was used as a substitute for primary antibodies.

Membranous staining for mesothelin, nuclear and cytoplasmic staining for calretinin, and nuclear staining for WT1 were considered positive. We categorized any tumor with ≥5% staining of any intensity as positive and <5% as negative.[12] Stained sections were evaluated independently by two observers.

Statistical analysis

Statistical analysis was performed using SPSS ver. 21.0 (IBM Corp., Armonk, NY, USA). Correlations between the expression of mesothelial markers in gastric adenocarcinoma and clinicopathological variables were assessed using Pearson's χ^2-test. The Kaplan-Meier method was used for DFS analysis, and differences were determined using log-rank test. The prognostic implications of mesothelin expression and clinicopathological parameters were analyzed by Cox univariate and multivariate proportional hazards models. DFS was calculated from the date of surgery to the time of first local recurrence or distant metastasis. Values of $p < .05$ were considered statistically significant.
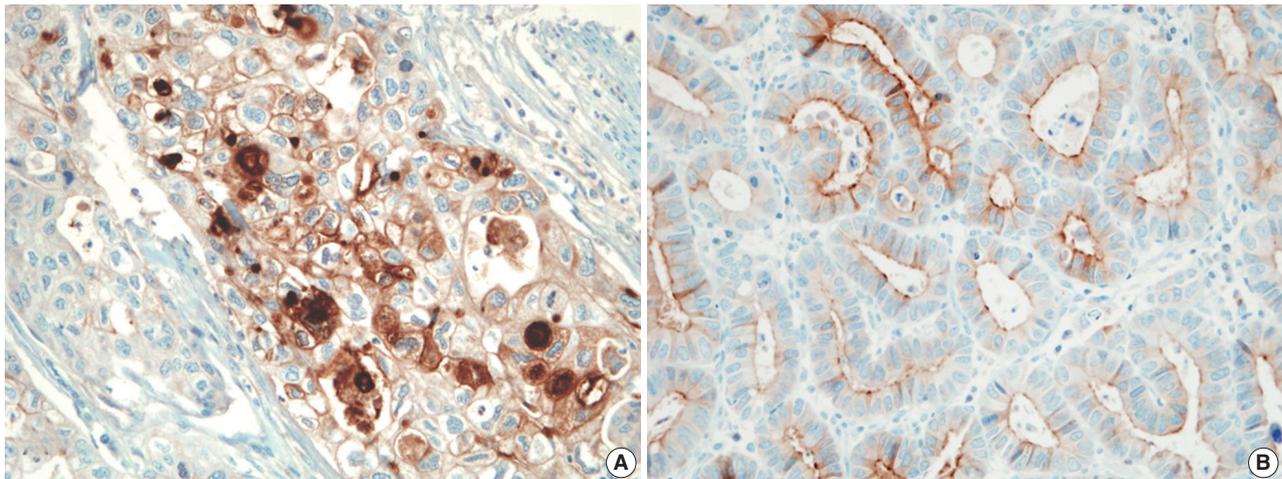
Fig. 1. The tumor cell membrane was stained with mesothelin in gastric adenocarcinomas, showing membranous (A) or apical patterns (B).
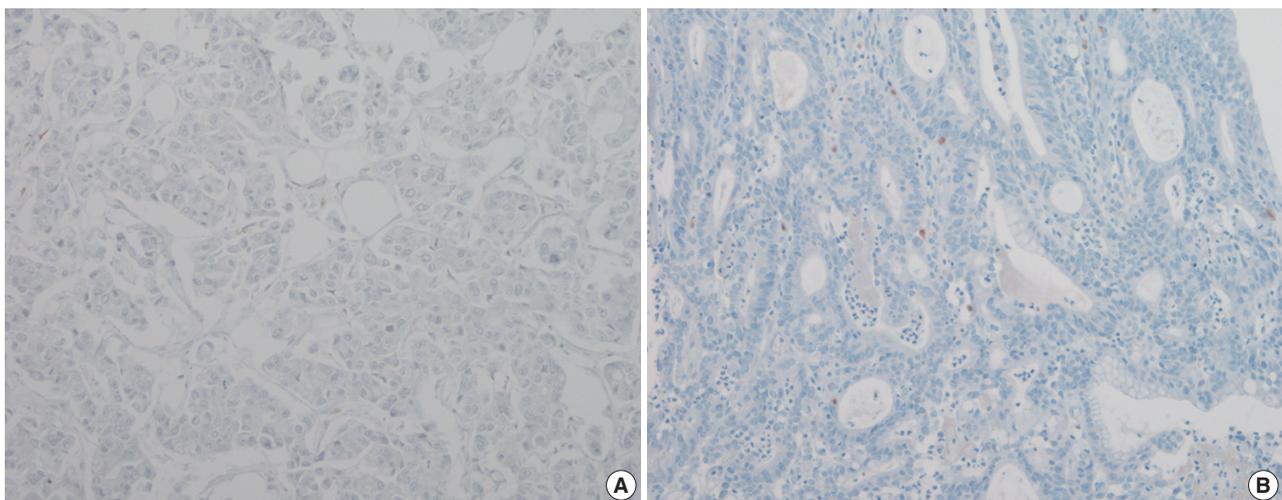
Fig. 2. Wilms tumor protein 1 (A) and calretinin (B) are not expressed in gastric adenocarcinoma.

RESULTS

Mesothelin, calretinin, and WT1 expression in gastric adenocarcinoma

The pattern of mesothelin expression was characterized by a diffuse and strong pattern with thick, membranous staining, especially along the apical cell membrane (Fig. 1). Some tumor cells showed cytoplasmic staining. Mesothelin was positively stained in 30 cases (25.6%). Staining only along the apical cell membrane was observed in 20 cases. In the remaining 10 cases, the staining was mixed membranous and cytoplasmic. Twenty-two cases exhibited cytoplasmic staining, which were considered negative. None of the 117 gastric adenocarcinomas (100%) stained for calretinin or WT1 (Fig. 2). In normal gastric mucosa, mesothelin, calretinin, and WT1 were not expressed.
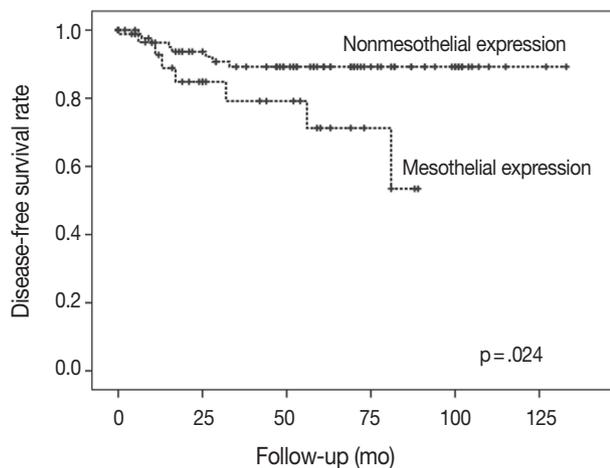
Fig. 3. The group with nonmesothelial expression had significantly better survival than the group with mesothelin expression.

Association of mesothelin expression with clinicopathological variables

The associations between mesothelin expression and clinicopathological characteristics in gastric adenocarcinoma are shown in Table 1. Mesothelin expression was related to increased depth of invasion (p = .002), lymph node metastasis (p = .013), presence of lymphovascular invasion (p = .015), and presence of perineural invasion (p = .004).

Mesothelin expression and DFS

There was a difference in DFS between patients with mesothelin expression and patients with no mesothelin expression (median, 29 months vs 57 months). Patients with mesothelin expression had significant shorter DFS rate compared with those with no mesothelin expression (p = .024) (Fig. 3).

Cox proportional hazards regression model was used to evaluate the association between mesothelin expression and DFS. On univariate analysis, factors associated with DFS included mesothelial expression, depth of invasion, and perineural invasion (Table 2). However, multivariate Cox regression analysis suggested that mesothelin expression was not an independent prognostic factor (Table 2).

DISCUSSION

In this study, we obtained clinicopathological data related to expression of mesothelin, one of the three mesothelial markers. Approximately 25.6% of gastric adenocarcinomas showed positive staining for mesothelin. Importantly, we found that mesothelin expression was related to advanced disease and DFS. Therefore, mesothelin might be a promising therapeutic target in patients with advanced disease.

Mesothelin is a 40-kDa cell surface glycoprotein.[17] Its gene

Table 2. Univariate and multivariate analyses for disease-free survival

Variable		Univariate			Multivariate		
		HR	95% CI	p-value	HR	95% CI	p-value
Stage	EGC	1	1.152–5.321	.001	1	2.036–9.922	.004
	AGC	3.240			3.521		
Lymphovascular invasion	Absent	1	0.572–2.801	.075	-	-	-
	Present	1.283			-		
Lymph node metastasis	Absent	1	0.961–5.027	.058	-	-	-
	Present	1.502			-		
Perineural invasion	Absent	1	1.254–6.455	.001	1	0.356–9.616	.475
	Present	2.428			1.847		
Mesothelin expression	Negative	1	1.523–5.212	.019	1	0.251–2.703	.770
	Positive	2.261			1.428		

HR, hazard ratio; 95% CI, 95% confidence interval; EGC, early gastric cancer; AGC, advanced gastric cancer.

encodes a precursor protein that is cleaved by proteases to form 40-kDa mesothelin that attaches to the cell membrane and a 31-kDa cleaved fragment, which is secreted into the blood. Mesothelin is believed to be involved in cell adhesion, though its biological function is not well known. Einama *et al.*[11] have investigated mesothelin expression in gastric adenocarcinoma, focusing on localization of mesothelin expression. They found that luminal membranous expression was a significant prognostic factor in gastric cancer, while cytoplasmic expression was not significantly correlated with prognosis of gastric cancer.[13] In their study, membranous or mixed membranous and cytoplasmic expression was considered positive staining. In addition to mesothelin expression pattern, previous studies have used various scoring systems to quantify immunohistochemically observed expression of mesothelin in different tumor types.[9-12,18] Because the staining patterns of mesothelin were quite distinct, such as diffuse and strong with thick, membranous staining or no staining, we considered ≥5% staining of any intensity as positive, using the cut-off described by Baba *et al.*[12] Thus, the rate of mesothelin expression in gastric adenocarcinomas was 25.6% in our study. However, the rate of mesothelin expression differed between studies. Taliano *et al.*[14] reported that mesothelin was expressed in 59% of gastric adenocarcinomas. Lugli *et al.*[13] found that mesothelin expression was 15.4% in the membrane. These differences between our results and prior studies may be attributed to the different sample sizes and distribution as well as different staining protocols and antibodies used.

Mesothelin is expressed in several cancers, including epithelioid mesotheliomas, pancreatic and biliary adenocarcinomas, and ovarian and gastric cancers.[11,12,18-20] The relationships between mesothelin expression and tumor aggressiveness and clinical outcomes have been studied in various cancers. The results of this study confirmed that mesothelin expression was strongly associated with depth of invasion, lymph node metastasis, and presence of lymphovascular and perineural invasion. Similarly, Baba *et al.*[12] reported that mesothelin expression was correlated with greater nodal involvement and deeper invasion. Einama *et al.*[11] also reported that mesothelin expression was associated with clinical stage, lymphatic and blood vessel permeation, and recurrence. However, previous studies have reported conflicting results regarding the relationship between mesothelin expression and clinical outcome. Kawamata *et al.*[9] reported that a mesothelin-positive group showed poor prognosis in several gastrointestinal malignancies, including biliary adenocarcinoma. In contrast, Yen *et al.*[10] demonstrated that mesothelin expression was associated with prolonged survival in patients with advanced stage

epithelial ovarian carcinomas. For patients with gastric cancer, studies of the association between mesothelin expression and survival have shown different results. Baba *et al.*[12] found that mesothelin expression was correlated with prolonged patient survival in AGC. In addition to our study, a previous study has reported that mesothelin expression was correlated with poor overall survival.[11]

Although the mechanism by which mesothelin affects survival of patients with gastric cancer remains unclear, discrepancies between studies may be related to the biological role of mesothelin. Recent studies have reported that mesothelin plays a role in tumorigenesis by increasing cellular proliferation and migration. Servais *et al.*[21] found that mesothelin promoted tumor cell invasion by increasing matrix metalloprotease-9 secretion in mesothelioma. Additionally, Rump *et al.*[22] observed that mesothelin bound to carbohydrate antigen 125/MUC16 with very high affinity and may contribute to the adhesion of tumor cells in peritoneal metastasis. Bharadwaj *et al.*[23] reported that mesothelin expression increased resistance to tumor necrosis factor-α–induced apoptosis through Akt/phosphoinositide 3-kinase/nuclear factor κB activation. Mesothelin-overexpressing pancreatic cancer cell lines showed increased cyclin E and cyclin-dependent kinase 2 expression, resulting in increased cell proliferation and cell cycle progression.[24] These findings suggest significant interplay between mesothelin-related proteins and/or genes and aggressive tumor behavior.

Increasing evidence has suggested that mesothelin is a strongly immunogenic protein. Thomas *et al.*[25] reported that pancreatic cancer patients who were vaccinated with granulocyte macrophage colony-stimulating factor–secreting pancreatic tumor cells showed a strong mesothelin-specific CD8+ T-cell immune response. Ho *et al.*[26] detected mesothelin-specific IgG antibodies in the serum of patients with advanced mesothelioma and ovarian cancer. These results indicate that mesothelin-specific B-cell and T-cell responses against mesothelin-expressing carcinoma cells contribute to overall prolonged survival. The reason for differences in clinical outcomes among various carcinomas remains unclear, and additional studies are necessary to explain these discrepancies.

Both silencing of mesothelin for inhibited cell proliferation and migration and increased mesothelin-specific immune response may be correlated with the control of tumor progression. Thus, mesothelin has been evaluated as a marker for biological malignancy from both genetic and immunological perspectives. Mesothelin is a promising target for immune-based therapy, specifically for mesothelioma and pancreatic and ovarian cancers.

Several ongoing clinical trials in patients with these carcinomas have revealed a beneficial effect.[27,28] For example, SS1P is a representative recombinant antimesothelin immunotoxin, and the therapy response rate of SS1P combined with chemotherapy exhibits good response.[28]

We hypothesized that calretinin and WT1 would show positive reactivity in gastric adenocarcinoma.[13-15] No prior studies have evaluated WT1 expression in gastric adenocarcinoma. A few studies have reported calretinin expression in a wide variety of poorly differentiated carcinomas, including gastric adenocarcinoma.[13] In this study, we found that neither calretinin nor WT1 was expressed. This discrepancy from previous study[13] is likely related to technique sensitivity, resulting in false-positive values, and may also be related to the diversity of antibodies used.

Given the conflicting results from previous investigations, we evaluated the expression pattern and prognostic value of mesothelin in gastric adenocarcinoma and the correlations of mesothelin expression with clinicopathological variables. We found that 25.6% of gastric adenocarcinomas expressed mesothelin, which was associated with poor prognosis. Our results suggest that mesothelin-targeted therapies, such as SS1P, are important alternatives for cancer patients with mesothelin expression.

Conflicts of Interest

No potential conflict of interest relevant to this article was reported.

REFERENCES

1. Ferlay J, Soerjomataram I, Dikshit R, et al. Cancer incidence and mortality worldwide: sources, methods and major patterns in GLOBOCAN 2012. Int J Cancer 2015; 136: E359-86.

2. Oh CM, Won YJ, Jung KW, et al. Cancer statistics in Korea: incidence, mortality, survival, and prevalence in 2013. Cancer Res Treat 2016; 48: 436-50.

3. Gotoda T. Endoscopic resection of early gastric cancer. Gastric Cancer 2007; 10: 1-11.

4. Oba K, Paoletti X, Bang YJ, et al. Role of chemotherapy for advanced/recurrent gastric cancer: an individual-patient-data meta-analysis. Eur J Cancer 2013; 49: 1565-77.

5. Wagner AD, Grothe W, Haerting J, Kleber G, Grothey A, Fleig WE. Chemotherapy in advanced gastric cancer: a systematic review and meta-analysis based on aggregate data. J Clin Oncol 2006; 24: 2903-9.

6. Kataoka H, Mori Y, Shimura T, et al. A phase II prospective study of the trastuzumab combined with 5-weekly S-1 and CDDP therapy for HER2-positive advanced gastric cancer. Cancer Chemother Pharmacol 2016; 77: 957-62.

7. Boku N. HER2-positive gastric cancer. Gastric Cancer 2014; 17: 1-12.

8. Ordóñez NG. Value of mesothelin immunostaining in the diagnosis of mesothelioma. Mod Pathol 2003; 16: 192-7.

9. Kawamata F, Kamachi H, Einama T, et al. Intracellular localization of mesothelin predicts patient prognosis of extrahepatic bile duct cancer. Int J Oncol 2012; 41: 2109-18.

10. Yen MJ, Hsu CY, Mao TL, et al. Diffuse mesothelin expression correlates with prolonged patient survival in ovarian serous carcinoma. Clin Cancer Res 2006; 12(3 Pt 1): 827-31.

11. Einama T, Homma S, Kamachi H, et al. Luminal membrane expression of mesothelin is a prominent poor prognostic factor for gastric cancer. Br J Cancer 2012; 107: 137-42.

12. Baba K, Ishigami S, Arigami T, et al. Mesothelin expression correlates with prolonged patient survival in gastric cancer. J Surg Oncol 2012; 105: 195-9.

13. Lugli A, Forster Y, Haas P, et al. Calretinin expression in human normal and neoplastic tissues: a tissue microarray analysis on 5233 tissue samples. Hum Pathol 2003; 34: 994-1000.

14. Taliano RJ, Lu S, Singh K, et al. Calretinin expression in high-grade invasive ductal carcinoma of the breast is associated with basal-like subtype and unfavorable prognosis. Hum Pathol 2013; 44: 2743-50.

15. Kao SC, Klebe S, Henderson DW, et al. Low calretinin expression and high neutrophil-to-lymphocyte ratio are poor prognostic factors in patients with malignant mesothelioma undergoing extrapleural pneumonectomy. J Thorac Oncol 2011; 6: 1923-9.

16. Qi XW, Zhang F, Wu H, et al. Wilms' tumor 1 (WT1) expression and prognosis in solid cancer patients: a systematic review and meta-analysis. Sci Rep 2015; 5: 8924.

17. Chang K, Pastan I. Molecular cloning of mesothelin, a differentiation antigen present on mesothelium, mesotheliomas, and ovarian cancers. Proc Natl Acad Sci U S A 1996; 93: 136-40.

18. Nomura R, Fujii H, Abe M, et al. Mesothelin expression is a prognostic factor in cholangiocellular carcinoma. Int Surg 2013; 98: 164-9.

19. Argani P, Iacubuzio-Donahue C, Ryu B, et al. Mesothelin is overexpressed in the vast majority of ductal adenocarcinomas of the pancreas: identification of a new pancreatic cancer marker by serial

analysis of gene expression (SAGE). Clin Cancer Res 2001; 7: 3862-8.

20. Hassan R, Kreitman RJ, Pastan I, Willingham MC. Localization of mesothelin in epithelial ovarian cancer. Appl Immunohistochem Mol Morphol 2005; 13: 243-7.

21. Servais EL, Colovos C, Rodriguez L, *et al*. Mesothelin overexpression promotes mesothelioma cell invasion and MMP-9 secretion in an orthotopic mouse model and in epithelioid pleural mesothelioma patients. Clin Cancer Res 2012; 18: 2478-89.

22. Rump A, Morikawa Y, Tanaka M, *et al*. Binding of ovarian cancer antigen CA125/MUC16 to mesothelin mediates cell adhesion. J Biol Chem 2004; 279: 9190-8.

23. Bharadwaj U, Marin-Muller C, Li M, Chen C, Yao Q. Mesothelin confers pancreatic cancer cell resistance to TNF-alpha-induced apoptosis through Akt/PI3K/NF-kappaB activation and IL-6/Mcl-1 overexpression. Mol Cancer 2011; 10: 106.

24. Bharadwaj U, Li M, Chen C, Yao Q. Mesothelin-induced pancreatic cancer cell proliferation involves alteration of cyclin E via activa-tion of signal transducer and activator of transcription protein 3. Mol Cancer Res 2008; 6: 1755-65.

25. Thomas AM, Santarsiero LM, Lutz ER, *et al*. Mesothelin-specific CD8(+) T cell responses provide evidence of in vivo cross-priming by antigen-presenting cells in vaccinated pancreatic cancer patients. J Exp Med 2004; 200: 297-306.

26. Ho M, Hassan R, Zhang J, *et al*. Humoral immune response to mesothelin in mesothelioma and ovarian cancer patients. Clin Cancer Res 2005; 11: 3814-20.

27. Hassan R, Ho M. Mesothelin targeted cancer immunotherapy. Eur J Cancer 2008; 44: 46-53.

28. Hassan R, Sharon E, Thomas A, *et al*. Phase 1 study of the antimesothelin immunotoxin SS1P in combination with pemetrexed and cisplatin for front-line therapy of pleural mesothelioma and correlation of tumor response with serum mesothelin, megakaryocyte potentiating factor, and cancer antigen 125. Cancer 2014; 120: 3311-9.

Comparison of the Mismatch Repair System between Primary and Metastatic Colorectal Cancers Using Immunohistochemistry

Jiyoon Jung · Youngjin Kang
Yoo Jin Lee · Eojin Kim
Bokyung Ahn · Eunjung Lee
Joo Young Kim · Jeong Hyeon Lee
Youngseok Lee · Chul Hwan Kim
Yang-Seok Chae

Department of Pathology, Korea University Anam Hospital, Seoul, Korea

Corresponding Author
Yang-Seok Chae, MD
Department of Pathology, Korea University Anam Hospital, 73 Inchon-ro, Seongbuk-gu, Seoul 02841, Korea
Tel: +82-2-920-5595
Fax: +82-2-920-6576
E-mail: chaeys21@korea.ac.kr

Background: Colorectal cancer (CRC) is one of the most common malignancies worldwide. Approximately 10%–15% of the CRC cases have defective DNA mismatch repair (MMR) genes. Although the high level of microsatellite instability status is a predictor of favorable outcome in primary CRC, little is known about its frequency and importance in secondary CRC. Immunohistochemical staining (IHC) for MMR proteins (e.g., MLH1, MSH2, MSH6, and PMS2) has emerged as a useful technique to complement polymerase chain reaction (PCR) analyses. **Methods:** In this study, comparison between the MMR system of primary CRCs and paired liver and lung metastatic lesions was done using IHC and the correlation with clinical outcomes was also examined. **Results:** Based on IHC, 7/61 primary tumors (11.4%) showed deficient MMR systems, while 13/61 secondary tumors (21.3%) showed deficiencies. In total, 44 cases showed proficient expression in both the primary and metastatic lesions. Three cases showed deficiencies in both the primary and paired metastatic lesions. In 10 cases, proficient expression was found only in the primary lesions, and not in the corresponding metastatic lesions. In four cases, proficient expression was detected in the secondary tumor, but not in the primary tumor. **Conclusions:** Although each IHC result and the likely defective genes were not exactly matched between the primary and the metastatic tumors, identical results for primary and metastatic lesions were obtained in 77% of the cases (47/61). These data are in agreement with the previous microsatellite detection studies that used PCR and IHC.

Key Words: Colorectal neoplasms; DNA mismatch repair; Microsatellite instability; Immunohistochemistry

Approximately 10%–15% of the colorectal cancer (CRC) cases have a defective DNA mismatch repair (MMR) gene.[1] As a result of these defects, microsatellites are predicted to accumulate during cell division.[2] Microsatellite instability (MSI) has received attention since the discovery of repetitive sequences in 1993.[3] Deficient mismatch repair (dMMR) is the molecular basis for MSI. Two distinct causal mechanisms have been identified to explain these deficiencies. One potential mechanism is germline mutations in *MLH1, MSH2, MSH6,* and *PMS2*. Approximately 3% of CRC cases are associated with germline mutations in MMR genes.[4] Lynch syndrome is caused by these germline mutations in MMR genes; it is associated with extraintestinal manifestations, including cancers in the endometrium, ovary, stomach, hepatobiliary tract, and urinary tract.[5] The other mechanism is related to the methylation of CpG (cytosine-phosphate-guanine) islands of *MLH1*.[1,5] This MSI phenotype holds clinical importance, as it provides predictive value with respect to prognosis and response to chemotherapy.[6]

Many groups have examined the correlation in MSI status between primary and secondary CRCs. In many cases, MSI is found in the primary tumor, but not in the metastatic lesion, suggesting that MMR deficiencies contribute to tumor initiation, rather than progression.[2] Although MSI groups show favorable outcomes compared to the microsatellite stable groups in primary CRCs, little is known about the frequency of MSI and its importance in secondary CRCs.

The current gold standard for assessing DNA MMR competency is polymerase chain reaction (PCR).[7] However, immunohistochemical staining (IHC) for DNA MMR proteins (e.g., MLH1, MSH2, MSH6, and PMS2) has emerged as a useful complementary technique.[8] Compared to PCR, the sensitivity of IHC is as high as 93% and the specificity is close to perfect.[5,9,10]

MMR proteins recognize and correct insertion/deletion loops, base mismatches, and damaged bases.[11] They can interact as heterodimeric complexes: MSH2-MSH6, MSH2-MSH3, MLH1-PMS2, MLH1-PMS1, or MLH1-MSH3.[6] In 1996, the expression

of the MSH2 antibody was first reported and developed as a marker using fresh-frozen tissues.[12] Later, antibodies against MLH1 and MSH2 became applicable to paraffin embedded tissues.[13] Since then, numerous MMR IHC studies have been performed.

Shia et al.[10] showed that the overall sensitivity of IHC for the prediction of germline mutations is 79%, with a specificity of 89%. In another study, IHC correctly predicted the MSI status in 76% of cases, with a specificity of 100%.

The aim of this study was to compare the MMR system between primary CRCs and paired liver and lung metastatic lesions using IHC and to determine whether there is a correlation with the clinical outcomes.

MATERIALS AND METHODS

Patient population

The database of the Korea University Anam Hospital, Seoul, Korea was searched for all CRC patients who underwent surgical resection between 2002 and 2013. A cohort of patients who underwent hepatic resection or pulmonary resection for CRC metastases was also identified. Patients with available tissue samples were analyzed for MMR using IHC. Patients who received neoadjuvant chemoradiotherapy were excluded. A total of 61 cases were included in the study. The corresponding clinical data were obtained from a retrospective review of patient records. Follow-up survival data were also obtained.

Immunohistochemistry

To characterize the MMR system, IHC was performed using 4-μm-thick paraffin tissue sections. The manufacturers and incubation conditions for primary antibodies are summarized in Table 1. Sections were incubated for 15 minutes with antibodies against MLH1 protein (1:200, ES05, Leica, Newcastle upon Tyne, UK), MSH2 protein (1:100, G219-1129, Cell Marque, Rocklin, CA, USA), MSH6 protein (1:50, 44, Cell Marque), and PMS2 (1:50, MRQ-28, Cell Marque).

Tumors were considered deficient in MLH1, MSH2, MSH6, and PMS2 expression when there was a complete absence of detectable nuclear staining in neoplastic cells. Intact nuclear staining of the adjacent non-neoplastic epithelium, stromal cells, or lymphocytes served as an internal positive control (Appendix 1).

Whole sections were stained and reviewed for cases that showed a loss of expression on a microarray.

Statistical analysis

Clinicopathological features, including age, size, gender, site of primary CRC, lymph node status, lymphovascular invasion, perineural invasion, carcinoembryonic antigen (CEA) levels at diagnosis, T category, tumor differentiation, and metastatic site, were compared between dMMR and proficient MMR (pMMR) patients used Fisher exact, χ^2 tests and Mann-Whitney test. Overall survival was calculated according to the Kaplan-Meier method. All statistical tests were implemented in SPSS ver. 21 (IBM Corp., Armonk, NY, USA).

This case was reviewed by the Institutional Review Board of Korea University Medical Center (AN15349-00).

RESULTS

Clinicopathological features

The clinicopathological features of 61 patients included in the study are detailed in Table 1. The mean patient age was 58 years (range, 31 to 78 years); 26% of the patients were female and 73% were male. The mean tumor size was 5.4 cm (range, 1.8 to 15 cm). The anatomical location of the primary tumor was classified as left (rectum, rectosigmoid colon, splenic flexure, and descending colon) or right side (ascending colon, hepatic flexure, and cecum). In total, 55/61 (90.1%) were T3 cancers that invade through the muscularis propria into pericolorectal tissues. Moderately differentiated CRCs accounted for 44/61 (72.1%).

There were two patients in their early thirties. Neither patient had a family history of cancer.

Relationship between MMR status and clinicopathological features

Using Fisher exact, χ^2 tests and Mann-Whitney tests to analyze the relationship between MMR status and clinicopathological features, significant relationships were not detected for age (p = .58), size (p = .14), sex (p = .34), site (p = .96), T stage (p = .36), tumor differentiation (p = .32) lymph node metastasis (p = .13), lymphovascular invasion (p = .75), perineural invasion (p = .30), or CEA level (p = .49).

Association between primary and metastatic tumors

A total of 61 CRCs were assessed using a tissue microarray. The results are detailed in Tables 2 and 3.

Of the primary tumors, 7/61 (11.4%) showed a dMMR system based on IHC, while secondary tumors showed a deficiency in 13/61 cases (21.3%). In total, 44 cases showed proficient expression of MMR in both primary and metastatic lesions. Three cases

Table 1. Clinicopathological features of the entire cohort

Variable	MMR-proficient (n = 44)	MMR-deficient (n = 17)	χ^2	p-value
Age at diagnosis (yr)	54 (31–78)	55 (41–74)	-	.58[a]
Size (cm)	5.1 (1.8–11.0)	6.1 (1.8–15.0)	-	.14[a]
Sex			0.897	.34[b]
Male	31	14		
Female	13	3		
Anatomic location			0.002	.96[b]
Right	8	3		
Left	36	14		
T stage			2.074	.36[b]
T1	0	0		
T2	4	0		
T3	39	16		
T4	1	1		
Differentiation			3.498	.32[b]
Well	12	3		
Moderate	31	13		
Poor	1	0		
Mucinous	0	1		
Lymph node metastasis			2.273	.13[b]
No	19	11		
Yes	25	6		
Lymphovascular space invasion			0.123	.75[b]
No	33	12		
Yes	11	5		
Perineural invasion			1.082	.30[b]
No	37	16		
Yes	7	1		
CEA at diagnosis (ng/mL)	37.1 (0.2–1,042.8)	63.4 (1.1–852.5)	-	.49[a]
Metastastic site				
Liver	21	15		
Lung	23	2		

Values are presented as mean (range) or number.
MMR, mismatch repair; CEA, carcinoembryonic antigen.
[a]Mann-Whitney test; [b]Fisher exact or χ^2 tests.

Table 2. MMR status based on the IHC analysis for primary and metastatic tumors

Metastasis	Primary		Total
	Intact	Loss	
Intact	44	4	48
Loss	10	3	13
Total	54	7	

MMR, mismatch repair; IHC, immunohistochemical staining.

Table 3. Immunohistochemical patterns of mismatch repair deficiencies

Loss	Tumor	
	Primary	Metastatic
MLH1/PMS2	0	0
MSH2/MSH6	6	8
MSH6 only	0	2
PMS2 only	1	1
Combined[a]	0	3

[a]Combined: MSH6 + PMS2 (1 case), MLH1 + MSH6 + PMS2 (1 case), MSH2 + PMS2 (1 case).

showed deficiencies in both the primary and the paired metastatic lesions. In 10 cases, proficient expression was found in the primary lesions, but not in the corresponding metastatic lesions. In four cases, proficient expression was detected in the secondary tumor, but not in the primary tumor.

Survival analysis

In total, 14 patients died of cancer, and the median survival was 33 months from the date of initial diagnosis.

A survival analysis was performed assuming that the primary and metastatic tumors showing intact expression using IHC
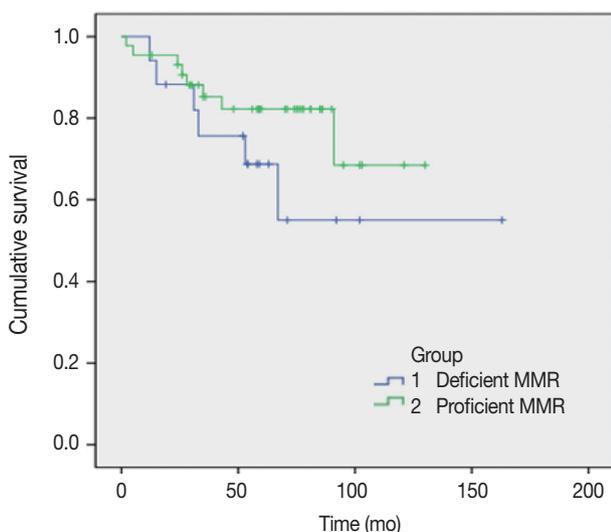
Fig. 1. Overall survival for the entire cohort (proficient mismatch repair [MMR] and deficient MMR patients).

group are pMMR and the loss of expression in either tumor indicates dMMR (Fig. 1). This result was not statistically significant (log-rank test, p = .22), but the pMMR group showed a more favorable prognosis compared to the dMMR group.

DISCUSSION

In this study, MMR proteins were evaluated by IHC for the following reasons: (1) IHC is less time consuming than PCR, (2) is easier to implement,[14] and (3) enables the simultaneous identification of affected MMR genes.[5]

However, the interpretation of IHC results requires caution for the following reasons. First, it is well known that the IHC staining patterns for MSH6 IHC are variable.[8] Second, stainability is dependent on tissue handling, including fixation and analytical variables. For instance, tissue hypoxia and delayed fixation reduce the sensitivity of detection of MMR gene expression or suppress MMR. Fewer proliferative cells result in lower levels of staining.[15] Third, some *MLH1* mutation-positive cases or even cases with *MLH1* promoter methylation show false-positive nuclear staining.[6,9] A missense mutation or an in-frame insertion/deletion mutation in *MLH1* does not affect MLH1-PMS2 interactions, and thus the protein reacts with the antibody used for IHC. Lastly, interpretation of MMR IHC results requires consideration that the MMR proteins act as heterodimers.[6] For example, CRCs that show loss of MLH1 and PMS2 expression, but intact MSH2 and MSH6 expression indicate an MLH1 deficiency. The loss of PMS2 expression results from *MLH1* mutations.

In this study, our major interest was investigating the con-

cordance in MMR deficiencies between the primary CRCs and its corresponding metastases.

Haraldsdottir *et al.*[16] reported matching IHC results between the primary tumor and metastatic tissue for all cases examined. However, Agoston *et al.*[17] found discordance in the MMR status between primary tumors and metastases in 20.2% of cases. Haddad *et al.*[18] found a very low frequency of MSI using PCR in resected CRC hepatic metastases in 190 patients. Unlike in primary CRCs, the rate of MSI in resectable CRC hepatic metastases is approximately 2.5%. Two potential explanations were proposed to explain this discrepancy. First, high-frequency MSI primary CRCs do not frequently metastasize to the liver. Second, high-frequency MSI primary CRCs spread to the liver extensively and therefore are considered unresectable.[18] Previous studies suggest divergent views regarding this issue.

Of the 61 cases, 47 showed concordance in the IHC staining results between the primary and metastatic tumors. The incidence of dMMR was similar to the previously reported incidence of 10%–20%.[19] However, the incidence was somewhat different between the primary (11.5%) and the metastatic (21.3%) cancer groups. In this study, among the 36 hepatic metastatic cancers, five cases showed dMMR in primary CRCs. This frequency of approximately 14% was not as low as that reported in the previous study.

We focused on dMMR cases that showed discordance between primary and metastatic tumors. The clinicopathological features and each MMR protein expressions of the cases with either primary or metastatic dMMR are summarized in Tables 4 and 5. Except one case, 16 cases were T3 cancers. Most of the cases (16/17) presented without perineural invasion. Based on IHC, primary and metastatic lesions of all the cases showed intact MLH1 expression. In 10 cases, proficient expression was found in the primary tumor, but not in the corresponding metastatic lesions. In four cases, proficient expression was detected in the secondary tumor, but not in the primary tumor. Furthermore, the precise MMR proteins that showed a loss of expression were not exactly matched in the primary and the metastatic tumors.

To further examine the data, we divided the dMMR cases into five groups. During heterodimeric complex formation, MMR proteins change concurrently. The loss of PMS2 is followed by the loss of MLH1 expression owing to functional dimerization. Similarly, the loss of MSH2 is accompanied by the loss of MSH6 (Fig. 2). However, the loss of isolated MSH6 or PMS2 is not accompanied by MLH1 or MSH2, reflecting mutations in *MSH6* or *PMS2*.[4] Although three cases were classified as a combined group that do not belong to the above four groups, most

Table 4. Clinicopathological features of dMMR cases

Case	Sex	Age (yr)	Location	Size	T stage	LN metastases	LVI	PNI	CEA (ng/mL)	Survival time (mo)	Evolution	Metastasis
1	M	62	R	5.2	III	+	+	–	2.8	31	D	Liver
2	F	46	R	2.5	IV	–	–	–	2.9	163	A	Liver
3	M	61	R	5	III	–	–	–	3.3	102	A	Liver
4	M	49	RS	5	III	+	+	–	7	53	D	Liver
5	M	74	S	8.8	III	–	–	–	1.2	54	A	Liver
6	F	67	S	1.8	III	–	+	+	3.6	71	A	Liver
7	M	53	S	7	III	–	–	–	7.8	59	A	Liver
8	F	41	As	15	III	–	–	–	4.4	15	D	Liver
9	M	58	S	3.5	III	+	–	–	2.7	58	A	Liver
10	M	57	Hf	7.5	III	–	–	–	852.5	54	A	Liver
11	M	57	RS	6	III	–	–	–	124.5	63	A	Liver
12	M	64	S	6.3	III	+	–	–	2.22	92	A	Liver
13	M	59	As	3	III	–	+	–	1.1	33	D	Liver
14	M	67	R	5.5	III	+	–	–	11.4	12	D	Liver
15	M	54	S	7.5	III	–	–	–	2	19	A	Liver
16	M	64	R	6.5	III	+	–	–	13.7	67	D	Lung
17	M	68	Sf	8	III	–	+	–	34.3	52	A	Lung

dMMR, deficient mismatch repair; LN, lymph node; LVI, lymphovascular invasion; PNI, perineural invasion; CEA, carcinoembryonic antigen; M, male; R, rectum; +, present; –, absent; D, death; F, female; A, alive; RS, rectosigmoid colon; S, sigmoid colon; As, ascending colon; Hf, hepatic flexure; Sf, splenic flexure.

Table 5. MMR protein expression status of primary and metastatic colorectal adenocarcinomas in dMMR cases

Case	MLH1 (P/M)	MSH2 (P/M)	MSH6 (P/M)	PMS2 (P/M)	MMR (P/M)
1	I/I	I/I	I/L	I/L	Pr/De
2	I/I	L/I	L/I	I/I	De/Pr
3	I/I	I/I	I/L	I/I	Pr/De
4	I/I	I/L	I/L	I/I	Pr/De
5	I/I	I/L	I/I	L/I	De/De
6	I/I	L/I	I/I	I/I	De/Pr
7	I/I	I/I	I/I	I/L	Pr/De
8	I/I	L/L	L/L	I/I	De/De
9	I/I	I/L	I/L	I/I	Pr/De
10	I/L	I/I	I/L	I/I	Pr/De
11	I/I	I/L	I/L	I/I	Pr/De
12	I/I	L/L	I/L	I/L	De/De
13	I/I	I/L	I/I	I/I	Pr/De
14	I/I	I/L	I/I	I/I	Pr/De
15	I/I	I/L	I/L	I/I	Pr/De
16	I/I	L/I	L/I	I/I	De/Pr
17	I/I	L/I	L/I	I/I	De/Pr

P, primary; M, netastatic; MMR, mismatch repair; I, intact; L, loss; Pr, proficient; De, deficient.

of the dMMR cases fit the classification, indicating that the IHC expression is consistent.

MLH1 mutations are the most common type among the MMR genes. However, the detected loss of the MLH1 protein was significantly less frequent than the loss of the MSH2 protein in this study. As stated above, we attributed this difference to the IHC technique. Most mutations in *MSH2* result in truncated proteins, which consequently showed a loss of expression in IHC analyses. However, *MLH1* mutations are non-functional missense mutations, and mutated-*MLH1* cases also show profi-

cient expression.[15] A meta-analysis showed that using IHC, only 74% of MLH1 losses were detected in the *MLH1* mutation-positive cases, compared to the 91% detected using MSI testing. However, *MSH2* mutations could be detected in up to 94% of the *MSH2* mutation-positive cases by IHC.[9] We infer that there may be false-positive MLH1 cases, and additional PCR studies are needed to identify the precise *MLH1* mutations.

In our study, cases were considered deficient if any target locus (e.g., MLH1, MSH2, MSH6, or PMS2) was not expressed. This is a limitation of our study, and variable patterns could lead to

erroneous interpretations. Shia et al.[8] analyzed MSH6 using IHC and showed limited staining in the MLH1/PMS2-deficient patients. In one case, we detected the losses of MLH1, MSH6, and PMS2 expression, suggesting a similar scenario.

Some cases showed a loss of MSH2 expression, but intact MSH6 expression. We attributed this discordance in IHC results to the variable reactivity and subjective data interpretations. Further evaluation by PCR is needed to obtain more definitive results.

All cases received adjuvant chemotherapy after resection of the primary tumor, because all cases included in this study were stage IV. Most of the patients (56 cases) were treated with FOLFOX regimens (combination of folic acid, 5-fluorouracil
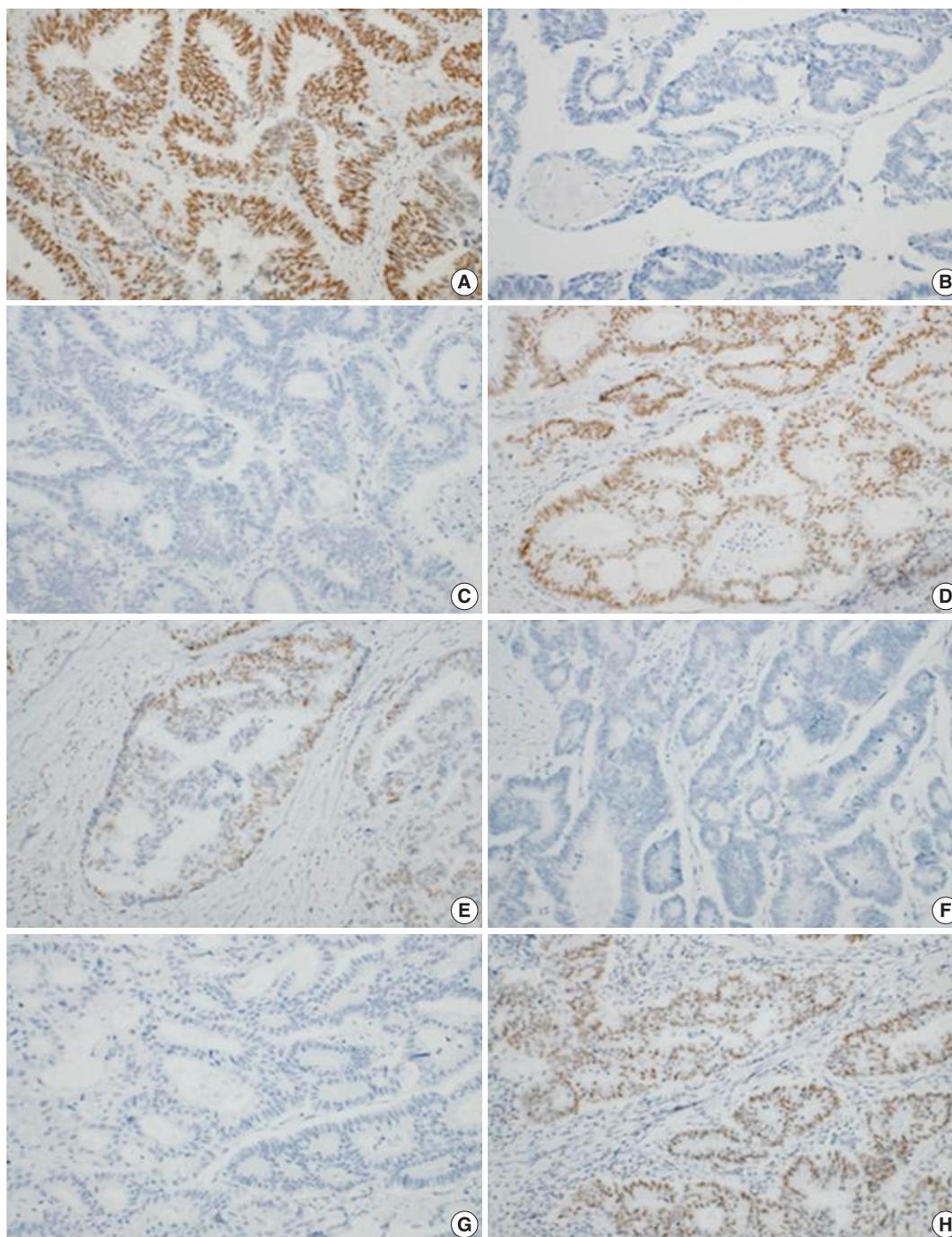

Fig. 2. Immunohistochemical analyses of primary colorectal cancer for MLH1 (A), MSH2 (B), MSH6 (C), and PMS2 (D). Immunohistochemical analyses of metastatic colorectal cancer for MLH1 (E), MSH2 (F), MSH6 (G), and PMS2 (H). A lack of staining for MSH2 and MSH6 indicates a primary defect in MSH2, with a secondary loss of MSH6 expression.

[5-FU] and oxaliplatin). Two cases were treated with leucovorin and 5-FU without oxaliplatin. Three cases were treated only with 5-FU–based chemotherapy. Among the 61 cases, 50 cases received chemotherapy before metastatectomy, wheres 11 cases received chemotherapy after metastatectomy. Of the 50 cases that received chemotherapy before metastatectomy, 11 cases (22%) showed discordance in IHC. In seven cases, proficient expression was found in the primary lesions, but not in the corresponding metastatic lesions. We assume that these losses of expression could be associated with chemotherapy-related effect.

MMR status was not a significant predictive marker in metastatic CRCs. This finding concurs with the results of previous studies.[20] Since all cases were stage IV tumors, the low survival rates were expected.

Despite these limitations, we detected a correlation between the MMR status of primary and metastatic CRCs using only IHC. These findings may improve our understanding of the metastatic processes in CRC patients. Further research should focus on the modifications in the biological and biochemical properties of DNA MMR proteins during metastatic processes.

Conflicts of Interest

No potential conflict of interest relevant to this article was reported.

REFERENCES

1. Kanthan R, Senger JL, Kanthan SC. Molecular events in primary and metastatic colorectal carcinoma: a review. Patholog Res Int 2012; 2012: 597497.

2. Yim KL. Microsatellite instability in metastatic colorectal cancer: a review of pathology, response to chemotherapy and clinical outcome. Med Oncol 2012; 29: 1796-801.

3. Aaltonen LA, Peltomäki P, Leach FS, et al. Clues to the pathogenesis of familial colorectal cancer. Science 1993; 260: 812-6.

4. Geiersbach KB, Samowitz WS. Microsatellite instability and colorectal cancer. Arch Pathol Lab Med 2011; 135: 1269-77.

5. Shia J. Evolving approach and clinical significance of detecting DNA mismatch repair deficiency in colorectal carcinoma. Semin Diagn Pathol 2015; 32: 352-61.

6. Vilar E, Gruber SB. Microsatellite instability in colorectal cancer: the stable evidence. Nat Rev Clin Oncol 2010; 7: 153-62.

7. Chen S, Watson P, Parmigiani G. Accuracy of MSI testing in predicting germline mutations of MSH2 and MLH1: a case study in Bayesian meta-analysis of diagnostic tests without a gold standard.

8. Shia J, Zhang L, Shike M, et al. Secondary mutation in a coding mononucleotide tract in MSH6 causes loss of immunoexpression of MSH6 in colorectal carcinomas with MLH1/PMS2 deficiency. Mod Pathol 2013; 26: 131-8.

9. Zhang L. Immunohistochemistry versus microsatellite instability testing for screening colorectal cancer patients at risk for hereditary nonpolyposis colorectal cancer syndrome. Part II. The utility of microsatellite instability testing. J Mol Diagn 2008; 10: 301-7.

10. Shia J, Klimstra DS, Nafa K, et al. Value of immunohistochemical detection of DNA mismatch repair proteins in predicting germline mutation in hereditary colorectal neoplasms. Am J Surg Pathol 2005; 29: 96-104.

11. Poulogiannis G, Frayling IM, Arends MJ. DNA mismatch repair deficiency in sporadic colorectal cancer and Lynch syndrome. Histopathology 2010; 56: 167-79.

12. Leach FS, Polyak K, Burrell M, et al. Expression of the human mismatch repair gene hMSH2 in normal and neoplastic tissues. Cancer Res 1996; 56: 235-40.

13. Thibodeau SN, French AJ, Roche PC, et al. Altered expression of hMSH2 and hMLH1 in tumors with microsatellite instability and genetic alterations in mismatch repair genes. Cancer Res 1996; 56: 4836-40.

14. Lindor NM, Burgart LJ, Leontovich O, et al. Immunohistochemistry versus microsatellite instability testing in phenotyping colorectal tumors. J Clin Oncol 2002; 20: 1043-8.

15. Shia J, Holck S, Depetris G, Greenson JK, Klimstra DS. Lynch syndrome-associated neoplasms: a discussion on histopathology and immunohistochemistry. Fam Cancer 2013; 12: 241-60.

16. Haraldsdottir S, Roth R, Pearlman R, Hampel H, Arnold CA, Frankel WL. Mismatch repair deficiency concordance between primary colorectal cancer and corresponding metastasis. Fam Cancer 2016; 15: 253-60.

17. Agoston EI, Baranyai Z, Dede K, et al. Occurrence, intratumoral heterogeneity, prognostic and predictive potential of microsatellite instability following surgical resection of primary colorectal carcinomas and corresponding liver metastases. Orv Hetil 2015; 156: 1460-71.

18. Haddad R, Ogilvie RT, Croitoru M, et al. Microsatellite instability as a prognostic factor in resected colorectal cancer liver metastases. Ann Surg Oncol 2004; 11: 977-82.

19. Koopman M, Kortman GA, Mekenkamp L, et al. Deficient mismatch repair system in patients with sporadic advanced colorectal cancer. Br J Cancer 2009; 100: 266-73.

20. Kim ST, Lee J, Park SH, et al. The effect of DNA mismatch repair (MMR) status on oxaliplatin-based first-line chemotherapy as in recurrent or metastatic colon cancer. Med Oncol 2010; 27: 1277-85.

Biostatistics 2005; 6: 450-64.
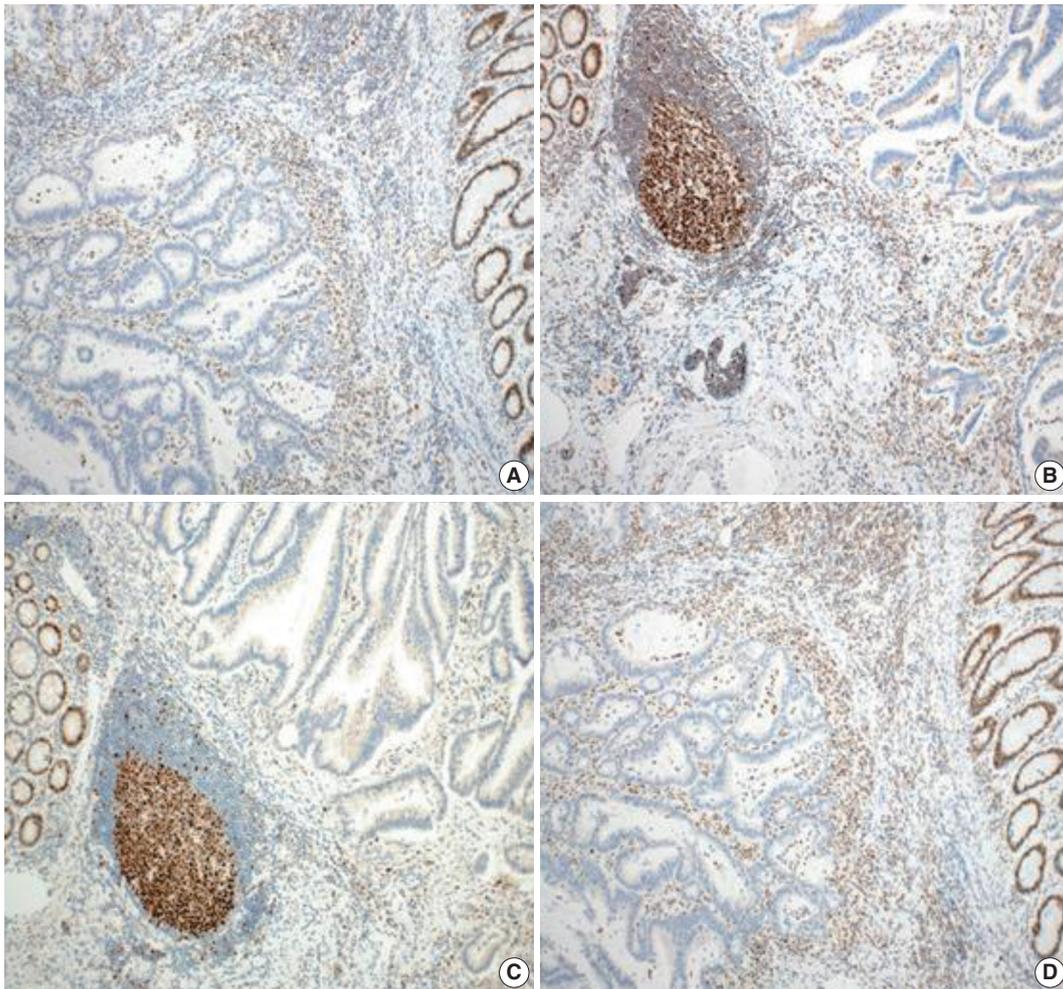
Appendix 1. Absence of immunohistochemical staining in tumor epithelium for MLH1 (A), MSH2 (B), MSH6 (C), and PMS2 (D). Note the presence of tumor-infiltrating lymphocytes and adjacent normal mucosal tissue that stain positively for each immunohistochemical staining.

Current Status of Pathologic Examinations in Korea, 2011–2015, Based on the Health Insurance Review and Assessment Service Dataset

Sun-ju Byeon

Department of Pathology, Asan Medical Center, University of Ulsan College of Medicine, Seoul, Korea

Corresponding Author
Sun-ju Byeon, MD
Department of Pathology, Asan Medical Center, University of Ulsan College of Medicine, 88 Olympic-ro 43-gil, Songpa-gu, Seoul 05505, Korea
Tel: +82-2-3010-1494
Fax: +82-2-472-7898
E-mail: byeon.sunju@welovedoctor.com

Background: Pathologic examinations play an important role in medical services. Until recently, the overall status of pathologic examinations in Korea has not been identified. I conducted a nationwide survey of pathologic examination status using the insurance reimbursements (IRs) dataset from the Health Insurance Review and Assessment Service (HIRA). The aims of this study were to estimate current pathologic examination status in Korea and to provide information for future resource arrangement in the pathology area. **Methods:** I asked HIRA to provide data on IR requests, including pathologic examinations from 2011 to 2015. Pathologic examination status was investigated according to the following categories: annual statistics, requesting department, type of medical institution, administrative district, and location at which pathologic examinations were performed. **Results:** Histologic mapping, immunohistochemistry, and cervicovaginal examinations have increased in the last 5 years. Internal medicine, general surgery, obstetrics/gynecology, and urology were the most common medical departments requesting pathologic examinations. The majority of pathologic examinations were frequently performed in tertiary hospitals. About 60.3% of pathologic examinations were requested in medical institutions located in Seoul, Gyeonggi-do, and Busan. More than half of the biopsies and aspiration cytologic examinations were performed using outside services. The mean period between IR requests and 99 percentile IR request completion inspections was 6.2 months. **Conclusions:** This survey was based on the HIRA dataset, which is one of the largest medical datasets in Korea. The trends of some pathologic examinations were reflected in the policies and needs for detailed diagnosis. The numbers and proportions of pathologic examinations were correlated with the population and medical institutions of the area, as well as patient preference. These data will be helpful for future resource arrangement in the pathology area.

Key Words: Insurance; Pathology, surgical; Cytological pathology; Reimbursement

Pathologic examinations play an important role in medical services. Until recently, overall pathologic examination status in Korea has not been investigated. Understanding the current pathologic examination status is important to establishing future plans for resource arrangement. Byeon and Kim[1] reported the estimated pathologic examination status in Korea using the Health Insurance Review and Assessment Service (HIRA)–National Patient Sample (NPS). Because the HIRA-NPS data was statistically extracted (selection probability, 0.03), some amount of statistical error is inevitable.[2] The current study is a follow-up study using the raw dataset from HIRA. The HIRA dataset did not contain any rejected inspections of insurance reimbursement (IR) requests or new diagnostic techniques that were not approved by various government organizations. However, this dataset is one of the largest medical datasets and it best reflects the current pathologic examination status in Korea.

The aims of this study are to estimate the current pathologic examination status according to multiple parameters in Korea, to provide information for future resource arrangement in the pathology era, and to compare differences between NPS and the raw data.

MATERIALS AND METHODS

I requested HIRA to provide the IRs for various pathologic examinations (Table 1) from 2011 to 2015 (data extraction was performed in May 2016). The HIRA provided the data after anonymizing the patient identification numbers and hospital identification numbers. Primary data processing was performed using the R Statistical Software (Foundation for Statistical Computing, Vienna, Austria) ver. 3.2.3 in a remote access system for HIRA. Secondary data processing was performed using the R

Table 1. Pathologic examination codes using in this study

Main category	Subcategory	Claim codes
Biopsy	1–3 pieces/4–6 pieces/7–9 pieces/10–12 pieces/ more than 13 pieces	C5911/C5912/C5913/C5914/C5915
Non-maligGro	NPB≤6/NPB≥7	C5916/C5917
MaligGro LND	NPB≤20/NPB≥21	C5918/C5919
MaligGro LNDX	NPB≤15/NPB≥16	C5500/C5504
MAPPING	LND/LNDX	C5505/C5508
FS	1–2 specimens/3–6 specimens/7–10 specimens/ equal and more than 11 specimens	C5511/C5512/C5513/C5514
BONE	-	C5520
SPECIAL	Reticulin/Massons' Trichrome/others	C5531/C5532/C5533
IF	IgG/IgA/IgM/IgE/C3/C4/HBsAg/fibrinogen/others	C5541/C5542/C5543/C5544/C5545/C5549/C5546/ C5547/C5548
EM	-	C5550
ENZYME	ATPase-pH 9.4/ATPase-pH 4.9/NADH/acetylcholinesterase/ chloroacetate esterase/others	C5561/C5562/C5563/C5564/C5565/C5566
Etc.	Et cetera	-
IHC	Interpretation by qualified doctor	C5575006
	Interpretation by non-qualified doctor	C5575
	HR	C5590
	EGFR pharmDx kit	CZ503006
	Morphometric Analysis	CY552
CERVIX	Smear/L-based	C5920/CX541
BFC	General/using cytospin examination/L-based	C5930/C5931/CZ521
AC	Conventional/L-AC	C5941/C5943
CB	After BFC/after AC/L-AC	C5940/C5942/C5944
HER2 (FISH)	-	C5967
HER2 (SISH)	-	CZ988
MSI test	-	CX574
OUTSIDE	-	Claim code+009 (subnumber)

Non-maligGro, resected specimen requiring gross sectioning; NPB, number of paraffin blocks; MaligGro, resected specimen for malignant tumor requiring gross sectioning; LND, with lymph node dissection; LNDX, without lymph node dissection; MAPPING, histologic mapping of tumor; FS, emergency histopathologic examination during surgery; BONE, histopathologic examination for bone; SPECIAL, special stain examinations; IF, tissue immunofluorescent microscopic examination; EM, tissue electron microscopy; ENZYME, enzyme histochemistry; IHC, immunohisto(cyto)chemistry; HR, examination of hormone receptor in tissue; CERVIX, cervicovaginal cytopathology; L-, liquid based; BFC, body fluid cytopathology; AC, aspiration cytopathology; CB, cell block; HER2 (FISH), *HER2* gene fluorescence *in situ* hybridization; HER2 (SISH), *HER2* gene silver *in situ* hybridization; MSI, microsatellite instability; OUTSIDE, outside slide interpretation.

Statistical Software ver. 3.3.1 using the t2.micro instance in the Amazon Elastic Compute Cloud (Amazon, Seattle, WA, USA). To evaluate the tendency of each pathologic examination number from 2011 to 2015, linear regression was applied. A p-value less than .05 was regarded as statistically significant.

I estimated the mean period between IR requests and completion of the IR inspections as follows. Since HIRA did not provide the exact date of completion for the IR inspections and provided their data on a monthly basisinstead, a table containing monthly pathologic examination status from January 2011 to December 2014 was formulated, as seen in Table 1 (pathologic examinations in 2015 were excluded due to incomplete IR request inspections). Using this table as the reference table, I obtained sequentially cumulative data by adding up the monthly number, thereby marking the period pertaining to the 33, 66,

and 99 percentile inspections of IR requests. Next, I made up the same table again as sequentially. I obtained the time more than 33, 66 and 99 percentile inspections of IR requests were done.

RESULTS

The abbreviations used in this study are as follows. AC, aspiration cytopathology; BFC, body fluid cytopathology; BONE, histopathologic examination for bone; CB, cell block; CERVIX, cervicovaginal cytopathology; EM, tissue electron microscopy; ENZYME, enzyme histochemistry; HER2 (FISH), *HER2* gene fluorescence *in situ* hybridization; HER2 (SISH), *HER2* gene silver *in situ* hybridization; HR, examination of hormone receptor in tissue; IF, tissue immunofluorescent microscopic examination;

IHC, immunohisto(cyto)chemistry; L-, liquid based; LND, with lymph node dissection; LNDX, without lymph node dissection; MaligGro, resected specimen for malignant tumor requiring gross sectioning; MAPPING, histologic mapping of tumor; MSI, microsatellite instability; Non-maligGro, resected specimen requiring gross sectioning; NPB, number of paraffin blocks; OUTSIDE, outside slide interpretation; SPECIAL, special stain examinations.

A summary and the details for annual pathologic examination status are given in Table 2 and Supplementary Table S1, respectively. Among the main categories, it was found that the total numbers of MAPPING, IF, EM, IHC, CERVIX, and BFC increased during 2011–2015, while the total numbers of ENZYME and CB were decreased. In more detail, the following pathologic examinations increased in 2011–2015: non-maligGro with NPB ≤6, MAPPING LND, MAPPING LNDX, Masson's trichrome stain, IF (IgG, IgA, IgM, C3, C4, fibrinogen, others), EM, IHC (interpretation by qualified doctor, HR, EGFR pharmDx kit), L-CERVIX, L-BFC, L-AC, CB after L-AC, and some of OUTSIDE (C5500009, C5912009, C5916009, C5917009). The following pathologic examinations decreased in 2011-2015: biopsy (more than 13 pieces), IF (IgE and hepatitis B surface antigen), ENZYME (acetylcholinesterase), CERVIX by smear, BFC (general), AC (conventional), and CB (AC). Note that no chloroacetate esterase examinations were performed during the last 5 years.

Most medical and dental departments requested various pathologic examinations (a summary is given in Tables 3 and 4 and the details are given in Supplementary Table S2), but the proportions were quite different. Internal medicine (13,917,799, 46.29%), general surgery (6,334,913, 21.07%), obstetrics/gynecology (3,444,796, 11.46%), and urology (1,769,651, 5.89%) were the most common medical departments (25,467,159, 84.70%) requesting pathologic examinations. These proportions were similar to those of the previous study.[1]

A summary and the details of the pathologic examination status according to type of medical institution are listed in Table 5 and Supplementary Table S3, respectively. The numbers of each type of medical institution were not included in this analysis. The majority of pathologic examinations were frequently performed in a tertiary hospital. Among the different pathologic examinations, biopsy and AC were frequently performed in clinics.

A summary and the details of the pathologic examination status according to the administrative district are listed in Tables 6, 7, and Supplementary Table S4, respectively. About 60.3% of pathologic examinations (20,787,770) were requested in medical institutions located in Seoul (12,249,590, 35.5%), Gyeonggi-do (5,517,990, 16.0%), and Busan (3,020,190, 8.8%).

A summary and the details of the pathologic examination status according to the location at which examinations were performed are listed in Table 8 and Supplementary Table S5, respectively. More than 90% of the resected specimens for malignant tumors requiring gross sectioning (MaligGro) LND, MaligGro LNDX, MAPPING, emergency histopathologic examination during surgery (FS), ENZYME, IHC, CB, and OUTSIDE were performed in their own hospitals. More than half of the biopsies and AC examinations were performed using outside services.

The mean periods between IR requests and the 33, 66, and 99 percentiles IR request inspection completions were 2.2, 2.8, and 6.2 months, respectively. The kernel density estimation plot for each percentile can be found in Fig. 1. The 95 and 99 percentile values of the period for 99 percentile IR request inspection completion were 11 and 25 months, respectively.

DISCUSSION

In this study, I investigated various pathologic examination status according to the following categories: annual statistics, requesting department, type of medical institution, administrative district, and location at which pathologic examinations were performed in Korea, 2011–2015. In the last 5 years, the total numbers of MAPPING and IHC increased. These trends reflect the need for a more accurate pathologic diagnosis. Contrary to how the number of conventional cytopathologic examinations decreased, the number of variable liquid-based cytopathologic examinations increased. After FISH and SISH based *HER2* gene examinations were approved by insurance companies in 2013, the number of *HER2* gene examinations increased. These trends reflect both insurance and public health policies.

Throughout many medical institutions in Korea, pathologists will order a large amount of pathologic examinations for diagnosis. However, only 0.04% of pathologic examinations have been claimed by pathologic departments. These discrepancies come from the difference between actual and administrative claims. In tertiary and general hospitals, various medical examinations were requested based on the inpatient department. In clinics, medical examinations were usually requested based on the major disease code of the patient.

According to HIRA (http://opendata.hira.or.kr/op/opc/olapMdclRcStatsInfo.do) and the Ministry of the Interior (http://

Table 2. Annual pathologic examination status and trend

Main category	2011	2012	2013	2014	2015	Total	Growth rates (%) by 2011	Slope	Adjusted R-squared	p-value
Biopsy	2,084,502 (20.24)	2,092,015 (20.31)	2,086,267 (20.25)	2,052,391 (19.92)	1,985,718 (19.28)	10,300,893 (100)	-4.7	-23,719.2	.617	.072
Non-maligGro	1,269,834 (18.90)	1,371,044 (20.41)	1,349,030 (20.08)	1,340,151 (19.95)	1,388,338 (20.66)	6,718,397 (100)	9.3	20,611.5	.354	.172
MaligGro LND	100,204 (20.04)	106,599 (21.32)	107,083 (21.42)	97,288 (19.46)	88,838 (17.77)	500,012 (100)	-11.3	-3,204.3	.273	.212
MaligGro LNDX	40,003 (18.99)	41,651 (19.77)	42,958 (20.39)	43,528 (20.66)	42,553 (20.20)	210,693 (100)	6.4	697.7	.524	.103
MAPPING	28,429 (15.16)	35,866 (19.12)	38,546 (20.55)	42,042 (22.42)	42,662 (22.75)	187,545 (100)	50.1	3,464.2	.867	.014
FS	111,477 (20.19)	116,373 (21.08)	114,943 (20.82)	107,726 (19.51)	101,583 (18.40)	552,102 (100)	-8.9	-2,843.5	.424	.141
BONE	15,705 (21.11)	15,267 (20.52)	14,275 (19.19)	14,516 (19.51)	14,643 (19.68)	74,406 (100)	-6.8	-287.5	.462	.126
SPECIAL	362,888 (19.53)	364,742 (19.63)	372,751 (20.07)	385,799 (20.77)	371,494 (20.00)	1,857,684 (100)	2.4	3,824.9	.266	.216
IF	59,173 (18.40)	63,043 (19.60)	64,959 (20.20)	66,347 (20.63)	68,110 (21.18)	321,632 (100)	15.1	2,117.8	.939	.004
EM	8,945 (19.07)	9,344 (19.92)	9,452 (20.15)	9,522 (20.30)	9,637 (20.55)	46,900 (100)	7.7	156.2	.821	.022
ENZYME	2,399 (27.80)	1,901 (22.03)	1,437 (16.65)	1,479 (17.14)	1,415 (16.39)	8,631 (100)	-41	-239	.717	.044
IHC	550,773 (17.15)	610,637 (19.01)	653,438 (20.34)	698,083 (21.73)	699,285 (21.77)	3,212,216 (100)	27	38,447	.909	.008
CERVIX	209,750 (17.67)	224,052 (18.88)	226,773 (19.11)	245,152 (20.65)	281,166 (23.69)	1,186,893 (100)	34	16,393.2	.849	.017
BFC	490,524 (18.99)	514,410 (19.92)	511,839 (19.82)	530,399 (20.54)	535,708 (20.74)	2,582,880 (100)	9.2	10,635.7	.861	.015
AC	292,502 (21.91)	314,290 (23.55)	294,545 (22.07)	231,264 (17.33)	202,235 (15.15)	1,334,836 (100)	-30.9	-26,356	.683	.053
CB	117,159 (21.76)	115,878 (21.52)	112,949 (20.98)	103,139 (19.15)	89,320 (16.59)	538,445 (100)	-23.8	-6,841.7	.817	.023
HER2	0 (NA)	0 (NA)	1,176 (10.28)	5,031 (43.96)	5,238 (45.77)	11,445 (100)	NA	1,550.7	.814	.023
MSI	11,837 (20.56)	10,763 (18.70)	10,831 (18.81)	11,919 (20.70)	12,219 (21.22)	57,569 (100)	3.2	192	-.060	.444
OUTSIDE	65,609 (18.04)	72,877 (20.04)	75,695 (20.81)	76,649 (21.07)	72,906 (20.04)	363,736 (100)	11.1	1,836.6	.267	.215

Values are presented as number (%).
Non-maligGro, resected specimen requiring gross sectioning; MaligGro, resected specimen for malignant tumor requiring gross sectioning; LND, with lymph node dissection; LNDX, without lymph node dissection; MAPPING, histologic mapping of tumor; FS, emergency histopathologic examination during surgery; BONE, histopathologic examination for bone; SPECIAL, special stain examinations; IF, tissue immunofluorescent microscopic examination; EM, tissue electron microscopy; ENZYME, enzyme histochemistry; IHC, immunohisto(cyto)chemistry; CERVIX, cervicovaginal cytopathology; BFC, body fluid cytopathology; AC, aspiration cytopathology; CB, cell block; HER2, HER2 gene fluorescence in situ hybridization and HER2 gene silver in situ hybridization; MSI, microsatellite instability; OUTSIDE, outside slide interpretation.

Table 3. Pathologic examination numbers according to requesting department in 2011–2015: part I (sort based on department codes)

Requesting department	Biopsy	Non-maligGro	MaligGro	MaligGro LND	MaligGro LNDX	MAPPING	FS	BONE	SPECIAL	IF	EM
General	1,983 (0.02)	1,891 (0.03)	5 (<0.01)	2 (<0.01)	0	0	0	3 (<0.01)	74 (<0.01)	0	0
Internal medicine	6,743,794 (65.47)	2,094,401 (31.17)	10,822 (2.16)	12,804 (6.08)	—	101,570 (54.16)	17,044 (3.09)	36,536 (49.10)	1,347,183 (72.52)	219,154 (68.14)	30,851 (65.78)
Neurology	26,860 (0.26)	9,082 (0.14)	78 (0.02)	205 (0.10)	50 (0.03)	573 (0.10)	174 (0.23)	10,438 (0.56)	834 (0.26)	1,083 (2.31)	
Psychiatry	7,026 (0.07)	1,895 (0.03)	11 (<0.01)	12 (0.01)	14 (0.01)	32 (0.01)	13 (0.02)	1,245 (0.07)	107 (0.03)	9 (0.02)	
General surgery	1,309,516 (12.71)	1,679,607 (25.00)	379,207 (75.84)	73,301 (34.79)	57,975 (30.91)	298,270 (54.02)	406 (0.55)	193,095 (10.39)	36,140 (11.24)	5,525 (11.78)	
Orthopedic surgery	128,100 (1.24)	452,910 (6.74)	649 (0.13)	6,321 (NA)	249 (0.13)	15,707 (2.84)	26,557 (35.69)	19,256 (1.04)	582 (0.18)	287 (0.61)	
Neurosurgery	56,583 (0.55)	181,773 (2.71)	347 (0.07)	13,422 (6.37)	35 (0.02)	29,625 (5.37)	2,979 (NA)	18,216 (0.98)	673 (0.21)	3,672 (7.83)	
Thoracic surgery	28,438 (0.28)	100,518 (1.50)	34,694 (6.94)	11,248 (5.34)	2,892 (1.54)	48,875 (8.85)	261 (0.35)	33,537 (1.81)	209 (0.06)	122 (0.26)	
Plastic surgery	8,598 (0.08)	110,218 (1.64)	1,916 (0.38)	8,022 (3.81)	1,337 (0.71)	14,533 (2.63)	420 (0.56)	4,498 (0.24)	98 (0.03)	56 (0.12)	
Anesthesiology	1,038 (0.01)	835 (0.01)	10 (<0.01)	8 (<0.01)	1 (<0.01)	20 (<0.01)	5 (0.01)	110 (0.01)	2 (<0.01)	0	
Obstetrics and gynecology	888,109 (8.62)	1,078,597 (16.05)	26,431 (5.29)	16,294 (7.73)	4,194 (2.24)	43,154 (7.82)	53 (0.07)	16,801 (0.90)	136 (0.04)	152 (0.32)	
Pediatrics	37,839 (0.37)	16,037 (0.24)	118 (0.02)	388 (0.18)	23 (0.01)	1,309 (0.24)	3,856 (5.18)	23,871 (1.28)	16,039 (4.99)	3,784 (8.07)	
Ophthalmology	20,154 (0.20)	22,715 (0.34)	36 (0.01)	611 (0.29)	10 (0.01)	1,317 (0.24)	14 (0.02)	3,399 (0.18)	132 (0.04)	85 (0.18)	
Otorhinolaryngology	123,136 (1.20)	396,701 (5.90)	31,590 (6.32)	17,180 (8.15)	464 (0.25)	50,489 (9.14)	148 (0.20)	46,797 (2.52)	254 (0.08)	197 (0.42)	
Dermatology	340,839 (3.31)	222,969 (3.32)	121 (0.02)	4,481 (2.13)	472 (0.25)	5,487 (0.99)	9 (0.01)	80,731 (4.35)	41,682 (12.96)	70 (0.15)	
Urology	286,191 (2.78)	215,571 (3.21)	12,449 (2.49)	45,382 (21.54)	17,938 (9.56)	22,137 (4.01)	70 (0.09)	15,361 (0.83)	1,916 (0.60)	542 (1.16)	
Radiology	89,520 (0.87)	7,732 (0.12)	1 (<0.01)	2 (<0.01)	1 (<0.01)	4 (<0.01)	300 (0.40)	1,113 (0.06)	0	4 (0.01)	
Radiation oncology	2,430 (0.02)	113 (<0.01)	0	0	0	1 (<0.01)	0	202 (0.01)	8 (<0.01)	1 (<0.01)	
Pathology	391 (<0.01)	15 (<0.01)	0	0	0	3 (<0.01)	0	3,249 (0.17)	19 (0.01)	4 (0.01)	
Laboratory medicine	338 (<0.01)	46 (<0.01)	0	0	0	0	24 (0.03)	921 (0.05)	0	1 (<0.01)	
Tuberculosis	233 (<0.01)	20 (<0.01)	0	0	0	0	6 (0.01)	122 (0.01)	0	0	
Rehabilitation medicine	8,784 (0.09)	4,392 (0.07)	37 (0.01)	181 (0.09)	30 (0.02)	385 (0.07)	104 (0.14)	2,131 (0.11)	500 (0.16)	135 (0.29)	
Nuclear medicine	118 (<0.01)	15 (<0.01)	0	0	1 (<0.01)	0	0	82 (<0.01)	0	0	
Family medicine	146,907 (1.43)	49,855 (0.74)	31 (0.01)	17 (0.01)	240 (0.13)	62 (0.01)	23 (0.03)	26,784 (1.44)	263 (0.08)	10 (0.02)	
Emergency medicine	15,072 (0.15)	6,035 (0.09)	166 (0.03)	190 (0.09)	41 (0.02)	276 (0.05)	97 (0.13)	5,778 (0.31)	1,381 (0.43)	309 (0.66)	
Occupational and environmental medicine	1,876 (0.02)	98 (<0.01)	0	0	0	0	1 (<0.01)	63 (<0.01)	0	0	
Preventive medicine	1,394 (0.01)	4,229 (0.06)	0	0	2 (<0.01)	0	0	3 (<0.01)	0	0	
Dental department	25,596 (0.25)	60,112 (0.89)	1,293 (0.26)	622 (0.30)	6 (<0.01)	2,799 (0.51)	2,347 (3.15)	2,624 (0.14)	1,503 (0.47)	1 (<0.01)	
Etc.	30 (<0.01)	15 (<0.01)	0	0	0	0	0	0	0	0	
Summary	10,300,893 (100)	6,718,397 (100)	500,012 (100)	210,693 (100)	187,545 (100)	552,102 (100)	74,406 (100)	1,857,684 (100)	321,632 (100)	46,900 (100)	

Values are presented as number (%).

Non-maligGro, resected specimen requiring gross sectioning; MaligGro, resected specimen for malignant tumor requiring gross sectioning; LND, with lymph node dissection; LNDX, without lymph node dissection; MAPPING, histologic mapping of tumor; FS, emergency histopathologic examination during surgery; BONE, histopathologic examination for bone; SPECIAL, special stain examinations; IF, tissue immunofluorescent microscopic examination; EM, tissue electron microscopy.

Table 4. Pathologic examination numbers according to requesting department in 2011–2015: part II (sort based on department codes)

Requesting department	ENZYME	IHC	CERVIX	BFC	AC	CB	HER2	MSI	OUTSIDE	Summary
General	0	5 (<0.01)	363 (0.03)	275 (0.01)	846 (0.06)	13 (<0.01)	1 (0.01)	0	0	5,461 (0.02)
Internal medicine	2,324 (26.93)	897,900 (27.95)	36,501 (3.08)	1,259,857 (48.78)	622,477 (46.63)	369,897 (68.70)	2,622 (22.91)	3,317 (5.76)	108,745 (29.90)	13,917,799 (46.29)
Neurology	2,312 (26.79)	5,100 (0.16)	1,412 (0.12)	53,245 (2.06)	2,423 (0.18)	1,852 (0.34)	5 (0.04)	8 (0.01)	148 (0.04)	115,882 (0.39)
Psychiatry	8 (0.09)	391 (0.01)	666 (0.06)	2,330 (0.09)	435 (0.03)	153 (0.03)	1 (0.01)	2 (<0.01)	24 (0.01)	14,374 (0.05)
General surgery	139 (1.61)	1,413,101 (43.99)	6,204 (0.52)	104,518 (4.05)	489,190 (36.65)	49,603 (9.21)	8,311 (72.62)	53,777 (93.41)	177,028 (48.67)	6,334,913 (21.07)
Orthopedic surgery	321 (3.72)	34,131 (1.06)	3,285 (0.28)	35,414 (1.37)	12,788 (0.96)	3,055 (0.57)	13 (0.11)	7 (0.01)	3,004 (0.83)	742,636 (2.47)
Neurosurgery	186 (2.16)	95,260 (2.97)	1,915 (0.16)	35,088 (1.36)	3,349 (0.25)	2,957 (0.55)	23 (0.20)	8 (0.01)	825 (0.23)	446,936 (1.49)
Thoracic surgery	6 (0.07)	91,268 (2.84)	314 (0.03)	42,808 (1.66)	3,034 (0.23)	13,872 (2.58)	30 (0.26)	92 (0.16)	7,707 (2.12)	419,925 (1.40)
Plastic surgery	91 (1.05)	24,684 (0.77)	107 (0.01)	991 (0.04)	482 (0.04)	388 (0.07)	130 (1.14)	2 (<0.01)	1,254 (0.34)	177,825 (0.59)
Anesthesiology	0	58 (<0.01)	70 (0.01)	371 (0.01)	135 (0.01)	31 (0.01)	0	0	5 (<0.01)	2,699 (0.01)
Obstetrics and gynecology	17 (0.20)	152,242 (4.74)	1,099,372 (92.63)	56,916 (2.20)	28,236 (2.12)	14,401 (2.67)	21 (0.18)	203 (0.35)	19,467 (5.35)	3,444,796 (11.46)
Pediatrics	2,489 (28.84)	31,051 (0.97)	116 (0.01)	38,929 (1.51)	1,821 (0.14)	1,494 (0.28)	0	4 (0.01)	1,258 (0.35)	180,426 (0.60)
Ophthalmology	63 (0.73)	10,629 (0.33)	59 (<0.01)	1,608 (0.06)	848 (0.06)	364 (0.07)	1 (0.01)	0	384 (0.11)	62,429 (0.21)
Otorhinolaryngology	4 (0.05)	125,340 (3.90)	460 (0.04)	9,871 (0.38)	83,493 (6.25)	27,339 (5.08)	1 (0.01)	7 (0.01)	21,799 (5.99)	935,270 (3.11)
Dermatology	197 (2.28)	77,791 (2.42)	308 (0.03)	4,179 (0.16)	3,150 (0.24)	219 (0.04)	7 (0.06)	0	4,957 (1.36)	787,669 (2.62)
Urology	9 (0.10)	193,693 (6.03)	26,181 (2.21)	876,070 (33.92)	31,351 (2.35)	11,392 (2.12)	4 (0.03)	24 (0.04)	13,370 (3.68)	1,769,651 (5.89)
Radiology	2 (0.02)	33,526 (1.04)	298 (0.03)	1,356 (0.05)	31,699 (2.37)	23,850 (4.43)	254 (2.22)	1 (<0.01)	856 (0.24)	190,519 (0.63)
Radiation oncology	0	915 (0.03)	3,773 (0.32)	100 (<0.01)	155 (0.01)	256 (0.05)	1 (0.01)	9 (0.02)	1,367 (0.38)	9,331 (0.03)
Pathology	1 (0.01)	81 (<0.01)	1 (<0.01)	206 (0.01)	3,255 (0.24)	3,488 (0.65)	1 (0.01)	0	10 (<0.01)	10,724 (0.04)
Laboratory medicine	0	7,006 (0.22)	112 (0.01)	22 (<0.01)	5 (<0.01)	2 (<0.01)	0	0	3 (<0.01)	8,480 (0.03)
Tuberculosis	0	75 (<0.01)	10 (<0.01)	1,276 (0.05)	43 (<0.01)	87 (0.02)	0	0	61 (0.02)	1,933 (0.01)
Rehabilitation medicine	392 (4.54)	1,884 (0.06)	648 (0.05)	6,636 (0.26)	606 (0.05)	940 (0.17)	10 (0.09)	8 (0.01)	65 (0.02)	27,868 (0.09)
Nuclear medicine	0	62 (<0.01)	7 (<0.01)	44 (<0.01)	2,514 (0.19)	682 (0.13)	0	0	58 (0.02)	3,583 (0.01)
Family medicine	5 (0.06)	3,524 (0.11)	2,536 (0.21)	16,582 (0.64)	11,341 (0.85)	4,132 (0.77)	1 (0.01)	5 (0.01)	398 (0.11)	262,716 (0.87)
Emergency medicine	64 (0.74)	3,939 (0.12)	2,156 (0.18)	31,115 (1.20)	514 (0.04)	7,460 (1.39)	8 (0.07)	95 (0.17)	293 (0.08)	74,989 (0.25)
Occupational and environmental medicine	0	18 (<0.01)	1 (<0.01)	159 (0.01)	81 (0.01)	2 (<0.01)	0	0	1 (<0.01)	2,300 (0.01)
Preventive medicine	0	5 (<0.01)	2 (<0.01)	24 (<0.01)	188 (0.01)	0	0	0	1 (<0.01)	5,848 (0.02)
Dental department	1 (0.01)	8,537 (0.27)	15 (<0.01)	2,875 (0.11)	372 (0.03)	516 (0.10)	0	0	648 (0.18)	109,867 (0.37)
Etc.	0	0	1 (<0.01)	15 (<0.01)	5 (<0.01)	0	0	0	0	66 (<0.01)
Summary	8,631 (100)	3,212,216 (100)	1,186,893 (100)	2,582,880 (100)	1,334,836 (100)	538,445 (100)	11,445 (100)	57,569 (100)	363,736 (100)	30,066,915 (100)

Values are presented as number (%).

ENZYME, enzyme histochemistry; IHC, immunohisto(cyto)chemistry; CERVIX, cervicovaginal cytopathology; BFC, body fluid cytopathology; AC, aspiration cytopathology; CB, cell block; HER2, *HER2* gene fluorescence *in situ* hybridization and *HER2* gene silver *in situ* hybridization; MSI, microsatellite instability; OUTSIDE, outside slide interpretation.

Table 5. Pathologic examination status according to types of medical institutions in 2011–2015

Pathologic examination	Tertiary hospital	General hospital	Hospital	Convalescent hospital	Clinic	Dental hospital	Dental clinic	Public health center	Public health center and county hospital	Oriental hospital	Summary
Biopsy	2,354,632 (22.86)	2,617,426 (25.41)	1,387,062 (13.47)	13,460 (0.13)	3,910,624 (37.96)	13,285 (0.13)	898 (0.01)	0	2,767 (0.03)	739 (0.01)	10,300,893 (100)
Non-maligGro	1,727,593 (25.71)	2,362,797 (35.17)	1,161,784 (17.29)	3,929 (0.06)	1,440,209 (21.44)	18,397 (0.27)	384 (0.01)	0	2,197 (0.03)	1,107 (0.02)	6,718,397 (100)
MaligGro LND	332,395 (66.48)	149,342 (29.87)	13,548 (2.71)	2 (<0.01)	4,032 (0.81)	693 (0.14)	0	0	0	0	500,012 (100)
MaligGro LNDX	151,392 (71.85)	56,436 (26.79)	1,999 (0.95)	16 (0.01)	567 (0.27)	282 (0.13)	0	0	1 (<0.01)	0	210,693 (100)
MAPPING	132,776 (70.80)	52,851 (28.18)	1,705 (0.91)	7 (<0.01)	205 (0.11)	1 (<0.01)	0	0	0	0	187,545 (100)
FS	388,171 (70.31)	158,797 (28.76)	3,730 (0.68)	21 (<0.01)	104 (0.02)	1,279 (0.23)	0	0	0	0	552,102 (100)
BONE	35,926 (48.28)	27,499 (36.96)	9,264 (12.45)	5 (0.01)	333 (0.45)	1,378 (1.85)	1 (<0.01)	0	0	0	74,406 (100)
SPECIAL	817,633 (44.01)	756,183 (40.71)	57,218 (3.08)	778 (0.04)	224,562 (12.09)	1,301 (0.07)	0	0	1 (<0.01)	8 (<0.01)	1,857,684 (100)
IF	226,147 (70.31)	91,857 (28.56)	519 (0.16)	503 (0.16)	1,450 (0.45)	1,156 (0.36)	0	0	0	0	321,632 (100)
EM	35,284 (75.23)	11,411 (24.33)	61 (0.13)	0	144 (0.31)	0	0	0	0	0	46,900 (100)
ENZYME	7,524 (87.17)	1,093 (12.66)	9 (0.10)	0	5 (0.06)	0	0	0	0	0	8,631 (100)
IHC	2,205,781 (68.67)	966,307 (30.08)	25,241 (0.79)	351 (0.01)	9,041 (0.28)	5,481 (0.17)	0	0	12 (<0.01)	2 (<0.01)	3,212,216 (100)
CERVIX	490,880 (41.36)	449,685 (37.89)	70,512 (5.94)	592 (0.05)	174,700 (14.72)	0	0	3 (<0.01)	503 (0.04)	18 (<0.01)	1,186,893 (100)
BFC	1,201,031 (46.50)	1,053,678 (40.79)	162,061 (6.27)	2,248 (0.09)	161,414 (6.25)	2,319 (0.09)	0	0	106 (<0.01)	23 (<0.01)	2,582,880 (100)
AC	219,121 (16.42)	335,929 (25.17)	152,361 (11.41)	645 (0.05)	626,573 (46.94)	145 (0.01)	1 (<0.01)	0	32 (<0.01)	29 (<0.01)	1,334,836 (100)
CB	293,874 (54.58)	196,885 (36.57)	20,101 (3.73)	124 (0.02)	27,092 (5.03)	369 (0.07)	0	0	0	0	538,445 (100)
HER2	8,605 (75.19)	2,747 (24.00)	86 (0.75)	6 (0.05)	1 (0.01)	0	0	0	0	0	11,445 (100)
MSI	49,100 (85.29)	8,318 (14.45)	151 (0.26)	0	0	0	0	0	0	0	57,569 (100)
OUTSIDE	276,885 (76.12)	75,385 (20.73)	1,391 (0.38)	47 (0.01)	9,667 (2.66)	360 (0.10)	0	0	0	1 (<0.01)	363,736 (100)
Summary	10,954,750 (36.43)	9,374,626 (31.18)	3,068,803 (10.21)	22,734 (0.08)	6,590,723 (21.92)	46,446 (0.15)	1,284 (<0.01)	3 (<0.01)	5,619 (0.02)	1,927 (0.01)	30,066,915 (100)

Values are presented as number (%).

Non-maligGro, resected specimen requiring gross sectioning; MaligGro, resected specimen for malignant tumor requiring gross sectioning; LND, with lymph node dissection; LNDX, without lymph node dissection; MAPPING, histologic mapping of tumor; FS, emergency histopathologic examination during surgery; BONE, histopathologic examination for bone; SPECIAL, special stain examinations; IF, tissue immunofluorescent microscopic examination; EM, tissue electron microscopy; ENZYME, enzyme histochemistry; IHC, immunohisto(cyto)chemistry; CERVIX, cervicovaginal cytopathology; BFC, body fluid cytopathology; AC, aspiration cytopathology; CB, cell block; HER2, HER2 gene fluorescence *in situ* hybridization and HER2 gene silver *in situ* hybridization; MSI, microsatellite instability; OUTSIDE, outside slide interpretation.

Table 6. Pathologic examination status according to administrative districts in 2011–2015: part I (sort based on administrative districts codes)

Administrative district	Biopsy	Non-maligGro	MaligGro LND	MaligGro LNDX	MAPPING	FS	BONE	SPECIAL	IF	EM
Etc.	0	21 (<0.01)	0	0	0	0	0	0	0	0
Seoul	3,569,090 (30.24)	2,487,048 (32.18)	267,423 (46.34)	113,181 (46.84)	109,012 (50.46)	317,546 (49.92)	22,231 (27.33)	830,214 (37.57)	169,672 (46.92)	26,715 (51.53)
Busan	1,007,783 (8.54)	718,747 (9.30)	57,598 (9.98)	26,132 (10.81)	18,263 (8.45)	61,611 (9.69)	9,156 (11.25)	101,122 (4.58)	39,230 (10.85)	5,599 (10.80)
Incheon	701,281 (5.94)	457,064 (5.91)	42,029 (7.28)	20,095 (8.32)	12,743 (5.90)	41,553 (6.53)	5,388 (6.62)	158,767 (7.18)	18,329 (5.07)	1,915 (3.69)
Daegu	914,814 (7.75)	505,092 (6.54)	43,935 (7.61)	13,662 (5.65)	9,264 (4.29)	35,356 (5.56)	10,090 (12.40)	161,162 (7.29)	22,793 (6.30)	3,466 (6.68)
Gwangju	419,909 (3.56)	314,418 (4.07)	9,260 (1.60)	2,575 (1.07)	1,216 (0.56)	7,133 (1.12)	635 (0.78)	31,555 (1.43)	6,476 (1.79)	1,167 (2.25)
Daejeon	435,340 (3.69)	309,986 (4.01)	19,421 (3.37)	3,075 (1.27)	3,934 (1.82)	13,359 (2.10)	6,968 (8.56)	66,516 (3.01)	12,276 (3.39)	1,732 (3.34)
Ulsan	250,163 (2.12)	168,514 (2.18)	8,207 (1.42)	4,827 (2.00)	138 (0.06)	8,178 (1.29)	2,136 (2.63)	41,843 (1.89)	6,577 (1.82)	698 (1.35)
Gyeonggi-do	1,978,367 (16.76)	1,287,772 (16.66)	67,488 (11.70)	28,882 (11.95)	37,470 (17.35)	78,222 (12.30)	11,599 (14.26)	436,544 (19.75)	49,950 (13.81)	5,760 (11.11)
Gangwon-do	228,857 (1.94)	150,249 (1.94)	6,447 (1.12)	3,586 (1.48)	4,503 (2.08)	10,730 (1.69)	3,151 (3.87)	67,670 (3.06)	7,882 (2.18)	758 (1.46)
Chungcheongbuk-do	250,413 (2.12)	171,847 (2.22)	5,083 (0.88)	1,591 (0.66)	590 (0.27)	5,706 (0.90)	1,927 (2.37)	61,513 (2.78)	2,266 (0.63)	385 (0.74)
Chungcheongnam-do	313,423 (2.66)	155,444 (2.01)	5,393 (0.93)	2,529 (1.05)	3,700 (1.71)	6,237 (0.98)	177 (0.22)	41,352 (1.87)	6,644 (1.84)	727 (1.40)
Jeollabuk-do	349,185 (2.96)	192,196 (2.49)	11,396 (1.97)	7,030 (2.91)	4,207 (1.95)	14,340 (2.25)	3,226 (3.97)	20,504 (0.93)	3,829 (1.06)	458 (0.88)
Jeollanam-do	295,622 (2.50)	177,955 (2.30)	16,774 (2.91)	7,613 (3.15)	30 (0.01)	11,400 (1.79)	245 (0.30)	35,185 (1.59)	1,056 (0.29)	200 (0.39)
Gyeongsangbuk-do	451,285 (3.82)	220,085 (2.85)	1,936 (0.34)	816 (0.34)	1,159 (0.54)	1,852 (0.29)	1,028 (1.26)	44,136 (2.00)	2,140 (0.59)	270 (0.52)
Gyeongsangnam-do	532,322 (4.51)	352,022 (4.55)	12,136 (2.10)	5,078 (2.10)	8,698 (4.03)	19,881 (3.13)	2,205 (2.71)	78,121 (3.54)	9,437 (2.61)	1,572 (3.03)
Jeju	100,466 (0.85)	57,359 (0.74)	2,538 (0.44)	961 (0.40)	1,094 (0.51)	3,023 (0.48)	1,194 (1.47)	33,540 (1.52)	3,070 (0.85)	426 (0.82)
Sejong-si	4,372 (0.04)	3,023 (0.04)	0	0	0	0	0	104 (<0.01)	0	0
Summary	11,802,692 (100)	7,728,842 (100)	577,064 (100)	241,633 (100)	216,021 (100)	636,127 (100)	81,356 (100)	2,209,848 (100)	361,627 (100)	51,848 (100)

Values are presented as number (%).
Non-maligGro, resected specimen requiring gross sectioning; MaligGro, resected specimen for malignant tumor requiring gross sectioning; LND, with lymph node dissection; LNDX, without lymph node dissection; MAPPING, histologic mapping of tumor; FS, emergency histopathologic examination during surgery; BONE, histopathologic examination for bone; SPECIAL, special stain examinations; IF, tissue immunofluorescent examination; EM, tissue electron microscopy.

Table 7. Pathologic examination status according to administrative districts in 2011–2015: part II (sort based on administrative districts codes)

Administrative district	ENZYME	IHC	CERVIX	BFC	AC	CB	HER2	MSI	OUTSIDE	Summary
Etc.	0	0	0	0	0	0	0	0	0	21 (<0.01)
Seoul	6,622 (71.09)	1,767,200 (46.85)	543,513 (40.40)	1,146,492 (39.19)	338,246 (22.66)	273,523 (44.02)	6,944 (52.83)	36,679 (55.68)	261,862 (61.69)	12,293,213 (35.55)
Busan	521 (5.59)	309,799 (8.21)	106,119 (7.89)	307,125 (10.50)	184,239 (12.34)	42,686 (6.87)	898 (6.83)	6,723 (10.21)	24,460 (5.76)	3,027,811 (8.76)
Incheon	144 (1.55)	234,731 (6.22)	86,153 (6.40)	235,529 (8.05)	92,453 (6.19)	38,392 (6.18)	1,297 (9.87)	4,462 (6.77)	19,867 (4.68)	2,172,192 (6.28)
Daegu	501 (5.38)	402,725 (10.68)	88,991 (6.62)	131,159 (4.48)	150,027 (10.05)	64,550 (10.39)	815 (6.20)	3,096 (4.70)	22,940 (5.40)	2,584,438 (7.47)
Gwangju	136 (1.46)	36,164 (0.96)	38,359 (2.85)	74,981 (2.56)	133,266 (8.93)	4,443 (0.72)	27 (0.21)	0	1,441 (0.34)	1,083,161 (3.13)
Daejeon	53 (0.57)	71,899 (1.91)	40,038 (2.98)	83,455 (2.85)	45,632 (3.06)	7,065 (1.14)	194 (1.48)	36 (0.05)	9,240 (2.18)	1,130,219 (3.27)
Ulsan	4 (0.04)	46,112 (1.22)	18,427 (1.37)	53,310 (1.82)	30,219 (2.02)	8,665 (1.39)	153 (1.16)	2 (<0.01)	3,367 (0.79)	651,540 (1.88)
Gyeonggi-do	849 (9.11)	569,103 (15.09)	219,328 (16.30)	374,113 (12.79)	221,132 (14.81)	92,707 (14.92)	1,820 (13.85)	10,526 (15.98)	58,704 (13.83)	5,530,336 (15.99)
Gangwon-do	24 (0.26)	63,272 (1.68)	35,913 (2.67)	69,897 (2.39)	15,218 (1.02)	17,189 (2.77)	208 (1.58)	624 (0.95)	1,517 (0.36)	687,695 (1.99)
Chungcheongbuk-do	0	13,816 (0.37)	11,057 (0.82)	45,783 (1.56)	30,046 (2.01)	8,844 (1.42)	55 (0.42)	371 (0.56)	2,802 (0.66)	614,095 (1.78)
Chungcheongnam-do	6 (0.06)	26,956 (0.71)	29,260 (2.18)	56,711 (1.94)	23,501 (1.57)	17,295 (2.78)	167 (1.27)	0	2,420 (0.57)	691,942 (2.00)
Jeollabuk-do	8 (0.09)	71,973 (1.91)	28,958 (2.15)	93,002 (3.18)	54,035 (3.62)	2,377 (0.38)	150 (1.14)	259 (0.39)	3,424 (0.81)	860,557 (2.49)
Jeollanam-do	3 (0.03)	55,684 (1.48)	27,585 (2.05)	55,997 (1.91)	68,206 (4.57)	5,211 (0.84)	285 (2.17)	798 (1.21)	6,128 (1.44)	765,977 (2.22)
Gyeongsangbuk-do	10 (0.11)	8,784 (0.23)	26,061 (1.94)	58,344 (1.99)	41,342 (2.77)	6,361 (1.02)	7 (0.05)	1 (<0.01)	330 (0.08)	865,947 (2.50)
Gyeongsangnam-do	339 (3.64)	70,854 (1.88)	30,645 (2.28)	109,302 (3.74)	54,687 (3.66)	29,855 (4.80)	92 (0.70)	2,266 (3.44)	5,066 (1.19)	1,324,578 (3.83)
Jeju	95 (1.02)	22,901 (0.61)	14,340 (1.07)	30,246 (1.03)	10,421 (0.70)	2,217 (0.36)	33 (0.25)	36 (0.05)	933 (0.22)	284,893 (0.82)
Sejong-si	0	5 (<0.01)	484 (0.04)	129 (<0.01)	331 (0.02)	12 (<0.01)	0	0	2 (<0.01)	8,462 (0.02)
Summary	9,315 (100)	3,771,978 (100)	1,345,231 (100)	2,925,575 (100)	1,493,001 (100)	621,392 (100)	13,145 (100)	65,879 (100)	424,503 (100)	34,577,077 (100)

Values are presented as number (%).

ENZYME, enzyme histochemistry; IHC, immunohisto(cyto)chemistry; CERVIX, cervicovaginal cytopathology; BFC, body fluid cytopathology; AC, aspiration cytopathology; CB, cell block; HER2, *HER2* gene fluorescence *in situ* hybridization and *HER2* gene silver *in situ* hybridization; MSI, microsatellite instability; OUTSIDE, outside slide interpretation.

Table 8. Summary of the types of institutions where pathologic examinations were done during 2011–2015

Pathologic examination	Performed in their own hospitals	Performed using outside services	Convalescent hospital	Etc.	Summary
Biopsy	4,484,330 (43.53)	5,784,009 (56.15)	28,542 (0.28)	4,012 (0.04)	10,300,893 (100)
Non-maligGro	3,621,714 (53.91)	3,034,515 (45.17)	61,635 (0.92)	533 (0.01)	6,718,397 (100)
MaligGro LND	475,825 (95.16)	20,673 (4.13)	3,512 (0.70)	2 (<0.01)	500,012 (100)
MaligGro LNDX	206,618 (98.07)	3,252 (1.54)	821 (0.39)	2 (<0.01)	210,693 (100)
MAPPING	185,267 (98.79)	1,123 (0.60)	1,152 (0.61)	3 (<0.01)	187,545 (100)
FS	545,200 (98.75)	4,089 (0.74)	2,806 (0.51)	7 (<0.01)	552,102 (100)
BONE	58,330 (78.39)	13,576 (18.25)	2,496 (3.35)	4 (0.01)	74,406 (100)
SPECIAL	1,487,782 (80.09)	363,521 (19.57)	5,793 (0.31)	588 (0.03)	1,857,684 (100)
IF	259,628 (80.72)	58,684 (18.25)	3,317 (1.03)	3 (<0.01)	321,632 (100)
EM	31,593 (67.36)	15,175 (32.36)	132 (0.28)	0	46,900 (100)
ENZYME	7,779 (90.13)	787 (9.12)	65 (0.75)	0	8,631 (100)
IHC	3,129,765 (97.43)	62,839 (1.96)	19,503 (0.61)	109 (<0.01)	3,212,216 (100)
CERVIX	901,312 (75.94)	278,397 (23.46)	1,057 (0.09)	6,127 (0.52)	1,186,893 (100)
BFC	2,068,613 (80.09)	490,820 (19.00)	22,888 (0.89)	559 (0.02)	2,582,880 (100)
AC	458,090 (34.32)	855,980 (64.13)	489 (0.04)	20,277 (1.52)	1,334,836 (100)
CB	505,034 (93.79)	29,688 (5.51)	3,073 (0.57)	650 (0.12)	538,445 (100)
HER2	9,856 (86.12)	1,587 (13.87)	2 (0.02)	0	11,445 (100)
MSI	35,244 (61.22)	22,325 (38.78)	0	0	57,569 (100)
OUTSIDE	356,892 (98.12)	6,640 (1.83)	165 (0.05)	39 (0.01)	363,736 (100)
Summary	18,828,872 (62.62)	11,047,680 (36.74)	157,448 (0.52)	32,915 (0.11)	30,066,915 (100)

Values are presented as number (%).

Non-maligGro, resected specimen requiring gross sectioning; MaligGro, resected specimen for malignant tumor requiring gross sectioning; LND, with lymph node dissection; LNDX, without lymph node dissection; MAPPING, histologic mapping of tumor; FS, emergency histopathologic examination during surgery; BONE, histopathologic examination for bone; SPECIAL, special stain examinations; IF, tissue immunofluorescent microscopic examination; EM, tissue electron microscopy; ENZYME, enzyme histochemistry; IHC, immunohisto(cyto)chemistry; CERVIX, cervicovaginal cytopathology; BFC, body fluid cytopathology; AC, aspiration cytopathology; CB, cell block; HER2, *HER2* gene fluorescence *in situ* hybridization and *HER2* gene silver *in situ* hybridization; MSI, microsatellite instability; OUTSIDE, outside slide interpretation.


Fig. 1. The kernel density estimation plot of each percentile inspection completion of insurance reimbursement requests (light gray, 33 percentile; dark gray, 66 percentile; black, 99 percentile).

rcps.egov.go.kr:8081/jsp/stat/ppl_stat_jf.jsp), there were 53,252 medical institutions and 51,677,054 people in Korea in December, 2015 (see Supplementary Table S6). The total number of pathologic examinations in each administrative district was positively correlated with both the number of medical institutions and people in the area (both p < .001). About 61.7% of OUTSIDE were performed in medical institutions located in Seoul. The proportion of OUTSIDE was higher than the population ratio of Seoul (10,022,181, 19.4%). This phenomenon reflects the patient preference for major medical institutions in Seoul.

Compared to previous studies using common pathologic examination codes in 2013 (approximately 5,440,288 pathologic examinations using the NPS data), there was a 3.2% increase in pathologic examinations (5,615,395 pathologic examinations in 2013). This difference was found to be in the acceptable range as determined by the pilot study. When using the raw HIRA data, implementation of basic algorithms using the NPS data is recommended.

In conclusion, even though this survey using the HIRA dataset did not reflect the exact current status, it is still quite accurate. I expect the present study to help with future operations for the Korean Society of Pathology in terms of understanding the current status and trends of pathologic examinations. I recommended that an in-depth analysis of the status of pathologic examinations

considering the period between IR requests and inspection completions be made after at least 1 year.

Electronic Supplementary Material

Supplementary materials are available at Journal of Pathology and Translational Medicine (http://jpatholtm.org).

Conflicts of Interest

No potential conflict of interest relevant to this article was reported.

REFERENCES

1. Byeon SJ, Kim WH. Analysis of surgical pathology data in the HIRA database: emphasis on current status and endoscopic submucosal dissection specimens. J Pathol Transl Med 2016; 50: 204-10.
2. Kim L, Kim JA, Kim S. A guide for the utilization of Health Insurance Review and Assessment Service National Patient Samples. Epidemiol Health 2014; 36: e2014008.

■ ORIGINAL ARTICLE ■

Higher Expression of Toll-like Receptors 3, 7, 8, and 9 in Pityriasis Rosea

Mostafa Abou El-Ela
Mohamed El-Komy
Rania Abdel Hay · Rehab Hegazy
Amin Sharobim[1] · Laila Rashed[2]
Khalda Amr[3]

Department of Dermatology, Faculty of Medicine, Cairo University, Cairo; [1]Department of Dermatology, National Research Center (NRC), Cairo University, Cairo; [2]Department of Clinical Biochemistry, Faculty of Medicine, Cairo University, Cairo; [3]Department of Molecular Genetics, National Research Center (NRC), Cairo University, Cairo, Egypt

Corresponding Author
Rania Abdel Hay, MD
Department of Dermatology, Faculty of Medicine, Cairo University, 13th Abrag Othman, Kournish el Maadi, Cairo 11431, Egypt
Tel: +20-1006084132
Fax: +20-23596724
E-mail: raniamounir@kasralainy.edu.eg

Background: Pityriasis rosea (PR) is a common papulosquamous skin disease in which an infective agent may be implicated. Toll-like receptors (TLRs) play an important role in immune responses and in the pathophysiology of inflammatory skin diseases. Our aim was to determine the possible roles of TLRs 3, 7, 8, and 9 in the pathogenesis of PR. **Methods:** Twenty-four PR patients and 24 healthy individuals (as controls) were included in this case control study. All recruits were subjected to routine laboratory investigations. Biopsies were obtained from one active PR lesion and from healthy skin of controls for the detection of TLR 3, 7, 8, and 9 gene expression using real-time polymerase chain reaction. **Results:** This study included 24 patients (8 females and 16 males) with active PR lesions, with a mean age of 28.62 years. Twenty four healthy age- and sex-matched individuals were included as controls (8 females and 16 males, with a mean age of 30.83 years). The results of the routine laboratory tests revealed no significant differences between both groups. Significantly elevated expression of all studied TLRs were detected in PR patients relative to healthy controls (p < .001). **Conclusions:** TLRs 3, 7, 8, and 9 might be involved in the pathogenesis of PR.

Although pityriasis rosea (PR) was identified some time ago, and much has been done to describe and diagnose the rash, little is known regarding PR's etiology. There are many studies supporting the theory that PR is caused by an infectious agent.[1] These studies were based on several facts, including the resemblance of PR's rash to viral exanthemas, the rare recurrences of PR suggesting lifelong immunity after a single episode,[2] the occurrence of seasonal variation, and the clustering in some communities, as well as the appearance of flu-like symptoms in some patients.[3] Some evidence suggests a relationship between human herpes virus (HHV) 6 and 7 and PR.[4,5]

Toll-like receptors (TLRs) are a group of pattern recognition receptors that are involved in mechanisms of host defense against a wide range of pathogenic microorganisms.[6] TLRs 3, 7, 8, and 9 are intracellular TLRs, in which they sense virus-derived pattern molecules and respond with the induction of antiviral genes, such as type I interferon.[7] Expression of TLRs 3, 7, and 9 has

previously been detected in blood lymphocytes from patients with PR.[8]

The aim of this study was to evaluate the possible role of TLRs 3, 7, and 9 in the pathogenesis of PR.

MATERIALS AND METHODS

The current case control study was approved by the Research Ethical Committee Office (REC), Department of Dermatology, Faculty of Medicine, Cairo University. All participants provided full informed written consent prior to this study.

This study included 24 patients with classic active PR and 24 age- and sex-matched and apparently healthy individuals serving as controls. All participants were recruited between May 2012 and January 2013 from the dermatology outpatient clinic of Kasr Al Ainy Hospital.

All patients in the PR group had classical findings of PR and

were in the active stage of the disease (having active lesions appearing within the same week of their visit to the clinic). All participants were otherwise healthy and immunocompetent, none had a recent history of immunization, and none were on systemic steroids or other immunosuppressive therapy.

All recruits were subjected to routine laboratory investigations including hemoglobin (Hb), white blood cells count, erythrocyte sedimentation rate first hour (ESR1), erythrocyte sedimentation rate second hour (ESR2), alanine aminotransferase (ALT), aspartate aminotransferase (AST), and urea and creatinine levels.

A 4-mm punch biopsy was obtained from the active edge of one of the lesions from each patient and from the apparently healthy skin of the trunk from each control. The biopsies were stored at –70°C until used for measurement of TLR mRNA.

Detection of TLR 3, 7, 8, and 9 gene expression levels using real-time polymerase chain reaction

Total RNA was extracted from skin tissue (TRIzol reagent, Invitrogen, Karlsruhe, Germany), and the quantity and purity of the extracted RNA were assessed by measuring absorbance at 260 nm and the ratio of absorbance at 260 nm to absorbance at 280 nm (A260/A280), using an ultraviolet spectrophotometer (NanoDrop Inc., Wilmington, DE, USA). Only samples with an A260/A280 ratio under 1.8 were considered valid for real-time polymerase chain reaction (RT-PCR). Reverse transcription of 1 μg of RNA into cDNA was performed (First Strand cDNA Synthesis Kit, TaKaRa, Bio Inc., Shiga, Japan) in accordance with the manufacturer's instructions.

Expression of the target gene TLR was quantified using the comparative threshold cycle (Ct) method, with the amount of target mRNA normalized to an internal control (glyceraldehyde phosphate dehydogenase [GAPDH]). RT-PCR was performed using a commercial kit (Light Cycler Fast Start DNA SYBR-Green I Kit, Roche Applied Sciences, Mannheim, Germany) in accordance with the provided protocol. Briefly, 10 μL amplification mixtures were prepared, containing the equivalent of 8 ng

Table 1. Sequence of primers used for real-time PCR

		Primer sequence
TLR3	Forward	5'- GCATTTGTTTTCTCACTCTTT-3'
	Reverse	5'-TTAGCCACTGAAAAGAAAAAT-3'
TLR7	Forward	5'-AAACTCCTTGGGGCTAGATG-3'
	Reverse	5'-AGGGTGAGGTTCGTGGTGTT-3'
TLR8	Forward	5'-CTGTGAGTTATGCGCCGAAGA-3'
	Reverse	5'-TGGTGCTGTACATTGGGGTTG-3'
TLR9	Forward	5'-CGCCCTGCACCCGCTGTCTCT-3'
	Reverse	5'-CGGGGTGCTGCCATGGAGAAG-3'

PCR, polymerase chain reaction; TLR, Toll-like receptor.

of reverse-transcribed RNA, along with 300 M primers (sequences of the PCR primer pairs used for each gene are shown in Table 1). Reactions were run on a cetection system (ABI Prism 7900 HT, Applied Biosystems, Foster City, CA, USA). PCR parameters were one cycle at 95°C for 10 minutes, followed by 40 cycles at 94°C for 15 seconds and 60°C for 1 minute. Data were analyzed and quantified using ABI Prism sequence detection system software (Sequence Detection Software v1.7, PE Applied Biosystems). Relative expression of studied genes was calculated using the comparative threshold cycle method, and all values were normalized to GAPDH genes.[9] The level of expression of each target gene was normalized relative to the expression of GAPDH mRNA in that sample using the ΔCt method. Relative differences in gene expression between groups were determined using the comparative Ct (ΔΔCt) method, and fold expression was calculated as $2^{-\Delta\Delta Ct}$, where ΔΔCt represents ΔCt values normalized relative to the mean ΔCt of control samples.

Statistical methods

Data were described in terms of mean ± standard deviation (± SD), frequencies (number of cases) and relative frequencies (%) when appropriate. Comparisons between groups were done using T-tests for all quantitative variables, and chi-square (χ^2) tests for categorical data (sex distribution). Correlations between various variables were calculated using Pearson moment correlation equations for linear relationships. $p < .05$ was considered statistically significant. All statistical calculations were done using the computer program Microsoft Excel (Microsoft Corporation, New York, NY, USA) and SPSS ver. 19 for Microsoft Windows (SPSS Inc., Chicago, IL, USA).

RESULTS

This case control study included 24 patients (8 females [33.3%] and 16 males [66.7%]) with classic active PR developing within the 2 weeks prior to recruitment. Their age ranged from 19 to 45 years with mean ± SD of 28.62 ± 8.30. Twenty-four apparently healthy age- and sex-matched individuals (p = .370 and p > .990, respectively) were also included in this study as controls. The controls included eight females (33.3%) and 16 males (66.7%), and their age ranged from 19–46 years with mean ± SD of 30.83 ± 8.59.

Routine laboratory data

Comparing routine laboratory findings between the patient and control groups revealed no significant differences (using

Table 2. Summary of descriptive data from routine laboratory investigations in pityriasis rosea patients and controls

Variable	Patient (n = 24)	Control (n = 24)	p-value
Hb (mg)	12.69 ± 1.27 (10.8–14.9)	12.97 ± 1.31 (10.8–14.9)	.431
WBC (mm³)	6.77 ± 1.63 (4.8–9.8)	6.46 ± 1.60 (3.9–9.8)	.512
ESR1 (mm/hr)	14.01 ± 6.27 (6–27)	12.04 ± 5.36 (6–25)	.251
ESR2 (mm/hr)	26.25 ± 7.62 (15–40)	23.37 ± 7.60 (15–40)	.198
ALT (U/L)	19.41 ± 10.40 (10–47)	21.91 ± 12.12 (10–47)	.081
AST (U/L)	20.41 ± 8.37 (10–40)	21.87 ± 7.90 (12–40)	.126
Urea (mg/dL)	28.29 ± 9.89 (15–48)	24.70 ± 8.62 (15–50)	.092
Creatinine (mg/dL)	0.88 ± 0.23 (0.5–1.3)	0.89 ± 0.28 (0.5–1.5)	.436

Values are presented as mean ± standard deviation (range).
Normal routine laboratory reference values: hemoglobin (Hb; male: 13–18 mg/female: 12–17 mg), white blood cells (WBCs; 4,000–12,000 mm³), erythrocyte sedimentation rate first hour (ESR1; up to 8 mm/hr), erythrocyte sedimentation rate second hour (ESR2; up to 18 mm/hr), alanine aminotransferase (ALT; 5–40 U/L), aspartate aminotransferase (AST; 7–56 U/L), urea (20–50 mg/dL), creatinine (0.5–1.5 mg/dL).

T-test) (Table 2). In the patient group, 14 patients had anemia (low Hb), none of the patients had leukocytosis or leucopenia, 18 patients showed elevated ESR1 and ESR2, none of the patients had elevated ALT or AST, and none showed elevated urea or creatinine levels. In the control group, 14 controls had anemia (low Hb), two controls showed leucopenia and none had leukocytosis, 15 controls showed elevated ESR1 and ESR2, none of the controls had elevated ALT or AST, and none showed elevated urea or creatinine levels.

Histopathologic findings among PR patients included focal parakeratosis, absent granular cell layer, mild acanthosis, mild spongiosis, papillary dermal edema, perivascular and superficial dermal interstitial infiltrate of lymphocytes and histiocytes, and focal extravasation of erythrocytes as previously described,[10] confirming the diagnosis of PR.

TLRs expression

Summary of the descriptive data of different studied TLRs in both groups were presented in Fig. 1. Comparing the TLR 3, 7, 8, and 9 expression levels between the patient and control groups revealed that the mean levels of all studied TLRs were significantly higher in patients relative to healthy controls (p < .001 for all, using T-test) (Fig. 1).

Our results revealed nonsignificant correlations between the studied TLRs in the patient group (using Pearson correlation test).

DISCUSSION

The current study highlights the possible roles played by different TLR pathways in the pathogenesis of PR. In this study, a significantly elevated expression of the studied TLRs 3, 7, 8, and 9 was documented in PR cases relative to healthy controls.

The results of the current study are in accordance with another,[8] which found the expression of TLRs 3, 7, and 9 to be signifi-
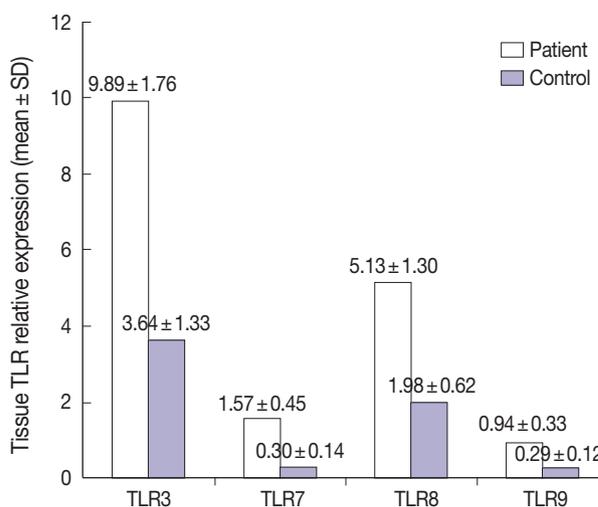

Fig. 1. Mean Toll-like receptors (TLRs) relative expression in patient and control groups. SD, standard deviation.

cantly elevated in the peripheral blood (PB) lymphocytes of patients with PR relative to normal controls. However, unlike in our study, that study did not find elevated levels in the skin. This discrepancy between skin and PB lymphocytes may support the concept of PR being induced through a systemic insult to the body, most likely an infective agent, with the primary and early burden on the immune system.

Our results revealed non-significant correlations among the studied TLRs in the patient group. This could suggest that each TLR can play an individual role in the pathogenesis of PR.

TLRs 3, 7, 8, and 9 have been shown to be involved in responses to viral infection,[11] but no studies have referred to their involvement with HHV. The use of TLRs 3, 7, 8, and 9 analogs as antiviral therapy supports the role of TLR in viral infections.[12,13]

The possible role of TLRs in PR can be attributed to several mechanisms. Vercammen *et al.*[14] demonstrated that TLR 3 triggering activates specific signaling pathways that mount an effec-

tive immune response through the induction of cytokines and other pro-inflammatory mediators. These mediators may participate in enhancing inflammation in the affected area of the PR. Renn et al.[15] also reported that after the stimulation of TLR 3, and to a lesser extent TLRs 7 and 8, langerhans cells are stimulated, which were found to be increased in lesions of PR; langerhans cells produce large amounts of chemoattractants, which may participate in the inflammation present in PR.

However, the fact that TLRs are involved with the initiation of innate and acquired immune responses for many other pathogens precludes us from asserting that their high expression in PR points to an infective etiology.

In conclusion, the current study indicated that TLRs 3, 7, 8 and 9 have a positive role in PR. Studying the link between HHV 6 and 7 and TLRs in cases of PR is part of our ongoing research in order to report a possible link between the TLRs and HHV in the pathogenesis of PR and to detect possible triggering factors for HHV reinfection or reactivation in PR.

Conflicts of Interest

No potential conflict of interest relevant to this article was reported.

REFERENCES

1. Chuh A, Chan H, Zawar V. Pityriasis rosea: evidence for and against an infectious aetiology. Epidemiol Infect 2004; 132: 381-90.
2. Drago F, Vecchio F, Rebora A. Use of high-dose acyclovir in pityriasis rosea. J Am Acad Dermatol 2006; 54: 82-5.
3. Watanabe T, Kawamura T, Jacob SE, et al. Pityriasis rosea is associated with systemic active infection with both human herpesvirus-7 and human herpesvirus-6. J Invest Dermatol 2002; 119: 793-7.
4. Drago F, Ciccarese G, Broccolo F, Cozzani E, Parodi A. Pityriasis rosea in children: clinical features and laboratory investigations. Dermatology 2015; 231: 9-14.
5. Broccolo F, Drago F, Careddu AM, et al. Additional evidence that pityriasis rosea is associated with reactivation of human herpesvirus-6 and -7. J Invest Dermatol 2005; 124: 1234-40.
6. Trinchieri G, Sher A. Cooperation of Toll-like receptor signals in innate immune defence. Nat Rev Immunol 2007; 7: 179-90.
7. Wagner H. The immunobiology of the TLR9 subfamily. Trends Immunol 2004; 25: 381-6.
8. Yang F, Han XP. Expression of Toll-like receptor 3, 7 and 9 in peripheral blood lymphocytes from patients with pityriasis rosea. Chin J Dermatol 2012: 45: 130-2.
9. Pfaffl MW. A new mathematical model for relative quantification in real-time RT-PCR. Nucleic Acids Res 2001; 29: e45.
10. Ataseven A, Kurtipek GS, Akyurek FT, Kucukosmanoglu I, Dilek N. Unilateral pityriasis rosea. Indian Dermatol Online J 2014; 5: 528-9.
11. Carty M, Bowie AG. Recent insights into the role of Toll-like receptors in viral infection. Clin Exp Immunol 2010; 161: 397-406.
12. Miller RL, Meng TC, Tomai MA. The antiviral activity of Toll-like receptor 7 and 7/8 agonists. Drug News Perspect 2008; 21: 69-87.
13. Lau YF, Tang LH, Ooi EE. A TLR3 ligand that exhibits potent inhibition of influenza virus replication and has strong adjuvant activity has the potential for dual applications in an influenza pandemic. Vaccine 2009; 27: 1354-64.
14. Vercammen E, Staal J, Beyaert R. Sensing of viral infection and activation of innate immunity by toll-like receptor 3. Clin Microbiol Rev 2008; 21: 13-25.
15. Renn CN, Sanchez DJ, Ochoa MT, et al. TLR activation of Langerhans cell-like dendritic cells triggers an antiviral immune response. J Immunol 2006; 177: 298-305.

■ ORIGINAL ARTICLE ■

GLUT1 as a Prognostic Factor for Classical Hodgkin's Lymphoma: Correlation with PD-L1 and PD-L2 Expression

Young Wha Koh · Jae-Ho Han
Seong Yong Park[1] · Dok Hyun Yoon[2]
Cheolwon Suh[2] · Jooryung Huh[3]

Departments of Pathology and [1]Thoracic and Cardiovascular Surgery, Ajou University School of Medicine, Suwon; Departments of [2]Oncology and [3]Pathology, Asan Medical Center, University of Ulsan College of Medicine, Seoul, Korea

Corresponding Author
Jooryung Huh, MD
Department of Pathology, Asan Medical Center,
University of Ulsan College of Medicine,
88 Olympic-ro 43-gil, Songpa-gu, Seoul 05505,
Korea
Tel: +82-2-3010-4553
Fax: +82-2-472-7898
E-mail: jrhuh@amc.seoul.kr

Background: Glucose transporter type 1 (GLUT1) expression is linked to glucose metabolism and tissue hypoxia. A recent study reported that GLUT1 was significantly associated with programmed death ligand 1 (PD-L1) as a therapeutic target in relapsed or refractory classical Hodgkin's lymphoma (cHL). The purpose of this study was to measure the expression of GLUT1 and assess its prognostic significance and potential relationships with PD-L1, programmed death ligand 2 (PD-L2), and programmed death-1 (PD-1) expressions in cHL. **Methods:** Diagnostic tissues from 125 patients with cHL treated with doxorubicin, bleomycin, vinblastine, and dacarbazine were evaluated retrospectively via immunohistochemical analysis of GLUT1, PD-L1, PD-L2, and PD-1 expression. **Results:** The median follow-up time was 4.83 years (range, 0.08 to 17.33 years). GLUT1, PD-L1, PD-L2, and PD-1 were expressed in 44.8%, 63.2%, 9.6%, and 13.6% of the specimens, respectively. Positive correlations were found between GLUT1 and PD-L1 expression (p = .004) and between GLUT1 and PD-L2 expression (p = .031). GLUT1 expression in Hodgkin/Reed-Sternberg (HRS) cells was not associated with overall survival or event-free survival (EFS) in the entire cohort (p = .299 and p = .143, respectively). A subgroup analysis according to the Ann Arbor stage illustrated that GLUT1 expression in HRS cells was associated with better EFS in advanced-stage disease (p = .029). A multivariate analysis identified GLUT1 as a marginally significant prognostic factor for EFS (p = .068). **Conclusions:** This study suggests that GLUT1 expression is associated with better clinical outcomes in advanced-stage cHL and is significantly associated with PD-L1 and PD-L2 expressions.

Key Words: Hodgkin lymphoma; GLUT1; Programmed death ligand 1; Programmed death ligand 2; Programmed death-1

Classical Hodgkin lymphoma (cHL) is considered a highly curable disease with modern therapy; however, at least 20% of the patients cannot be cured with the standard treatment.[1,2] Although the International Prognostic Score (IPS) is a powerful tool for risk stratification, it does not fully reflect the biological nature of cHL. Furthermore, the prognostic significance of IPS is limited in advanced-stage disease.[3]

Glucose transporter type 1 (GLUT1) is responsible for the cellular glucose uptake, and it is often overexpressed in malignant tumors, which are characterized by an increased glycolytic rate to meet the intense energy requirements for cell proliferation.[4] GLUT1 overexpression has been correlated with a poor prognosis in several cancers including the lung,[5] breast,[6] colon,[7] and stomach cancers.[8] Although GLUT1 expression was evaluated in cHL,[9,10] it was not associated with clinical outcomes in a previous study.[9] Some cancer prediction systems such as the IPS are useful only for certain stages; however, previous studies did not perform

subgroup analyses according to the Ann Arbor stage.

The programmed death-1 (PD-1) pathway has emerged as an important mechanism for tumor evasion from anti-tumor immune responses.[11] Two ligands for PD-1, programmed death ligand 1 (PD-L1) and programmed death ligand 2 (PD-L2), act as negative immune regulators via interactions with the PD-1 receptor.[12] PD-1/PD-L1 and PD-L2 have been reported as prognostic biomarkers for hepatocellular carcinoma,[13] urothelial carcinoma,[14] breast cancer,[15] lung cancer,[16] and colorectal cancer.[17]

Hypoxia-inducible factors (HIFs) play an important role in tumor immune responses.[18] HIF-1a and HIF-2α stabilized by hypoxia promote the expression of PD-L1 via binding to a specific hypoxia-response element in the promoter of PD-L1 in myeloid-derived suppressor cells, dendritic cells, and macrophages, as well as in prostate, breast, and colorectal cancer cell lines.[19-22] It will be interesting to evaluate the relationship between GLUT1 and PD-L1 because GLUT1 is a well-known target gene of the

HIF pathways.[19,22,23] A recent study reported that PD-L1 expression is regulated by GLUT1 in clear cell renal cell carcinoma.[24] An anti–PD-1 monoclonal antibody (nivolumab) has exhibited substantial therapeutic activity and an acceptable safety profile in relapsed or refractory cHL.[25] A GLUT1-specific inhibitor (STF-31) also suppressed glucose uptake and induced apoptosis in myeloma cells with high GLUT1 expression.[26] However, no study has examined the relationship between PD-L1 and GLUT1 in patients with cHL. This retrospective study evaluated the expression of GLUT1 and assessed its prognostic significance and potential relationships with PD-L1, PD-L2, and PD-1 expressions in cHL.

MATERIALS AND METHODS

Patients

A retrospective analysis of 125 consecutive patients diagnosed with cHL at Asan Medical Center between 1995 and 2012 and at Ajou University Hospital between 2008 and 2015 was performed. All patients were pathologically confirmed to have cHL and treated with the doxorubicin, bleomycin, vinblastine, and dacarbazine (ABVD) therapy regimen, with or without radiation. The patients were ≥15 years of age at diagnosis, and they had no previous treatment or history of malignancy. Paraffin-embedded tumor tissues and follow-up data were available for all patients included in the study. The median follow-up time was 4.83 years (range, 0.08 to 17.33 years). Response criteria were based on standard guidelines. Routine follow-up imaging analyses were performed every 3 months for the first 2 years, every 6 months for the next 3 years, and annually (or whenever clinically indicated) thereafter. The results of PD-L1, PD-L2, and PD-1 expressions from a previously reported study were used.[27] The research was approved by the Institutional Review Board of Asan Medical Center.

Histopathological analysis and immunohistochemistry

All histological and immunophenotypic data were reviewed by two pathologists (J.H. and Y.W.K.). The cases of cHL were subtyped according to the World Health Organization criteria as nodular sclerosis, lymphocyte-rich, mixed cellularity, lymphocyte-depleted, or not otherwise specified cHL. Tissue microarrays (TMAs) were constructed using three 1-mm-diameter tumor cores from selected areas of formalin-fixed, paraffin-embedded tumor samples. TMA sections were stained using a Benchmark XT automatic immunohistochemistry staining device (Ventana Medical Systems, Tucson, AZ, USA). Anti-

GLUT1 (Cell Marque, Rocklin, CA, USA), anti–PD-L1 (Cell Signaling Technology, Danvers, MA, USA), anti–PD-L2 (R&D Systems, Minneapolis, MN, USA), and anti–PD-1 antibodies (Cell Marque) were used. In the TMA, each case was represented by three tissue cores, and at least 10 CD30-positive Hodgkin/Reed-Sternberg (HRS) cells in at least one of the three core cylinders from each patient were read. To minimize the counting of cells, other than small lymphocytes, with nonspecific PD-1 staining we counted only the cells with staining that were morphologically compatible with small lymphocytes in the microenvironment (excluded fibroblasts, endothelial cells, HRS cells, and macrophages) based on their size, shape, and CD30 staining. We examined the protein expression of GLUT1, PD-L1, PD-L2, and PD-1 in 5% increments. The cut-off values of GLUT1, PD-L1, PD-L2, and PD-1 associated with the most significant differences in overall survival (OS) were selected. A sample was considered GLUT1-, PD-L1–, or PD-L2–positive if the expression of these markers was detected in ≥20% of HRS cells. A sample was considered PD-1–positive if PD-1 expression was detected in ≥20% of the peritumoral microenvironment. *In situ* hybridization analysis of Epstein-Barr virus–encoded RNA-1 and RNA-2 was performed and scored as previously described.[28]

Statistical analyses

Event-free survival (EFS) was defined as the interval between the date of diagnosis and that of disease progression, relapse, or death from any cause. OS was defined as the interval between the date of diagnosis and that of death from any cause. The follow-up of patients was censored at their last follow-up date. Cumulative OS or EFS was analyzed using the Kaplan-Meier method, and comparisons were performed via log-rank testing. Multivariate prognostic analyses was performed with the Cox proportional hazards regression model using the enter method. Categorical variables were compared using the chi-squared test. All statistical analyses were performed using the SPSS statistical software program ver. 18.0 (SPSS Inc., Chicago, IL, USA). All p-values were two-sided associations, and p < .05 was considered statistically significant.

RESULTS

Patient characteristics

The clinical characteristics of the 125 patients are summarized in Table 1. The median age of the patients was 39 years (range, 15 to 78 years). Twenty-five patients died. The median OS was not achieved, and the median EFS was 11 years. The estimated

Table 1. Demographic and clinical characteristics of patients

Characteristics at diagnosis	No. of patients (%)
Age, median (range, yr)	39 (15–78)
Male gender	74 (59.2)
Histologic subtype	
Nodular sclerosis	83 (66.4)
Mixed cellularity	27 (21.6)
Lymphocyte-rich	6 (4.8)
Lymphocyte-depleted	3 (2.4)
Not classifiable	6 (4.8)
Ann Arbor stage	
I	26 (20.8)
II	41 (32.8)
III	29 (23.2)
IV	29 (23.2)
Stage (limited vs advanced)	
Limited	48 (38.4)
Advanced	77 (61.6)
B symptoms present	41 (32.8)
International Prognostic Score ≥3 (high-risk)	49 (39.2)
EBER positivity	49 (39.2)
Primary treatment	
Chemotherapy	95 (76.0)
Chemoradiotherapy	30 (24.0)

EBER, Epstein-Barr virus–encoded RNA-1 and RNA-2 assessed by *in situ* hybridization.

5-year OS and EFS rates were 84% and 61%, respectively.

GLUT1 expression in cHL tissues

The correlations between GLUT1 and clinical variables are summarized in Table 2. Fifty-six patients (44.8%) displayed membranous positivity for GLUT1 (Fig. 1A). There was no correlation between GLUT1 expression and clinical variables.

Correlations of PD-L1, PD-L2, and PD-1 expression with GLUT1 expression

PD-L1, PD-L2, and PD-1 were expressed in 63.2%, 9.6%, and 13.6% of the specimens, respectively (Fig. 1B–D). The correlations of PD-L1, PD-L2, and PD-1 expression with GLUT1 expression are summarized in Table 3. GLUT1 protein expression was associated with high PD-L1 (p = .004) and high PD-L2 protein expression in HRS cells (p = .031). However, there was no correlation between GLUT1 levels in HRS cells and PD-1 expression in the peritumoral microenvironment (p = .198).

Prognostic significance of GLUT1 expression

GLUT1 expression was not associated with EFS and OS rates (p = .143 and p = .299, respectively). As the prognostic significance of the IPS is limited in advanced-stage disease,[3] we performed a

Table 2. Correlations between clinical variables and GLUT1 expression in all cases

Characteristic	GLUT1 expression		p-value
	Low (<20%) (n=69)	High (≥20%) (n=56)	
Age (yr)			.858[a]
<45	38 (55.1)	32 (57.1)	
≥45	31 (44.9)	24 (42.9)	
Gender			.276[a]
Male	44 (63.8)	30 (53.6)	
Female	25 (36.2)	26 (46.4)	
Disease subtype			.182[b]
Nodular sclerosis	43 (62.3)	40 (71.4)	
Mixed cellularity	14 (20.3)	13 (23.2)	
Lymphocyte-rich	6 (8.7)	0	
Lymphocyte-depleted	2 (2.9)	1 (1.8)	
Not classifiable	4 (5.8)	2 (3.6)	
B symptom			.184[a]
Absent	50 (72.5)	34 (60.7)	
Present	19 (27.5)	22 (39.3)	
Ann Arbor stage			.586[a]
Limited	28 (40.6)	20 (35.7)	
Advanced	41 (59.4)	36 (64.3)	
IPS			.467[a]
<3	44 (63.8)	32 (57.1)	
≥3	25 (36.2)	24 (42.9)	
EBER			.467[a]
Negative	44 (63.8)	32 (57.1)	
Positive	25 (36.2)	24 (42.9)	
Primary treatment			.674[a]
Chemotherapy	51 (73.9)	44 (78.6)	
Chemoradiotherapy	18 (26.1)	12 (21.4)	

Values are presented as number (%).
GLUT1, glucose transporter 1; IPS, International Prognostic Score; EBER, Epstein-Barr virus-encoded RNA-1 and RNA-2 assessed by *in situ* hybridization.
[a]Chi-squared test by two-sided Pearson's test; [b]Chi-squared test by two-sided Fisher test.

subgroup analysis according to the disease stage to determine whether GLUT1 expression has prognostic significance in certain stages. In limited-stage cHL, GLUT1 expression was not associated with EFS and OS rates (p = .906 and p = .833, respectively). In advanced-stage cHL, GLUT1 positivity was associated with better EFS (p = .029) (Fig. 2A). However, there was no association between GLUT1 expression and OS in advanced-stage cHL (p = .168) (Fig. 2B).

Univariate analysis revealed that EFS was associated with advanced age and anemia (Table 4). Multivariate analysis identified GLUT1 as a marginally significant prognostic factor for EFS, together with advanced age and anemia (hazard ratio, 0.462; p = .068) (Table 4).
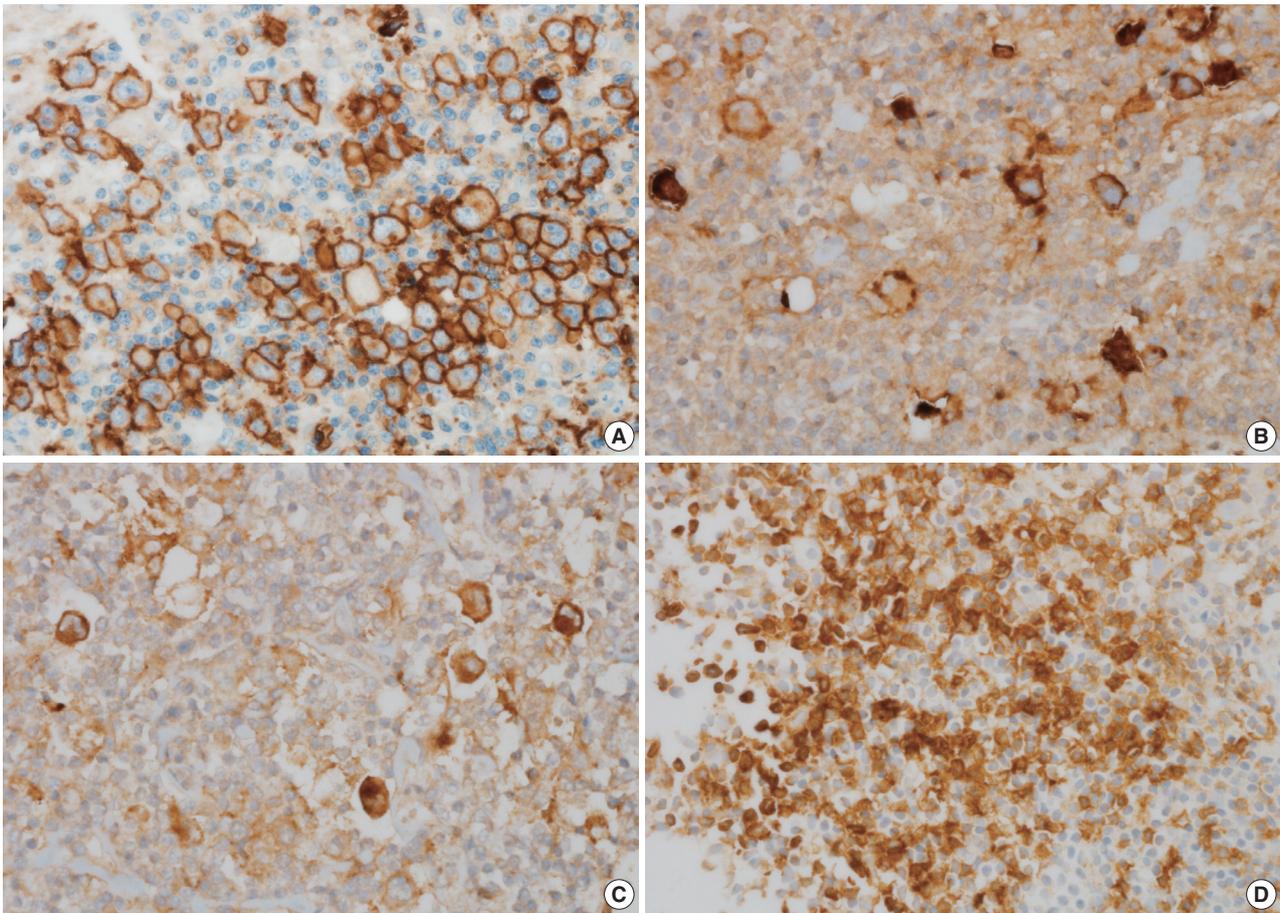
Fig. 1. Glucose transporter type 1 (GLUT1), programmed death ligand 1 (PD-L1), programmed death ligand 2 (PD-L2), and programmed death-1 (PD-1) expression in classical Hodgkin's lymphoma tissues. (A) High GLUT1 expression in Hodgkin/Reed–Sternberg (HRS) cells (≥ 20%). (B) High PD-L1 expression in HRS cells (≥ 20%). (C) High PD-L2 expression in HRS cells (≥ 20%). (D) High PD-1 expression in the peritumoral microenvironment (≥ 20%).

Table 3. Correlations between GLUT1, PD-L1, PD-L2, and PD-1 expression in all cases

| Characteristic | GLUT1 expression | | p-value |
	Low (< 20%) (n = 69)	High (≥ 20%) (n = 56)	
PD-L1 expression in HRS cells			.004[a]
Low (< 20%)	19 (33.3)	4 (8.9)	
High (≥ 20%)	38 (66.7)	41 (91.1)	
PD-L2 expression in HRS cells			.299[a]
Low (< 20%)	54 (94.7)	36 (80.0)	
High (≥ 20%)	3 (5.3)	9 (20.0)	
PD-1 expression in peritumoral microenvironment			.198[a]
Low (< 20%)	57 (82.6)	51 (91.1)	
High (≥ 20%)	12 (17.4)	5 (8.9)	

Values are presented as number (%).
GLUT1, glucose transporter type 1; PD-L1, programmed death ligand 1; PD-L2, programmed death ligand 2; PD-1, programmed death-1; HRS, Hodgkin/Reed–Sternberg.
[a]Chi-squared test by two-sided Pearson's test.

DISCUSSION

In the present study, the expression of GLUT1 was significantly correlated with PD-L1 and PD-L2 expression, supporting the hypothesis that GLUT1-related signaling pathways play an important role in the PD-L1 or PD-L2 pathway. In particular, GLUT1 expression was marginally associated with better EFS in advanced-stage cHL.

There are several explanations for the relationships between PD-1 pathways and GLUT1 expression. HIF-2α overexpression stabilized by hypoxia increased PD-L1 mRNA and protein levels in a kidney clear cell carcinoma cell line.[19] A previous study also revealed the direct binding of HIF-2α to a transcriptionally active hypoxia-response element in the human PD-L1 proximal promoter.[19] GLUT1 is an important downstream target of HIF-2α.[19,22] Therefore, a significant correlation between GLUT1 and PD-L1 expression was identified in clear cell renal cell carcino-
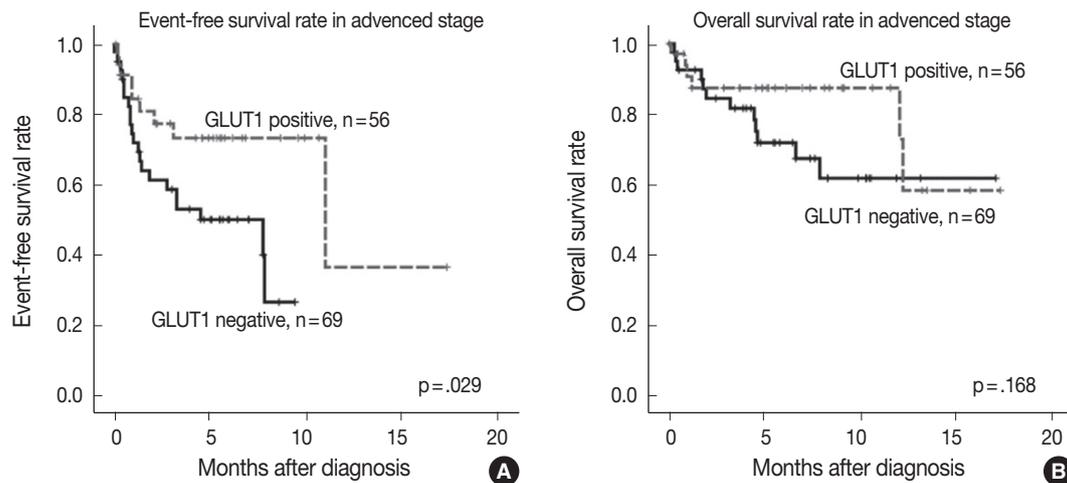
Fig. 2. Comparison of survival rates according to glucose transporter type 1 (GLUT1) expression in advanced-stage classical Hodgkin's lymphoma. The event-free survival rate is significantly higher in the GLUT1-positive group than in the GLUT1-negative group (A). GLUT1 expression is not significantly associated with the overall survival rate (B).

Table 4. Univariate and multivariate analysis of event-free survival in advanced stage

Covariate		HR	95% CI	p-value[a]
Univariate analysis				
Age	<45 yr vs ≥45 yr	3.22	1.47–7.05	.003
Sex	Female vs male	1.52	0.72–3.20	.271
B symptoms	(–) vs (+)	1.85	0.86–3.96	.112
EBER	(–) vs (+)	1.64	0.94–2.85	.081
Lymphopenia	(–) vs (+)	1.32	0.31–5.55	.706
Leukocytosis	(–) vs (+)	1.38	0.46–4.14	.563
Hypoalbuminemia	(–) vs (+)	1.65	0.62–4.31	.311
Anemia	(–) vs (+)	2.31	1.07–4.94	.032
GLUT1 expression	(-) vs (+)	0.42	0.18–0.94	.035
Multivariate analysis				
Age	<45 yr vs ≥45 yr	2.47	1.08–5.61	.031
Anemia	(–) vs (+)	1.92	0.86–4.24	.107
GLUT1 expression	(–) vs (+)	0.46	0.20–1.05	.068

HR, hazard ratio; CI, confidence interval; EBER, Epstein-Barr virus–encoded RNA-1 and RNA-2 assessed by *in situ* hybridization; GLUT1, glucose transporter 1.
[a]Cox univariate analysis.

ma.[24] In our study, 91% of patients with GLUT1-positive status had PD-L1 positive status, supporting the HIF-2α–Glut1–PD-L1 pathway identified in a previous study. However, 48% of patients with PD-L1–positive status had GLUT1 negative status. Further studies are needed to confirm the precise mechanism of the PD-L1 pathway, regardless of GLUT1 expression, in patients with cHL.

In the present study, GLUT1 expression was associated with better EFS in advanced-stage cHL, although the result was of borderline statistical significance. GLUT1 expression was not associated with EFS or OS rates in the entire patient cohort. Hartmann *et al.*[9] reported no prognostic significance for GLUT1 expression in cHL. However, Hartmann *et al.*[9] did not perform subgroup analysis according to the Ann Arbor stage. Some

prognostic biomarkers have limited importance in certain clinical stages. The IPS also has prognostic significance in advanced-stage cHL. Moreover, further research is needed to confirm the prognostic impact of GLUT1 expression.

Although our results revealed a favorable clinical outcome in patients with GLUT1-positive advanced-stage cHL, previous studies revealed correlations between high GLUT1 expression and poor survival in other solid malignancies.[5-8] In the present study, all patients received the ABVD regimen. Doxorubicin and vinblastine are associated with DNA damage. Doxorubicin inhibits the progression of the enzyme topoisomerase II, which relaxes supercoils in DNA for transcription.[29] Vinblastine can suppress microtubule dynamics, resulting in mitotic block and apoptosis.[30] Therefore, HRS cells with higher proliferation rates

would be more susceptible to chemotherapy-associated DNA damage. GLUT1 overexpression increases glucose metabolism in tumors to enhance cellular proliferation in melanoma and gastric cancer.[31,32] Some studies ascribed the superior survival of patients with diffuse large B-cell lymphoma or cHL to increased sensitivity to chemotherapy due to higher cell proliferation rates.[33,34] Although we did not examine the proliferation rates of HRS cells in our series, the superior survival of cHL patients with GLUT1 expression in our study may imply higher proliferation rates of HRS cells.

Differential expression of GLUT1 was detected according to the histologic type of cHL in a previous study.[9] GLUT1 expression was more rarely observed in HRS cells in the lymphocyte-rich classical cHL subtype (30%) than in the nodular sclerosis (56%), mixed cellularity (41%), or lymphocyte-depleted subtype (100%). Our series also identified lower expression of GLUT1 in the lymphocyte-rich classical cHL subtype (0%) than in other subtypes.

A GLUT1-specific inhibitor (STF-31) induces apoptosis and sensitizes multiple myeloma cells to conventional chemotherapeutic agents.[26] A recent study found that the GLUT1-specific inhibitor apigenin induces growth retardation and apoptosis through metabolic and oxidative stress caused by the suppression of glucose utilization in lung cancer and adenoid cystic carcinoma.[35] WZB117 also exerts inhibitory effects on cancer cell growth in breast and lung cancer cell lines.[36,37] Nivolumab has been tested in patients with advanced cHL, and impressive results were obtained in phase I trial.[25] Pembrolizumab, an IgG4 monoclonal antibody directed against PD-1, also induced favorable responses in a heavily pretreated patient with cHL.[38] Although an objective response was reported in 87% of patients with advanced cHL treated with nivolumab, only 17% of patients exhibited complete responses.[25] Based on the significant correlations of GLUT1 with PD-L1 and PD-L2 in this study and a previous study,[24] the HIF-2α–GLUT1–PD-L1 pathway may be efficiently inhibited by GLUT1-specific inhibitor and PD-1–specific inhibitor.

In summary, our results suggest that GLUT1 expression is significantly associated with the expression of PD-L1 and PD-L2. GLUT1 expression has prognostic significance in advanced-stage cHL. Further efforts to understand the mechanisms of the correlations of GLUT1 with PD-L1 and PD-L2 may help the development of effective therapeutic agents for the treatment of cHL.

REFERENCES

1. Björkholm M, Axdorph U, Grimfors G, et al. Fixed versus response-adapted MOPP/ABVD chemotherapy in Hodgkin's disease: a prospective randomized trial. Ann Oncol 1995; 6: 895-9.

2. Quddus F, Armitage JO. Salvage therapy for Hodgkin's lymphoma. Cancer J 2009; 15: 161-3.

3. Hasenclever D, Diehl V. A prognostic score for advanced Hodgkin's disease: international prognostic factors project on advanced Hodgkin's disease. N Engl J Med 1998; 339: 1506-14.

4. Barron CC, Bilan PJ, Tsakiridis T, Tsiani E. Facilitative glucose transporters: implications for cancer detection, prognosis and treatment. Metabolism 2016; 65: 124-39.

5. Osugi J, Yamaura T, Muto S, et al. Prognostic impact of the combination of glucose transporter 1 and ATP citrate lyase in node-negative patients with non-small lung cancer. Lung Cancer 2015; 88: 310-8.

6. Pinheiro C, Sousa B, Albergaria A, et al. GLUT1 and CAIX expression profiles in breast cancer correlate with adverse prognostic factors and MCT1 overexpression. Histol Histopathol 2011; 26: 1279-86.

7. Haber RS, Rathan A, Weiser KR, et al. GLUT1 glucose transporter expression in colorectal carcinoma: a marker for poor prognosis. Cancer 1998; 83: 34-40.

8. Kawamura T, Kusakabe T, Sugino T, et al. Expression of glucose transporter-1 in human gastric carcinoma: association with tumor aggressiveness, metastasis, and patient survival. Cancer 2001; 92: 634-41.

9. Hartmann S, Agostinelli C, Diener J, et al. GLUT1 expression patterns in different Hodgkin lymphoma subtypes and progressively transformed germinal centers. BMC Cancer 2012; 12: 586.

10. Shim HK, Lee WW, Park SY, Kim H, Kim SE. Relationship between FDG uptake and expressions of glucose transporter type 1, type 3, and hexokinase-II in Reed-Sternberg cells of Hodgkin lymphoma. Oncol Res 2009; 17: 331-7.

11. Weber J. Immune checkpoint proteins: a new therapeutic paradigm for cancer: preclinical background: CTLA-4 and PD-1 blockade. Semin Oncol 2010; 37: 430-9.

12. Keir ME, Butte MJ, Freeman GJ, Sharpe AH. PD-1 and its ligands

in tolerance and immunity. Annu Rev Immunol 2008; 26: 677-704.

13. Zeng Z, Shi F, Zhou L, *et al*. Upregulation of circulating PD-L1/PD-1 is associated with poor post-cryoablation prognosis in patients with HBV-related hepatocellular carcinoma. PLoS One 2011; 6: e23621.

14. Bellmunt J, Mullane SA, Werner L, *et al*. Association of PD-L1 expression on tumor-infiltrating mononuclear cells and overall survival in patients with urothelial carcinoma. Ann Oncol 2015; 26: 812-7.

15. Muenst S, Schaerli AR, Gao F, *et al*. Expression of programmed death ligand 1 (PD-L1) is associated with poor prognosis in human breast cancer. Breast Cancer Res Treat 2014; 146: 15-24.

16. Zhang Y, Wang L, Li Y, *et al*. Protein expression of programmed death 1 ligand 1 and ligand 2 independently predict poor prognosis in surgically resected lung adenocarcinoma. Onco Targets Ther 2014; 7: 567-73.

17. Droeser RA, Hirt C, Viehl CT, *et al*. Clinical impact of programmed cell death ligand 1 expression in colorectal cancer. Eur J Cancer 2013; 49: 2233-42.

18. Kumar V, Gabrilovich DI. Hypoxia-inducible factors in regulation of immune responses in tumour microenvironment. Immunology 2014; 143: 512-9.

19. Messai Y, Gad S, Noman MZ, *et al*. Renal cell carcinoma programmed death-ligand 1, a new direct target of hypoxia-inducible factor-2 alpha, is regulated by von Hippel-Lindau gene mutation status. Eur Urol 2016; 70: 623-32.

20. Noman MZ, Desantis G, Janji B, *et al*. PD-L1 is a novel direct target of HIF-1alpha, and its blockade under hypoxia enhanced MDSC-mediated T cell activation. J Exp Med 2014; 211: 781-90.

21. Barsoum IB, Smallwood CA, Siemens DR, Graham CH. A mechanism of hypoxia-mediated escape from adaptive immunity in cancer cells. Cancer Res 2014; 74: 665-74.

22. Li QQ, Sun YP, Ruan CP, *et al*. Cellular prion protein promotes glucose uptake through the Fyn-HIF-2alpha-Glut1 pathway to support colorectal cancer cell survival. Cancer Sci 2011; 102: 400-6.

23. Rapisarda A, Uranchimeg B, Scudiero DA, *et al*. Identification of small molecule inhibitors of hypoxia-inducible factor 1 transcriptional activation pathway. Cancer Res 2002; 62: 4316-24.

24. Ruf M, Moch H, Schraml P. PD-L1 expression is regulated by hypoxia inducible factor in clear cell renal cell carcinoma. Int J Cancer 2016; 139: 396-403.

25. Ansell SM, Lesokhin AM, Borrello I, *et al*. PD-1 blockade with nivolumab in relapsed or refractory Hodgkin's lymphoma. N Engl J Med 2015; 372: 311-9.

26. Matsumoto T, Jimi S, Migita K, Takamatsu Y, Hara S. Inhibition of glucose transporter 1 induces apoptosis and sensitizes multiple myeloma cells to conventional chemotherapeutic agents. Leuk Res 2016; 41: 103-10.

27. Koh YW, Jeon YK, Yoon DH, Suh C, Huh J. Programmed death 1 expression in the peritumoral microenvironment is associated with a poorer prognosis in classical Hodgkin lymphoma. Tumour Biol 2016; 37: 7507-14.

28. Huh J, Cho K, Heo DS, Kim JE, Kim CW. Detection of Epstein-Barr virus in Korean peripheral T-cell lymphoma. Am J Hematol 1999; 60: 205-14.

29. Pommier Y, Leo E, Zhang H, Marchand C. DNA topoisomerases and their poisoning by anticancer and antibacterial drugs. Chem Biol 2010; 17: 421-33.

30. Jordan MA, Wilson L. Microtubules as a target for anticancer drugs. Nat Rev Cancer 2004; 4: 253-65.

31. Koch A, Lang SA, Wild PJ, *et al*. Glucose transporter isoform 1 expression enhances metastasis of malignant melanoma cells. Oncotarget 2015; 6: 32748-60.

32. Yan S, Wang Y, Chen M, Li G, Fan J. Deregulated SLC2A1 promotes tumor cell proliferation and metastasis in gastric cancer. Int J Mol Sci 2015; 16: 16144-57.

33. Uddin S, Hussain AR, Ahmed M, *et al*. Inhibition of c-MET is a potential therapeutic strategy for treatment of diffuse large B-cell lymphoma. Lab Invest 2010; 90: 1346-56.

34. Dinand V, Malik A, Unni R, Arya LS, Pandey RM, Dawar R. Proliferative index and CD15 expression in pediatric classical Hodgkin lymphoma. Pediatr Blood Cancer 2008; 50: 280-3.

35. Lee YM, Lee G, Oh TI, *et al*. Inhibition of glutamine utilization sensitizes lung cancer cells to apigenin-induced apoptosis resulting from metabolic and oxidative stress. Int J Oncol 2016; 48: 399-408.

36. Liu Y, Cao Y, Zhang W, *et al*. A small-molecule inhibitor of glucose transporter 1 downregulates glycolysis, induces cell-cycle arrest, and inhibits cancer cell growth *in vitro* and *in vivo*. Mol Cancer Ther 2012; 11: 1672-82.

37. Zhao F, Ming J, Zhou Y, Fan L. Inhibition of Glut1 by WZB117 sensitizes radioresistant breast cancer cells to irradiation. Cancer Chemother Pharmacol 2016; 77: 963-72.

38. Armand P, Shipp MA, Ribrag V, *et al*. Programmed death-1 blockade with pembrolizumab in patients with classical Hodgkin lymphoma after brentuximab vedotin failure. J Clin Oncol 2016 Jun 27 [Epub]. https://doi.org/10.1200/JCO.2016.67.3467.

A Pyloric Gland-Phenotype Ovarian Mucinous Tumor Resembling Lobular Endocervical Glandular Hyperplasia in a Patient with Peutz-Jeghers Syndrome

Eun Na Kim · Gu-Hwan Kim[1]
Jiyoon Kim · In Ah Park
Jin Ho Shin · Yun Chai
Kyu-Rae Kim

Department of Pathology, Asan Medical Center, University of Ulsan College of Medicine, Seoul; [1]Department of Medical Genetics, Asan Medical Center Children's Hospital, Seoul, Korea

Corresponding Author
Kyu-Rae Kim, MD
Department of Pathology, Asan Medical Center, University of Ulsan College of Medicine, 88 Olympic-ro 43-gil, Songpa-gu, Seoul 05505, Korea
Tel: +82-2-3010-4514
Fax: +82-2-472-7898
E-mail: krkim@amc.seoul.kr

We describe an ovarian mucinous neoplasm that histologically resembles lobular endocervical glandular hyperplasia (LEGH) containing pyloric gland type mucin in a patient with Peutz-Jeghers syndrome (PJS). Although ovarian mucinous tumors rarely occur in PJS patients, their pyloric gland phenotype has not been clearly determined. The histopathologic features of the ovarian mucinous tumor were reminiscent of LEGH. The cytoplasmic mucin was stained with periodic acid-Schiff reaction after diastase treatment but was negative for Alcian blue pH 2.5, suggesting the presence of neutral mucin. Immunohistochemically, the epithelium expressed various gastric markers, including MUC6, HIK1083, and carbonic anhydrase-IX. Multiple ligation-dependent probe amplification detected a germline heterozygous deletion mutation at exons 1–7 of the *STK11* gene (c.1-?_920+?del) in peripheral blood leukocytes and mosaic loss of heterozygosity in ovarian tumor tissue. Considering that LEGH and/or gastric-type cervical adenocarcinoma can be found in patients with PJS carrying germline and/or somatic *STK11* mutations, our case indicates that *STK11* mutations have an important role in the proliferation of pyloric-phenotype mucinous epithelium at various anatomical locations.

Key Words: Pyloric gland type; Lobular endocervical glandular hyperplasia; Mucinous; Ovary; Peutz-Jeghers syndrome

Peutz-Jeghers syndrome (PJS) is an autosomal dominant hereditary disorder characterized by hamartomatous polyposis of the gastrointestinal tract and mucocutaneous pigmentation around the lips. Patients with PJS have a higher incidence of benign or malignant neoplasia of the female genital tract, including minimal deviation adenocarcinoma of the uterine cervix, sex cord tumor with annular tubules, Sertoli cell tumor of the ovary,[1] and mucinous metaplasia of the fallopian tube and endometrium, as well as extragenital tumors, such as carcinomas of the breast, pancreas, and gastrointestinal tract. Germline mutation of the serine/threonine kinase 11 (*STK11*)/liver kinase B1 (*LKB1*) gene in patients with PJS[2] and somatic mutation of the *STK11* gene in patients with sporadic cases of minimal deviation adenocarcinoma of the uterine cervix[3] have suggested that the protein product of the *STK11* gene has a putative tumor suppressor function and that mutation of the gene plays an important role in the pathogenesis of mucin-producing tumors at various sites. On the other hand, lobular endocervical glandular hyperplasia (LEGH) of the uterine cervix has rarely been reported in patients with PJS; however, ovarian tumor resembling LEGH is even rarer in these patients.

We encountered an ovarian mucinous neoplasm in a patient with PJS (confirmed by *STK11* germline mutation), in which the histopathologic features of the ovarian mass were reminiscent of LEGH. The epithelium contained pyloric gland-type mucin and expressed immunohistochemical markers for pyloric glands. Here, we describe the clinicopathologic findings in a PJS patient with an ovarian mucinous tumor with a pyloric gland type mucin.

CASE REPORT

A 47-year-old postmenopausal woman presented with slowly increasing abdominal girth with a palpable abdominal mass and vaginal bleeding. At the age of 15, she underwent abdominal
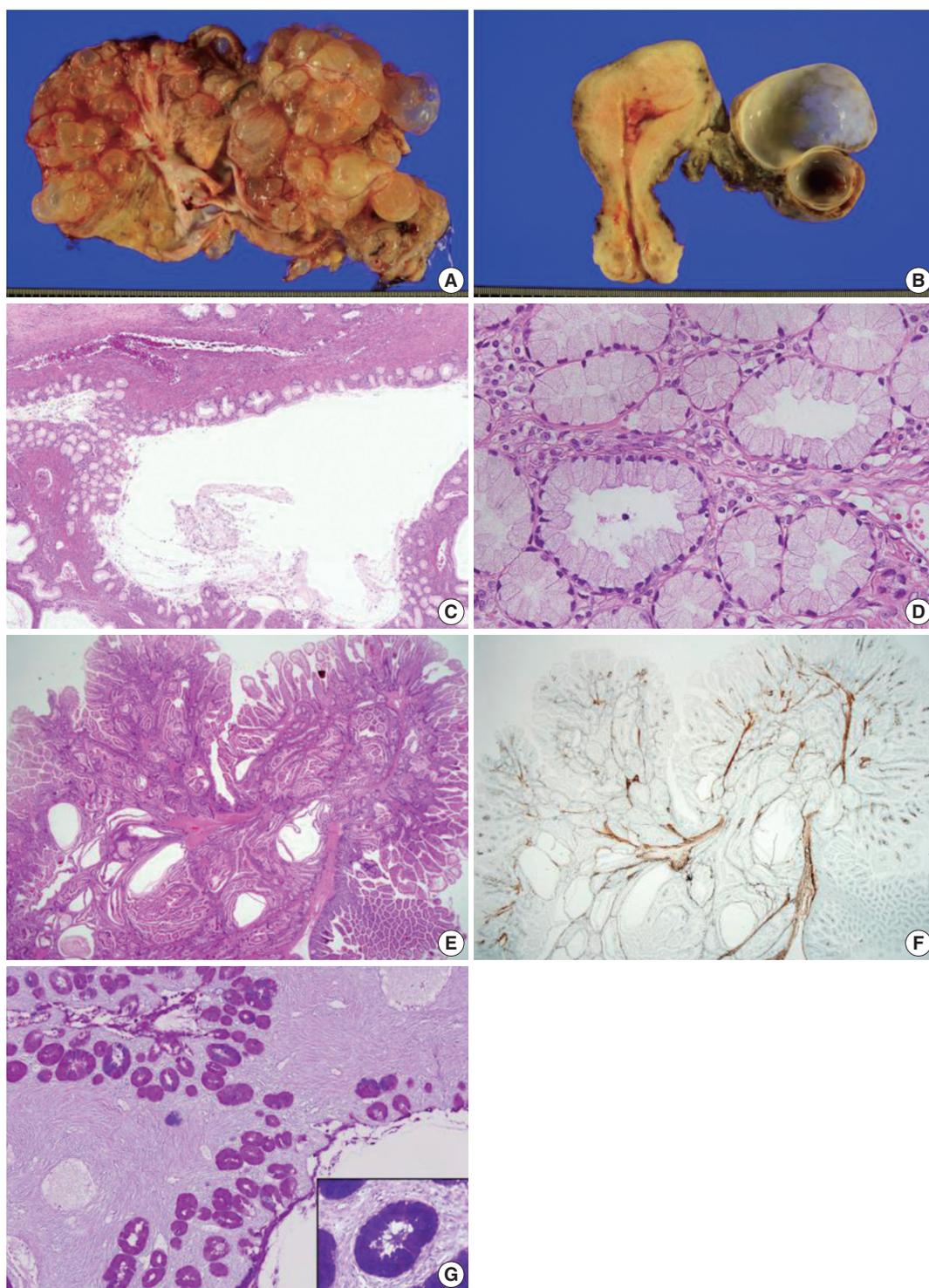
Fig. 1. Sectioned surface of the left ovary showing multilocular cysts filled with mucinous fluid (A) and the cut surface of the right ovary (B). No apparent abnormality is identified on the surface of the uterine cervix and endometrium. Microscopically, the ovarian mucinous tumor is composed of a large dilated duct-like structure with clusters of small glands, reminiscent of lobular endocervical glandular hyperplasia of the uterine cervix (C). At higher magnification, the cysts are lined by a single layer of mucinous epithelium with bland nuclei and pale eosinophilic cytoplasm. Stratification or mitosis is not identified (D). The small bowel polyps in this patient show hyperplastic mucosa with arborizing strands of smooth muscle in various directions (E), highlighted by desmin immunostaining (F). Combined Alcian blue pH 2.5 and periodic acid-Schiff stains after diastase treatment show bright pink-colored cytoplasm, indicating predominant neutral mucin in the cytoplasm of the ovarian mucinous epithelium (G) in contrast to the purple-violet color in normal endocervical epithelium (G, inlet).
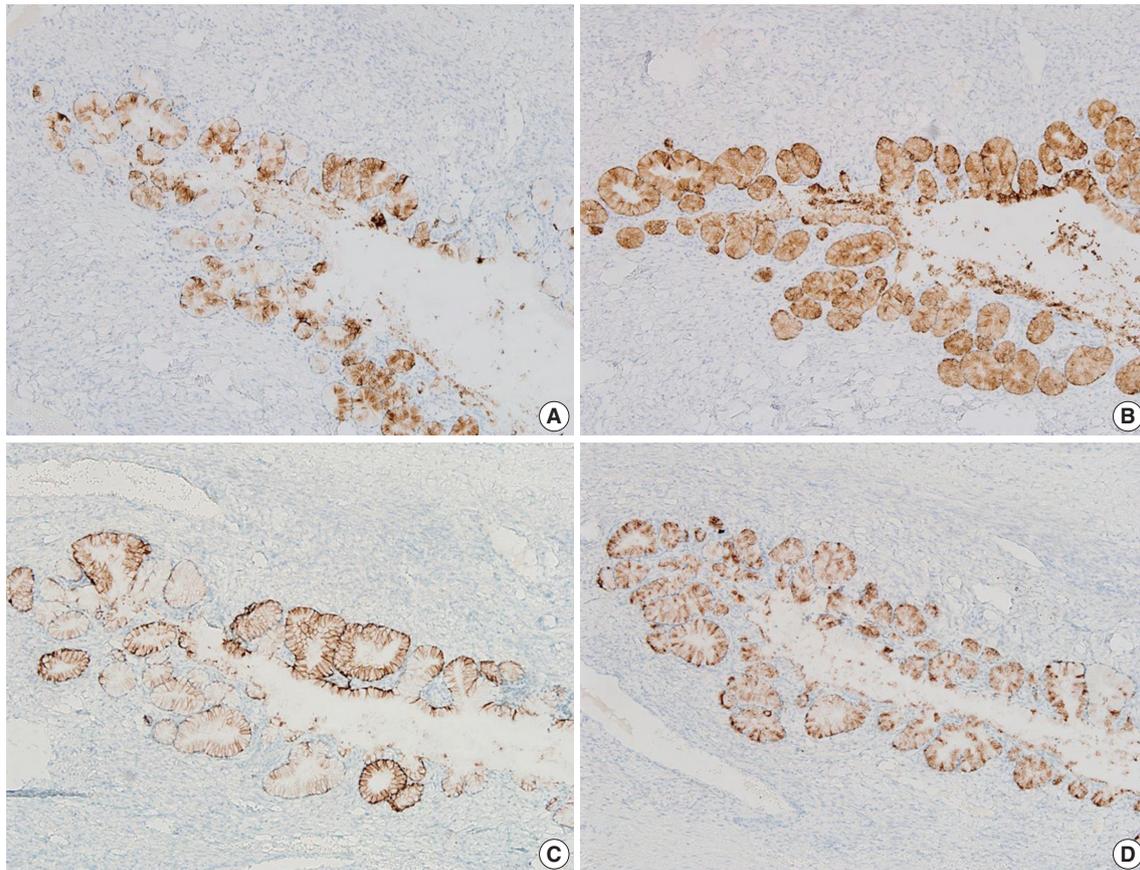
Fig. 2. The mucinous epithelium of the ovary shows immunoreactivity for various gastric markers, including MUC5AC (A), MUC6 (B), carbonic anhydrase-IX (C), and HIK1083 (D), indicating the gastric phenotype of the mucinous epithelium.

surgery due to intussusception of the small bowel of unknown cause. During the preoperative evaluation, colonoscopy identified eight hamartomatous polyps, nine hyperplastic polyps, and two tubulovillous adenomas in her large intestine. She had abundant mucocutaneous melanin pigmentation around the lips. Based on her clinical features and the histopathological diagnosis of hamartomatous polyps and mucocutaneous pigmentation, she was clinically diagnosed with PJS. No other family members had clinical signs of PJS. On pelvic and abdominal ultrasonography and computed tomography, she was found to have huge bilateral ovarian cystic masses with ascites in the pelvic cavity. On exploratory laparotomy, the left ovarian mass was ruptured, and approximately 1,500 mL of ascitic fluid was identified. The patient underwent hysterectomy, bilateral salpingo-oophorectomy, and small bowel polypectomy via small bowel enterostomy.

Grossly, the left ovarian tumor was a multilocular cyst measuring $22 \times 20 \times 6$ cm (Fig. 1A), whereas the right ovarian tumor was an oligolocular cyst measuring $8 \times 7 \times 5$ cm (Fig. 1B). The septa of the cysts were thin and the internal surface was smooth. Both cystic tumors contained mucinous fluid without any solid

Table 1. PCR primers for the *STK11* gene

STK11 exon	Sense (5' to 3')	Antisense (5' to 3')
Exon 1a	tggagaagggaagtcggaa	tgaggatcttgacggccc
Exon 1b	tcggcaagtacctgatggg	gaaagtccgtaacgcaggc
Exon 2	gtacgccacttccacaggg	ggaaccagggaaggccac
Exon 3	cctccagagccccttttct	gcttgcagtgagccgagat
Exon 4	ctgtggtgtttgggaggct	agaaggtgtccaggccgtt
Exon 5	ggggaacctgctgctcac	tgtggccagagagggtctg
Exon 6	cctctggtccagcagcca	tcggcctctccactcagtc
Exon 7	ccagggcctgacaacagag	actgcccagagaccccact
Exon 8	ctcctgagtgtgtggcaggt	caccagagggcagaagctg
Exon 9	cagctgtaagtgcgtcccc	ccatgactgactagcgcgg

PCR, polymerase chain reaction.

area. Microscopically, both ovarian tumors showed cysts of varying sizes lined by a single layer of columnar epithelium, and the architecture of the glandular arrangement was characterized by clusters of small glands budding from surrounding a centrally located large duct-like structures, forming a lobular arrangement at lower magnification (Fig. 1C). The mucinous epithelium had pale eosinophilic cytoplasm with basally located nuclei (Fig. 1D). Neither epithelial stratification nor nuclear atypia

was identified. There were no foci of sex cord tumor with annular tubules in both ovaries. The uterine cervix, endometrium, and fallopian tubes were meticulously examined, but no histologic

evidence of mucinous epithelial lesions or metaplasia was identified.

Polyps of the small intestine showed a branching polypoid
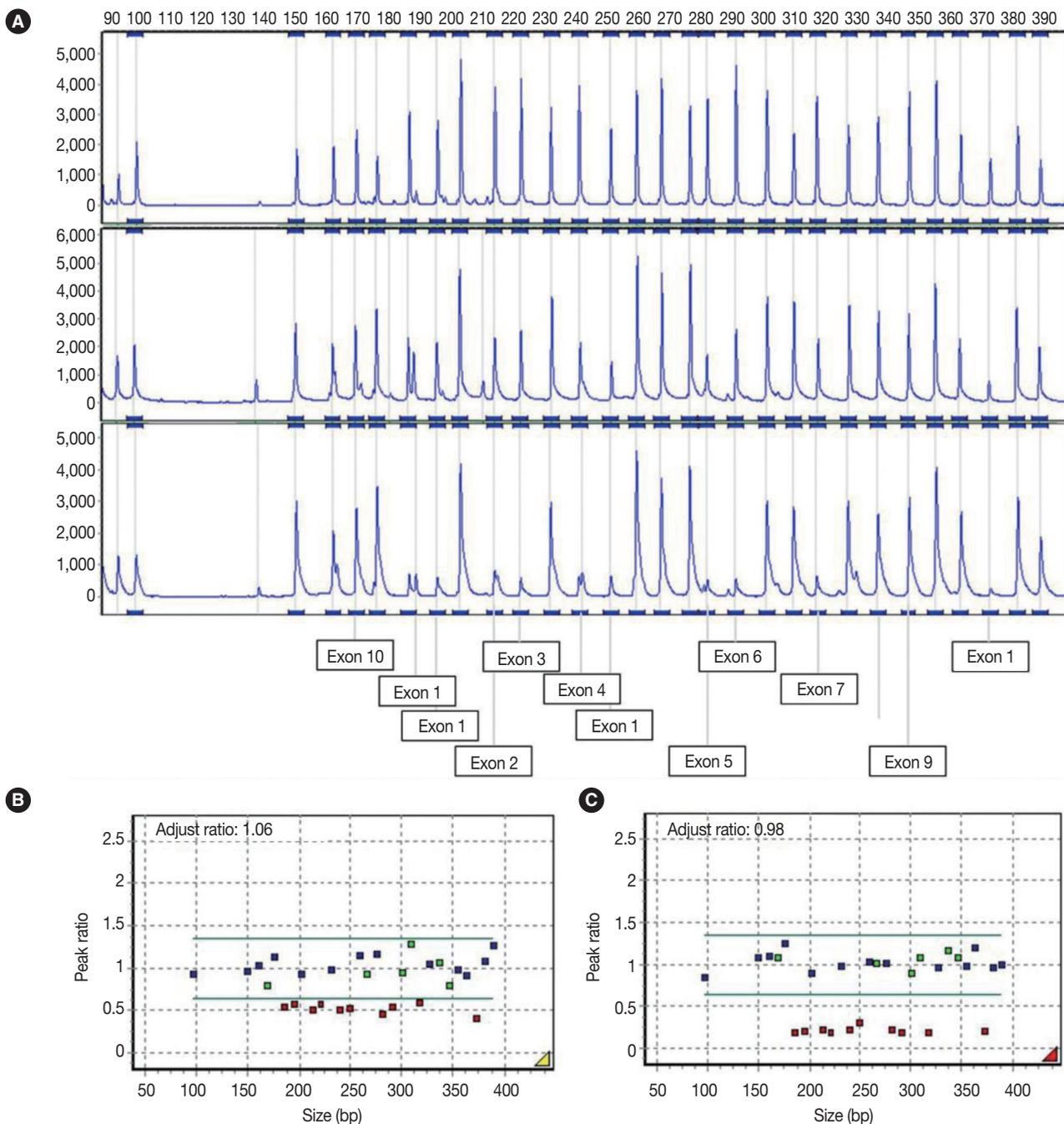
Fig. 3. (A) Electrogram showing multiple ligation-dependent probe amplification analysis of the *STK11* gene. The X-axis indicates product size (bp) and the Y-axis indicates the fluorescence intensities as the dosage of the products. The exon numbers of *STK11* are marked below the electrogram. The peaks are those of a normal control (A, upper), peripheral blood leukocyte (A, middle), and left ovarian mucinous cystadenoma (A, lower). (B) In the peripheral blood leukocytes, a peak ratio less than 0.65 represented the deletion mutation in the *STK11* gene. (C) Ovarian mucinous tumor with lobular endocervical glandular hyperplasia-like features showing mosaic loss of heterozygosity on mutation analysis (heteroplasmy) through exon 1 to 7 with a peak ratio of about 0.25. The X-axis indicates product size (bp) and the Y-axis represents the adjusted peak ratios with normal controls. The adjusted ratio was standardized to the control sample, and the median point was considered to be 1.0.

structure with crypts and villi of variable lengths and cystically dilated glands, which were divided by muscularis mucosa branching in various directions (Fig. 1E), as highlighted by desmin immunostaining (Fig. 1F). On combined Alcian blue (pH 2.5) and periodic acid-Schiff after diastase (DPAS) staining, the intracytoplasmic mucin in the epithelium of the ovarian tumor was negative for Alcian blue pH 2.5 and positive for DPAS. The cytoplasm stained bright pink for combined Alcian blue pH2.5/DPAS, implying that the mucinous contents of the ovarian tumor were neutral (Fig. 1G), in contrast to mucin in the normal endocervical mucosa, which was positive for both Alcian blue pH 2.5 and DPAS and showed a purple-violet color for combined Alcian blue pH2.5/DPAS (Fig. 1G, inlet).

Immunohistochemistry

We performed immunohistochemical staining using formalin-fixed, paraffin-embedded, 4-μm-thick tissue sections with an OptiView DAB immunohistochemical detection kit (Roche Diagnostics, Mannheim, Germany) on a Benchmark XT auto-immunostainer (Ventana Medical System, Tucson, AZ, USA). The mucinous epithelium of the ovary showed diffuse immunoreactivity for MUC6 (Novo, Newcastle upon Tyne, UK), moderately intense immunoreactivity for carbonic anhydrase-IX (Novus Biologicals, Littleton, CO, USA), and focal immunoreactivity for MUC5AC (marker of foveolar-type mucin; Novo) and HIK1083 (TOYO 2CHOME, Tokyo, Japan) (Fig. 2A–D). The epithelium did not show immunoreactivity for p16 (Santa Cruz Biotechnology, Santa Cruz, CA, USA), estrogen receptor (Novo), progesterone receptor (Novo), or p53 (Oncogene, Uniondale, NY, USA). The Ki-67 labelling index was less than 5%.

Mutation analysis

Genomic DNA was extracted from peripheral blood samples by a QIAamp DNA blood kit (Qiagen GmbH, Hilden, Germany) and from fresh frozen tissue of the left ovarian tumor by a QuickGene DNA tissue kit (Fujifilm Life Science, Tokyo, Japan). The STK11 gene was amplified via polymerase chain reaction by using 10 sets of primers in intronic flanking regions containing all exons (Table 1). Sequencing analysis was performed by a cycle sequencing kit (Thermo Fisher Scientific, Waltham, MA, USA) following the manufacturer's instructions.

Multiple ligation-dependent probe amplification (MLPA) was performed to detect deletions and duplications in the STK11 gene by STK11 MLPA kit P101 (MRC-Holland, Amsterdam, The Netherlands). The peak height of the probes was analyzed using GeneMarker software v.1.7 (SoftGenetics LLC, State Col-

lege, PA, USA). A peak ratio less than 0.65 was interpreted as a 'deletion,' whereas a peak ratio greater than 1.35 was interpreted as a 'duplication.'

Sequencing analysis did not detect any mutation in the exons and exon-intron boundaries of the STK11 gene in the blood and ovarian tumor samples. Using MLPA analyses, however, peripheral blood leukocytes showed a germline heterozygous deletion mutation at exons 1–7 of the STK11 gene (c.1-?_920+?del) and the tumor tissue showed mosaic loss of heterozygosity due to the mutation (heteroplasmy) (Fig. 3A–C).

DISCUSSION

Minimal deviation adenocarcinoma (an extremely well-differentiated form of gastric type adenocarcinoma) of the cervix and ovarian sex cord tumor with annular tubules are the most well-known tumors of the female genital organs associated with PJS, but association with ovarian mucinous tumors has rarely been described.[4] Moreover, gastric phenotype of the mucinous epithelium in patients with PJS has not been clearly determined, and there is only one case briefly mentioning ovarian mucinous tumor with pyloric/gastric differentiation.[4] In that case report, the pyloric gland differentiation involved the lesions of multiple organs, including the jejunum, urinary bladder, uterine cervix, fallopian tube, and ovary. In the extragenital organs, Peutz-Jeghers polyps in duodenum and jejunum have small areas of normal superficial gastric-type epithelium, suggesting that the proliferations of gastric-type mucinous epithelium are common features in any organs of the patients with PJS. Although the gastric subtype is very rare among mucinous tumors, it must be a distinct subtype of the ovarian mucinous tumors, which should be differentiated from the usual intestinal subtype.

LEGH in the uterine cervix is thought to be a precursor lesion of gastric-type cervical adenocarcinoma,[5] which is often identified in patients with PJS. Therefore, the premalignant potential of an ovarian mucinous tumor resembling LEGH should be closely monitored.

In our case, a germline heterozygous deletion mutation in STK11 (c.1-?_920+?del) (exon1–7del) and mosaic loss of heterozygosity were detected in the left ovarian mucinous cystadenoma by MLPA assay, but direct sequencing did not detect the deletion of the large exon.

In conclusion, our case combined with previously described cases suggests that STK11 gene mutations play an important role in the proliferation of pyloric gland-phenotype mucinous epithelium in various anatomical locations.

REFERENCES

1. Ferry JA, Young RH, Engel G, Scully RE. Oxyphilic Sertoli cell tumor of the ovary: a report of three cases, two in patients with the Peutz-Jeghers syndrome. Int J Gynecol Pathol 1994; 13: 259-66.

2. Jenne DE, Reimann H, Nezu J, *et al*. Peutz-Jeghers syndrome is caused by mutations in a novel serine threonine kinase. Nat Genet 1998; 18: 38-43.

3. Kuragaki C, Enomoto T, Ueno Y, *et al*. Mutations in the STK11 gene characterize minimal deviation adenocarcinoma of the uterine cervix. Lab Invest 2003; 83: 35-45.

4. Kato N, Sugawara M, Maeda K, Hosoya N, Motoyama T. Pyloric gland metaplasia/differentiation in multiple organ systems in a patient with Peutz-Jegher's syndrome. Pathol Int 2011; 61: 369-72.

5. Kondo T, Hashi A, Murata S, *et al*. Endocervical adenocarcinomas associated with lobular endocervical glandular hyperplasia: a report of four cases with histochemical and immunohistochemical analyses. Mod Pathol 2005; 18: 1199-210.

Thymoma and Synchronous Primary Mediastinal Seminomas with Florid Follicular Lymphoid Hyperplasia in the Anterior Mediastinum: A Case Report and Review of the Literature

Hyang-im Lee[1] · In-seok Jang[2,3,4]
Kyung Nyeo Jeon[3,4,5]
Gyung Hyuck Ko[3,4,6] · Jong Sil Lee[3,4,6]
Dong Chul Kim[3,4,6] · Dae Hyun Song[1,3]
Jeong-Hee Lee[3,4,6]

[1]Department of Pathology, Gyeongsang National University Changwon Hospital, Changwon; [2]Department of Thoracic and Cardiovascular Surgery, Gyeongsang National University Hospital, Jinju; [3]Gyeongsang National University School of Medicine, Jinju; [4]Institute of Health Science, Gyeongsang National University, Jinju; [5]Department of Radiology, Gyeongsang National University Changwon Hospital, Changwon; [6]Department of Pathology, Gyeongsang National University Hospital, Jinju, Korea

Corresponding Author
Jeong-Hee Lee, MD, PhD
Department of Pathology, Gyeongsang National University School of Medicine, 15 Jinju-daero 816beon-gil, Jinju 52727, Korea
Tel: +82-55-772-8062
Fax: +82-55-759-7952
E-mail: jhlee7@gnu.ac.kr

Thymoma is the most common neoplasm of the anterior mediastinum and has malignant potential. Germ cell tumors (GCTs) found in the anterior mediastinum are usually benign, and malignant GCTs, such as seminomas, are rare. Histologically, mediastinal seminoma is indistinguishable from testicular seminoma except for site-associated morphological features such as lymphoid follicular hyperplasia. Therefore, excluding metastasis is very important. Recently, we treated a young adult patient with multiple thymic masses that occurred simultaneously. The patient underwent a thymectomy for the removal of the mediastinal masses, one of which was diagnosed as type B2 invasive thymoma, and two of which were diagnosed as primary mediastinal seminomas with massive follicular hyperplasia. The patient received adjuvant chemotherapy after surgical resection. To our knowledge, this is the first description of a thymoma and a mediastinal seminoma occurring simultaneously in the thymus. We present this case along with a literature review.

In general, thymomas are rare tumors; however, they are the most common mediastinal tumors in adults, comprising approximately 50% of all anterior mediastinal tumors. Germ cell tumors (GCTs) of the mediastinum are also uncommon in adults and account for 10% to 20% of anterior mediastinal tumors.[1-3] Teratomas are the most common mediastinal GCTs, accounting for 44% of all mediastinal GCTs, and seminomas are the second most common, with an incidence of approximately 37%.[4] Thymomas occur most frequently in adults between the ages of 55 and 65 years, and thus, they are exceedingly rare in children and adolescents. Seminomas are primarily seen in young adult patients. According to previous reports, thymomas are commonly associated with thymic epithelial tumors, and seminomas are occasionally associated with smooth muscle tumors or multilobular thymic cysts.[5-7] Recently, Weissferdt *et al.*[8] described two cases of adult men, who were 32 and 34 years old, with mediastinal tumors that contained both a thymoma and seminoma component in a single mass. These are very rare cases that have not been previously reported. Interestingly, our group examined a patient with multiple thymic masses including one thymoma and two seminomas occurring as separate tumors. The seminomas showed prominent lymphoid follicular hyperplasia.

Because mediastinal seminomas are both rare and morphologically similar to their gonadal counterparts, the possibility of metastasis from testicular or ovarian tumors should always be excluded during the workup of these patients. Fortunately, mediastinal GCTs can be associated with secondary changes that are rarely found in testicular or ovarian tumors. These changes include reactive proliferation of remnant thymic epithelium, multiple cystic formations, epithelioid granulomatous reactions, fibrosis, and follicular lymphoid hyperplasia.[4,7,9-11] To the best of our knowledge, the simultaneous occurrence of thymomas and seminomas in the thymus has not been previously reported. Here, we report a case with a brief review of the literature.

CASE REPORT

A 35-year-old man presented with a 7.0 cm anterior mediastinal mass on a chest radiograph during a routine medical evaluation at an outside hospital. The patient was transferred to the Department of Thoracic and Cardiovascular Surgery for further evaluation and treatment. The patient did not present with any specific medical problems or symptoms and had no family history of cancer or prior surgeries except for an operation due to a pneumothorax that was performed 12 years prior to presentation. A whole body radiological study was performed. Fluorodeoxyglucose (FDG)-positron emission tomography/computed

tomography (CT) revealed two heterogenic hypermetabolic foci in the anterior mediastinum, with standard uptake values of 3.3 and 3.4. No significant FDG uptake was observed in the lymph nodes or anywhere else in the body to suggest distant metastasis, except for physiological uptake in both testes (Fig. 1A). Contrast-enhanced chest CT images showed multiple tumors in the anterior mediastinum. Specifically, a 5.0 cm mass compressing the superior vena cava, a 1.5 cm nodule, and a 1.0 cm nodule were observed (Fig. 1B, C). Radiologically, the differential diagnosis included invasive thymoma and GCT. Ultrasonography of the testes revealed a normal shape and echogenicity without focal mass or infiltrative lesions. The serum levels of β human chorionic gonadotropin (0.1 IU/L) and α-fetoprotein (12.8 ng/mL) were in the normal range.

A biopsy was performed in the operating room, and the diagnosis of thymoma was determined based on frozen tissue sections. The patient underwent a thymectomy to remove the mediastinal masses. The thymectomy specimen showed three well-circumscribed solid masses on cross section. The largest mass (5.0 × 5.0 cm in size) showed a lobulated, homogeneous, firm, cut surface with a partial hemorrhage. In the normal thymic tissue surrounding the largest tumor, two smaller masses (1.5 × 1.2 cm and 1.0 × 0.5 cm in size) were seen, which had a well-defined, round, homogeneous, soft appearance. The medium-sized mass was located 1.5 cm from the largest tumor, and the smallest
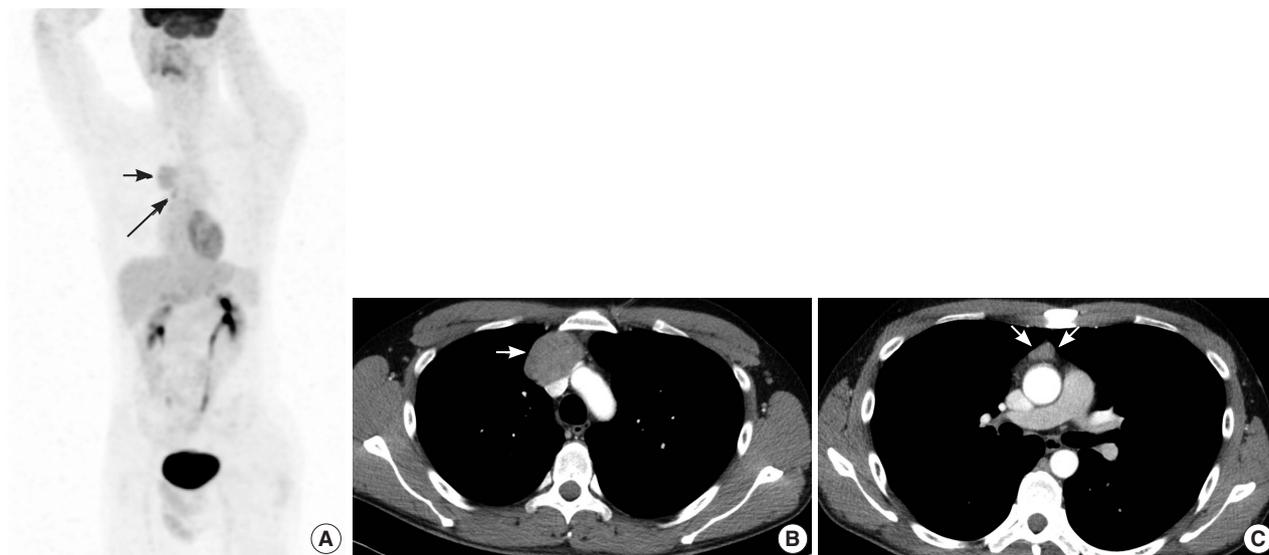

Fig. 1. Radiologic findgings of the anterior mediastinal masses. (A) Maximum intensity projection image of fluorodeoxyglucose–positron emission tomography/computed tomography (PET/CT) shows two faint hypermetabolic foci in the anterior mediastinum. The larger one (short arrow) is 4.8 cm (standard uptake value [SUV], 3.3) and the smaller one (long arrow) is 2.0 cm (SUV, 3.4). The smaller one looks like single mass due to limited spatial resolution of PET/CT image (coronal view). (B, C) Axial contrast enhanced chest CT images show multiple tumors in the anterior mediastinum; about 5-cm-sized mass (thymoma, arrow) compressing superior vena cava (B) and 1.5 cm-sized nodule (seminoma, arrows) (C).
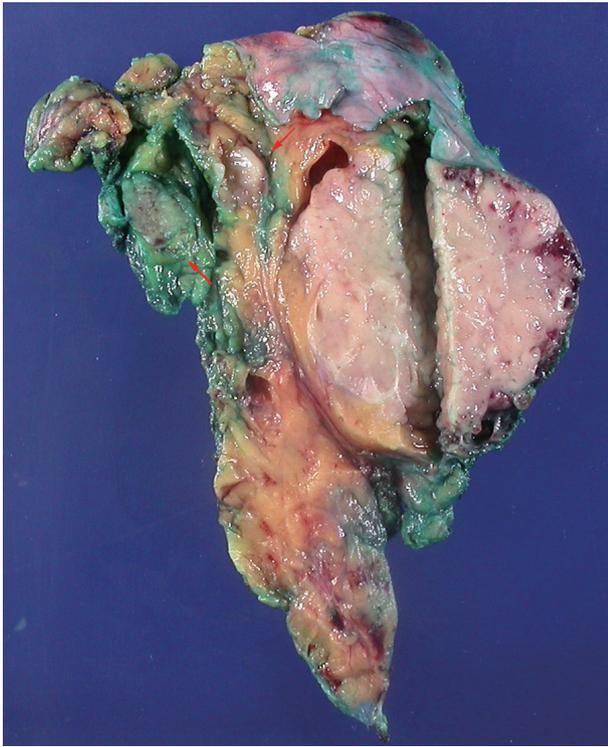
Fig. 2. Macroscopic findings of the thymectomy specimen. Three well circumscribed round masses are seen. The largest one is thymoma and two small round masses (arrows) are seminomas. The seminomas are 1.5 cm and 0.5 cm apart from the thymoma.

mass was 0.5 cm away (Fig. 2). On histologic examination, low-power magnification of the largest mass showed a well-circumscribed, thick-walled capsule with a partially incomplete area, lobular architecture, and perivascular spaces containing proteinaceous fluid and lymphocytes. The tumor was composed of a dual population of lymphocytes and epithelial cells in equal proportions. Under high-power magnification, the epithelial cells had a bland nuclear appearance with small inconspicuous nucleoli. The lymphocytes that were intermixed with the epithelial cells were small and mature-appearing. Mitotic figures were not identified within either the epithelial cells or the lymphocytes. These histologic patterns are characteristic of a type B2 thymoma (Fig. 3A, B). The two small masses without a capsule revealed clusters or islands of large epithelioid cells with prominent nucleoli and pale cytoplasm that were intermingled with small, infiltrating lymphocytic cells. These findings are similar to the characteristics of seminomas in the testes. Interestingly, these two small tumors revealed a prominent lymphoid follicular hyperplasia with the formation of germinal centers, some microscopic cysts, and Hassall's corpuscles in the surrounding area of the seminomatous component (Fig. 3C, D).

On immunohistochemical staining, the epithelial cells of the thymoma showed diffuse positive reactions for cytokeratin 19 and p63 and negative reactions for placental-like alkaline phosphatase, CD5, CD117, and D2-40 (Fig. 3E, F). The lymphoid cells were positive for TdT. In contrast, the epithelial cells of the seminoma-like tumors showed diffuse positive reactions for CD117, partially strong positive reactions for placental alkaline phosphatase (PLAP) and D2-40, and negative reactions for α-fetoprotein, cytokeratin 19, and p63 (Fig. 3G, H). Epithelial membrane antigen staining was observed in Hassall's epithelial cells of the thymoma and in microcystic epithelial cells of the seminomas. In summary, histological and immunohistochemical analyses of the anterior mediastinal masses revealed a type B2 invasive thymoma and two seminomas. The results of the immunohistochemical staining are summarized in Table 1. A biopsy of the testes was not performed.

DISCUSSION

The simultaneous occurrence of a thymoma and seminoma in the thymus has not yet been reported except for two cases described by Weissferdt et al.[8] in 2014. However, they reported a thymoma with a component of a thymic seminoma combined within a single tumor. The seminomatous component showed seminoma-like epithelioid cells with distinct hyalinization adjacent to the area of the conventional thymoma. Our case included one large thymoma and two small seminomas in the anterior mediastinum, with distances of 1.5 cm and 0.5 cm between the thymoma and the seminomas. Because multiple thymic masses containing a thymoma and small seminomas are very rare, the possibility of metastasis from another organ or a morphological transformation of the thymic epithelial tumor cells into thymic carcinoma should be considered. The two small masses showed negative reaction for CD5 and pan-cytokeratin and positive reaction for PLAP and D2-40 by immunohistochemical staining. Although CD5 loss in thymic carcinoma is known,[12] the other immunohistochemical findings favor seminoma rather than thymic carcinoma. We could not find a case of a thymic carcinoma with a positive reaction for PLAP or D2-40 in the literature. Our case showed site-associated features such as the presence of multiple cysts, reactive remnant thymic epithelium, epithelioid granulomatous reaction, fibrosis, and follicular lymphoid hyperplasia.[10,11] In the seminomatous tumor, no evidence of metastasis was found in the clinical workup. Fortunately, site-associated morphologic features of mediastinal masses are rare in gonadal tumors. Although a biopsy of the testes was not performed, metastatic seminoma in the mediastinum from an intra-
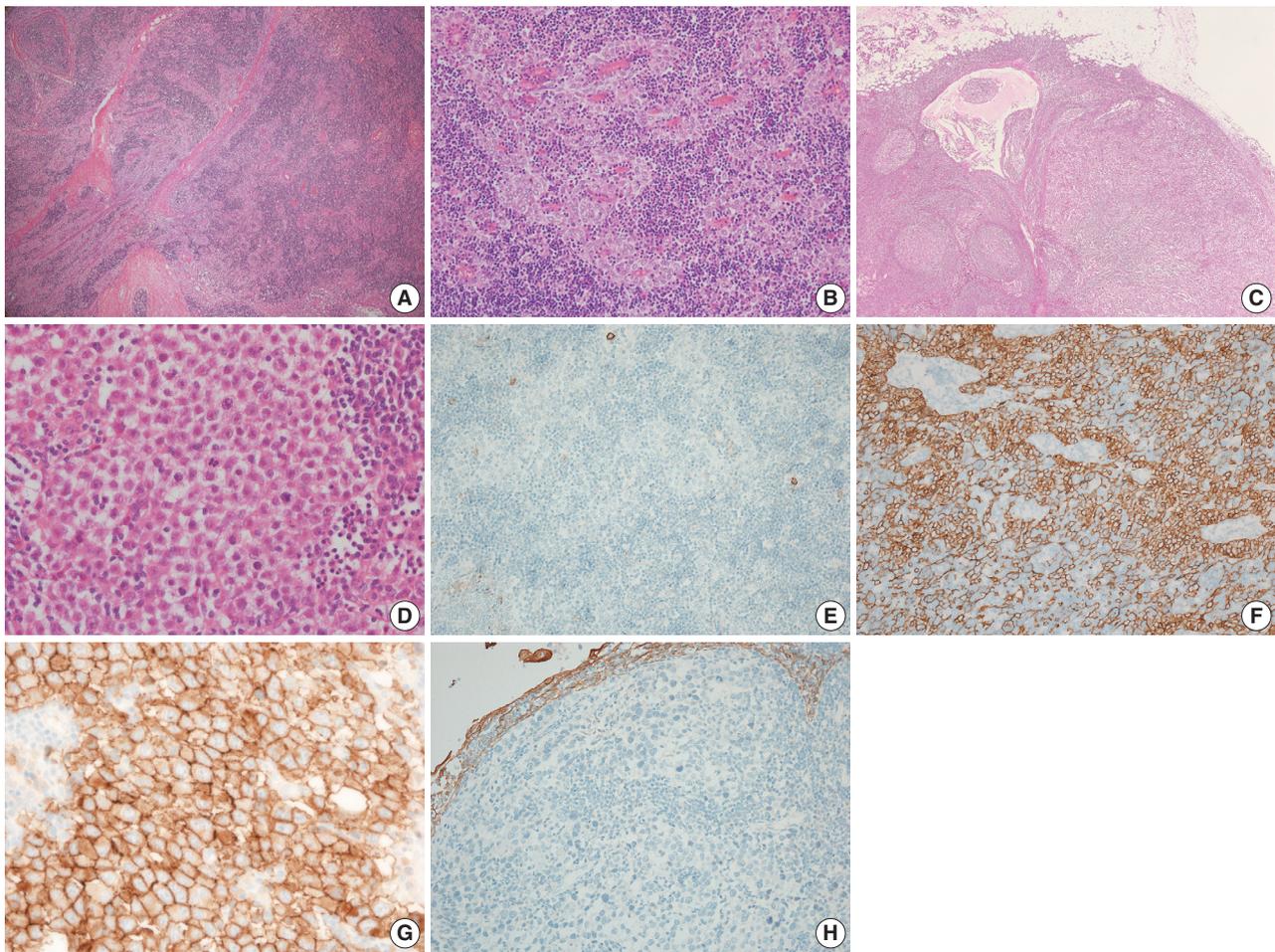
Fig. 3. Histologic findings and immunohistochemical staining results of the thymoma and seminoma of the anterior mediastinal masses. (A) At low power, thymoma shows relatively well demarcated round lobulated mass separated by thick collagenous blands consisting of dual population of lymphocytes and epithelial cells. (B) The epithelial cells show a bland appearance; round to oval with vesicular nuclei, eosinophilic to amphophilic cytoplasm, and small inconspicuous nucleoli. (C) Mediastinal seminoma show numerous lymphoid follicles with germinal center and microcystic change in left area. Seminoma component is seen in right area. (D) Seminoma cells displaying their classical features; indistinct cell border, clear to eosinophilic cytoplasm, vesicular nuclei with eosinophilic nucleoli, and increased mitotic activity. (E) CD117 staining reveals negative reaction for epithelial component of thymoma. (F) Thymic epithelial cells of thymoma highlighted by a cytokeratin 19 immunostain. (G) CD117 staining confirming a diagnosis of seminoma. (H) Cytokeratin 19 staining demonstrates thymic remnant associated with cystic change but is negative for seminoma component around thymic remnant.

tubular germ cell neoplasia is unusual in the absence of retroperitoneal lymph node metastasis.[13] These clinical and histological findings support the conclusion that these seminomas are of mediastinal origin rather than due to metastasis.

Primary mediastinal seminomas were first described in 1955 by Woolner *et al.*[14] and have been well recognized for over 50 years. Their histogenesis is controversial. Normal germ cells in the thymus have yet to be identified. However, it is believed that mediastinal seminomas originate from extragonadal germ cells in the thymic gland due to chromosomal abnormalities.[15] Chromosome 12p abnormalities, which are specific genetic alterations found in testicular seminomas, are also present in

mediastinal seminomas.[16] However, primary mediastinal seminomas show different genetic findings from those of testicular seminomas. Specifically, Przygodzki *et al.*[17] reported a unique pattern of a *KIT* exon 17 mutations in mediastinal seminomas, which are rare in testicular seminomas. This may imply that the mediastinal seminoma develops through different pathways than that of its gonadal counterpart. Regardless of the tumor location, seminomas show KIT protein expression, which is also seen in thymic carcinomas but not in thymomas.

Histopathological analyses show that thymomas have heterogeneous morphological features such as spindle cells, lymphocytic infiltrate, and rhabdomyomatous components. Additionally,

Table 1. Results of the immunohistochemical studies

Immunohistochemical marker	Thymoma component	Seminoma component
CK19	+	−
AFP	−	−
TdT	+ in lymphocytes	− in lymphocytes
PAX-8	−	−
D2-40	−	+
CD5	−	−
CD117	−	+
PLAP	−	+

CK19, cytokeratin 19; AFP, α-fetoprotein; TdT, terminal deoxynucleotidyl transferase; PLAP, placental alkaline phosphatase.

cytokeratin expression in seminoma tumor cells, which reflects the differential potential or the morphological transformation of the seminoma into another nonseminomatous GCTs, has been reported.[16] Moreover, a thymic carcinoma or seminoma may occur in combination with a thymoma within a single tumor. Therefore, we cautiously hypothesize that thymoma, thymic carcinoma, and seminoma occur from cells of the same origin, such as embryonic stem cells or primordial germ cells, which have the ability to differentiate into a diverse population of cells. They obtain chromosomal and molecular abnormalities such as chromosome 12p abnormalities and *KIT* mutations and transform from thymic epithelial tumors into GCTs (seminoma) or from seminomas into thymic epithelial tumors. The etiology and pathogenesis of thymomas and seminomas in the thymus are unknown, and further research is required in this area.

Follicular lymphoid hyperplasia of the thymus can be seen in reactive, autoimmune diseases like myasthenia gravis. Normal thymus and thymic epithelial tumors also exhibit germinal centers.[18,19] In seminoma, follicular lymphoid hyperplasia may be associated with specific antigens produced by the microenvironment of the seminoma.[20] Weissferdt and Moran[9] postulated that the specific distribution of antigen-presenting dendritic cells in mediastinal seminomas is related to the pathogenesis of follicular lymphoid hyperplasia.

In short, we report a case of one thymoma and two mediastinal seminomas that developed simultaneously in the thymus of a young adult. The seminomas revealed florid follicular lymphoid hyperplasia and microcystic changes that do not appear in testicular seminomas. In addition, no clinical or radiological evidence of GCTs was found elsewhere. Therefore, even though multiple masses were present, we considered these tumors to be synchronous primary thymic tumors rather than metastases from an occult tumor of the testis. To our knowledge, this is the first description of a synchronous occurrence of a separate thymoma and

mediastinal seminomas within the thymus.

Conflicts of Interest

No potential conflict of interest relevant to this article was reported.

REFERENCES

1. Moran CA, Suster S. Primary germ cell tumors of the mediastinum: I. Analysis of 322 cases with special emphasis on teratomatous lesions and a proposal for histopathologic classification and clinical staging. Cancer 1997; 80: 681-90.

2. Strollo DC, Rosado de Christenson ML, Jett JR. Primary mediastinal tumors. Part 1: tumors of the anterior mediastinum. Chest 1997; 112: 511-22.

3. Bokemeyer C, Nichols CR, Droz JP, *et al*. Extragonadal germ cell tumors of the mediastinum and retroperitoneum: results from an international analysis. J Clin Oncol 2002; 20: 1864-73.

4. Moran CA, Suster S, Przygodzki RM, Koss MN. Primary germ cell tumors of the mediastinum: II. Mediastinal seminomas: a clinicopathologic and immunohistochemical study of 120 cases. Cancer 1997; 80: 691-8.

5. Suster S, Moran CA. Primary thymic epithelial neoplasms showing combined features of thymoma and thymic carcinoma: a clinicopathologic study of 22 cases. Am J Surg Pathol 1996; 20: 1469-80.

6. Moran CA, Suster S, Perino G, Kaneko M, Koss MN. Malignant smooth muscle tumors presenting as mediastinal soft tissue masses: a clinicopathologic study of 10 cases. Cancer 1994; 74: 2251-60.

7. Moran CA, Suster S. Mediastinal seminomas with prominent cystic changes: a clinicopathologic study of 10 cases. Am J Surg Pathol 1995; 19: 1047-53.

8. Weissferdt A, Kalhor N, Moran CA. Combined thymoma-thymic seminoma: report of 2 cases of a heretofore unreported association. Hum Pathol 2014; 45: 2168-72.

9. Weissferdt A, Moran CA. Mediastinal seminoma with florid follicular lymphoid hyperplasia: a clinicopathological and immunohistochemical study of six cases. Virchows Arch 2015; 466: 209-15.

10. Burns BF, McCaughey WT. Unusual thymic seminomas. Arch Pathol Lab Med 1986; 110: 539-41.

11. Schantz A, Sewall W, Castleman B. Mediastinal germinoma: a study of 21 cases with an excellent prognosis. Cancer 1972; 30: 1189-94.

12. Ohue Y, Matsuoka S, Kumeda H, *et al*. Development of combined thymic carcinoma and thymoma in an extrathymic lesion during long follow-up for recurrent thymoma. Mol Clin Oncol 2016; 4:

139-42.

13. Hailemariam S, Engeler DS, Bannwart F, Amin MB. Primary mediastinal germ cell tumor with intratubular germ cell neoplasia of the testis: further support for germ cell origin of these tumors: a case report. Cancer 1997; 79: 1031-6.

14. Woolner LB, Jamplis RW, Kirklin JW. Seminoma (germinoma) apparently primary in the anterior mediastinum. N Engl J Med 1955; 252: 653-7.

15. Chaganti RS, Rodriguez E, Mathew S. Origin of adult male mediastinal germ-cell tumours. Lancet 1994; 343: 1130-2.

16. Sung MT, Maclennan GT, Lopez-Beltran A, Zhang S, Montironi R, Cheng L. Primary mediastinal seminoma: a comprehensive assessment integrated with histology, immunohistochemistry, and fluorescence in situ hybridization for chromosome 12p abnormalities in 23 cases. Am J Surg Pathol 2008; 32: 146-55.

17. Przygodzki RM, Hubbs AE, Zhao FQ, O'Leary TJ. Primary mediastinal seminomas: evidence of single and multiple KIT mutations. Lab Invest 2002; 82: 1369-75.

18. Middleton G. The incidence of follicular structures in the human thymus at autopsy. Aust J Exp Biol Med Sci 1967; 45: 189-99.

19. Vetters JM, Macadam RF. Fine structural evidence for hormone secretion by the human thymus. J Clin Pathol 1973; 26: 194-7.

20. Willis SN, Mallozzi SS, Rodig SJ, *et al*. The microenvironment of germ cell tumors harbors a prominent antigen-driven humoral response. J Immunol 2009; 182: 3310-7.

Malignant Solitary Fibrous Tumor with Heterologous Rhabdomyosarcomatous Differentiation: A Case Report

Jeong-Hwa Kwon · Joon Seon Song
Hye Won Jung[1] · Jong-Seok Lee[2]
Kyung-Ja Cho

Department of Pathology, [1]Department of
Radiology, Research Institute of Radiology,
[2]Department of Orthopedic Surgery, Asan
Medical Center, University of Ulsan College of
Medicine, Seoul, Korea

Corresponding Author
Joon Seon Song, MD, PhD
Department of Pathology, Asan Medical Center,
University of Ulsan College of Medicine, 88
Olympic-ro 43-gil, Songpa-gu, Seoul 05505, Korea
Tel: +82-2-3010-4548
Fax: +82-2-472-7898
E-mail: songjs@amc.seoul.kr

Malignant solitary fibrous tumor (MSFT) is a well-described entity, from which heterologous differentiation is extremely rare. We encountered a case of MSFT with rhabdomyosarcomatous differentiation in a 56-year-old man. This patient presented with a large mass in his posterior thigh. He had been treated with chemoradiation for sarcoma involving the cervical spine, right femoral head, and both lungs 6 months earlier. A wide excision was performed. The mass measured 10.6 cm and showed a fish-flesh cut surface with necrotic foci. Microscopically, the tumor showed heterogeneous cellularity with a hemangiopericytic vascular pattern. A hypercellular area showed spindle cells or epithelioid cells with high mitotic activity (63/10 high-power fields) and immunoreactivity for CD34 and CD99. A hypocellular area and a cystic area showed pleomorphic rhabdoid cells with immunoreactivity for desmin and myogenin. This is a report of a rare case of MSFT with rhabdomyosarcomatous differentiation and presents new histologic features of MSFT.

An extrapleural solitary fibrous tumor (SFT) is an uncommon mesenchymal spindle cell tumor characterized by its unpredictable behavior.[1,2] It can occur in any site of the body.[3] Approximately 10% of SFTs are found to be locally aggressive and may present local or distant recurrence many years after primary treatment.[4] The distinction between benign and malignant SFT (MSFT) is difficult and does not have established specific criteria in the current literature. According to the World Health Organization classification of soft tissue tumors, MSFT is designated as a tumor that has features of hypercellularity, at least focal moderate to marked cellular atypia, tumor necrosis, 4 mitoses/10 high-power fields (HPFs), and infiltrative margins.[5]

Heterologous differentiation of MSFT is extremely rare and has been described in only one article with osteosarcomatous and rhabdomyosarcomatous elements.[6] We herein present another case of MSFT with heterologous rhabdomyosarcomatous differentiation.

CASE REPORT

A 56-year-old man presented with a newly-developed large mass in his left posterior thigh. He had been treated 6 months earlier with palliative chemoradiation for unclassified sarcomas of the cervical spine, the right femoral head, and both lungs. Magnetic resonance imaging revealed a poorly marginated, 8.5-cm, heterogeneously enhancing mass in the left thigh with nodular, heterogeneous bone marrow signal intensity in the right femur neck, in the proximal femoral shaft, and in the pelvic bone, suggesting intramedullary bone metastasis. Wide excision of the thigh mass was performed under the assumption of high-grade sarcoma. The resected mass showed a multinodular, dark yellow, fish-flesh appearance with necrotic foci measuring 10.6 × 6.4 × 2.3 cm (Fig. 1).

Microscopically, the tumor showed heterogeneous cellularity with partly cystic changes and a hemangiopericytic vascular pattern. A hypercellular area showed spindle cells or epithelioid cells with high mitotic activity (63/10 HPFs), whereas a hypocellular
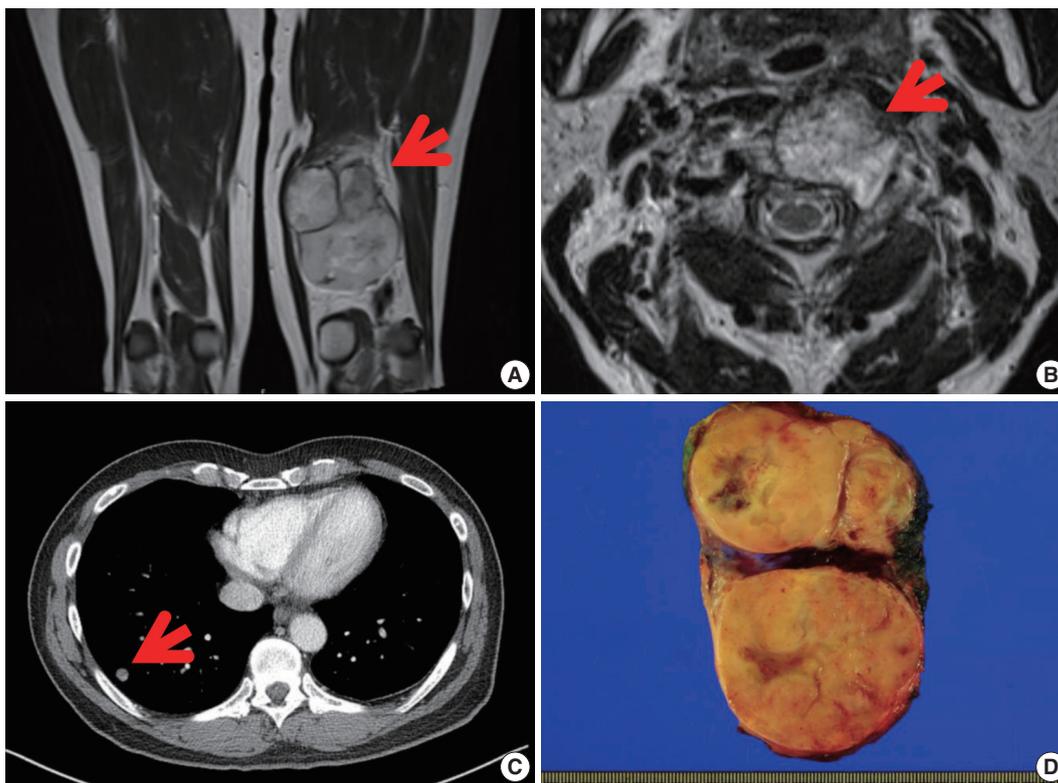
Fig. 1. Magnetic resonance image revealing a well-defined enhancing mass in the postero-medial compartment of the left thigh (arrow) (A), with metastasis in the C2 vertebral body (arrow) (B). (C) Chest computed tomography showing multiple nodules in both lungs. (D) Grossly, a large lobulated mass is observed in the left thigh. The cut surface of the mass is yellow-tan and firm with necrotic foci.

area and cystic wall showed pleomorphic rhabdoid cells (Fig. 2). The hypercellular area was immunopositive for CD34 (1:500, Immunotech, Marseille, France) and CD99 (1:200, Dako, Glostrup, Denmark), whereas the hypocellular area and cystic wall showed immunoreactivity for desmin (1:200, Dako) and myogenin (1:200, Dako, Carpinteria, CA, USA) (Fig. 3). The patient received adjuvant chemoradiation therapy (pazopanib 2 cycles and 3,000 cGy radiation 7 cycles) and had shown no recurrence after 7 months of follow-up.

DISCUSSION

SFT is a mesenchymal tumor that is characteristically "patternless" with an arborescent vascular frame.[5] It can occur at any site of body and can vary in appearance, including hyaline, cellular, and epithelioid elements. It presents as well-demarcate and slow growing.[7] A malignant form of SFT is rare, and it has been proposed to arise either *de novo* or within a preexisting benign SFT.[8] There are some reported cases of MSFT arising from benign SFT. Yokoi *et al*.[8] previously described three cases of malignant transformation from benign SFT. The tumors had both a

malignant-looking and a benign-looking component. The malignant-looking component had highly atypical cells with hyperchromatic nuclei and increased mitotic activity and had markedly high expression of p53, Ki-67, and CD34 and immunonegativity for desmin and myogenin, whereas the benign-looking component included low- or intermediate-grade tumors with typical SFT features. Another five cases of *de novo* MSFT have also been described.[8] These cases had heterogeneous, high- to low-grade pathologic features.

As previously mentioned, only one case of MSFT with heterologous components has been described to date.[6] This patient was a 59-year-old male with a 10-cm-sized mass in the medial aspect of the thigh who underwent a wide excision. The tumor had three distinct characteristics. First, it was a typical SFT with strong immunopositivity for CD34 and Bcl-2 and low mitotic activity (2/10 HPFs). Second, it consisted of pleomorphic cells with nuclear atypia and many bizarre multinucleate tumor giant cells with immunonegativity for CD34 and a high mitotic activity (23/10 HPFs). In addition, this area was also admixed with desmin- and myogenin-immunopositive rhabdomyosarcomatous elements. Third, the tumor showed osteosar-
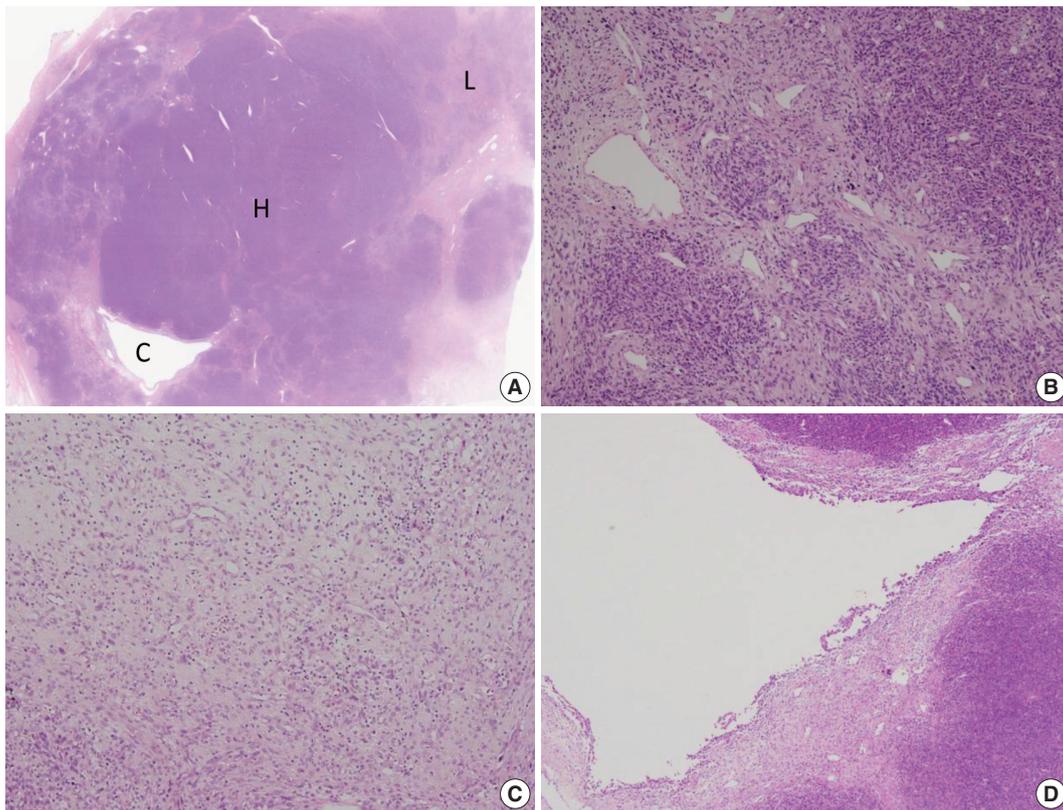
Fig. 2. Microscopic findings. (A) The mass consists of a hypercellular area (H), a hypocellular area (L), and a cystic area (C). (B) The hypercellular area is composed of short spindle or epithelioid cells with a hemangiopericytic vasculature. (C) The hypocellular area shows plump epithelioid cells with inflammatory cells. (D) The cystic area is unilocular and contacted both the hypercellular and the hypocellular areas.

comatous differentiation with distinct malignant osteoid cells. After wide excision, that patient proceeded to postoperative radiotherapy and remained free of disease for 7 months.

In our case, the patient was a 56-year-old man that had a 10.6-cm-sized, newly developed large mass in his left posterior thigh. He had been treated with palliative chemoradiation 6 months earlier for unclassified sarcomas of multiple metastasis. Microscopically, the tumor showed three different components: hypercellular, hypocellular, and partly cystic components. Cystic components presented with a hemangiopericytic vascular pattern. A hypercellular area showed spindle cells or epithelioid cells with high mitotic activity and showed immunopositivity for CD34 and CD99, whereas a hypocellular area and cystic wall showed pleomorphic rhabdoid cells and immunoreactivity for desmin and myogenin. The patient received adjuvant chemoradiation therapy and has shown no recurrence after 7 months of follow-up.

The differential diagnosis of MSFT includes benign and malignant lesions, such as malignant peripheral nerve sheath tumor (MPNST), synovial sarcoma (SS), fibrosarcoma, undifferentiated pleomorphic sarcoma (previously malignant fibrous histiocytoma),

and dermatofibrosarcoma protuberans (DFSP).[5,9] MPNST has features of heterogeneous spindle cells with variable growth pattern and arrangement and has bizarre giant cells, high mitotic activities, and distinguishing patterns of necrosis.[10] MPNST also shows focal immunopositivity for S100 protein.

SS has three major histological subtypes: biphasic, monophasic, and poorly differentiated. The biphasic subtype shows co-existence of epithelioid cells and spindle cells. However, the monophasic subtype is entirely composed of spindle cells; in this case, immunonegativity for CD34 is helpful to exclude the diagnosis.[11]

Fibrosarcoma consists of highly cellular fibroblasts with variable collagen production. It has a herringbone-like growth pattern and consists of scant cytoplasm, hyperchromatic nuclei, and variable nucleoli.[5] It also presents immunonegativity for CD34.

Undifferentiated pleomorphic sarcoma has high cellularity lesions, mixed with spindle cells and often rounded histiocyte-like cells. Some cases have extensive fibrous stroma. This tumor has a storiform growth pattern and pleomorphic tumor cells with foamy cytoplasm and marked nuclear atypia. Multinucleated giant cells may also be seen.

DFSP presents with a non-circumscribed, highly cellular lesion

H&E	CD34	Desmin	Myogenin
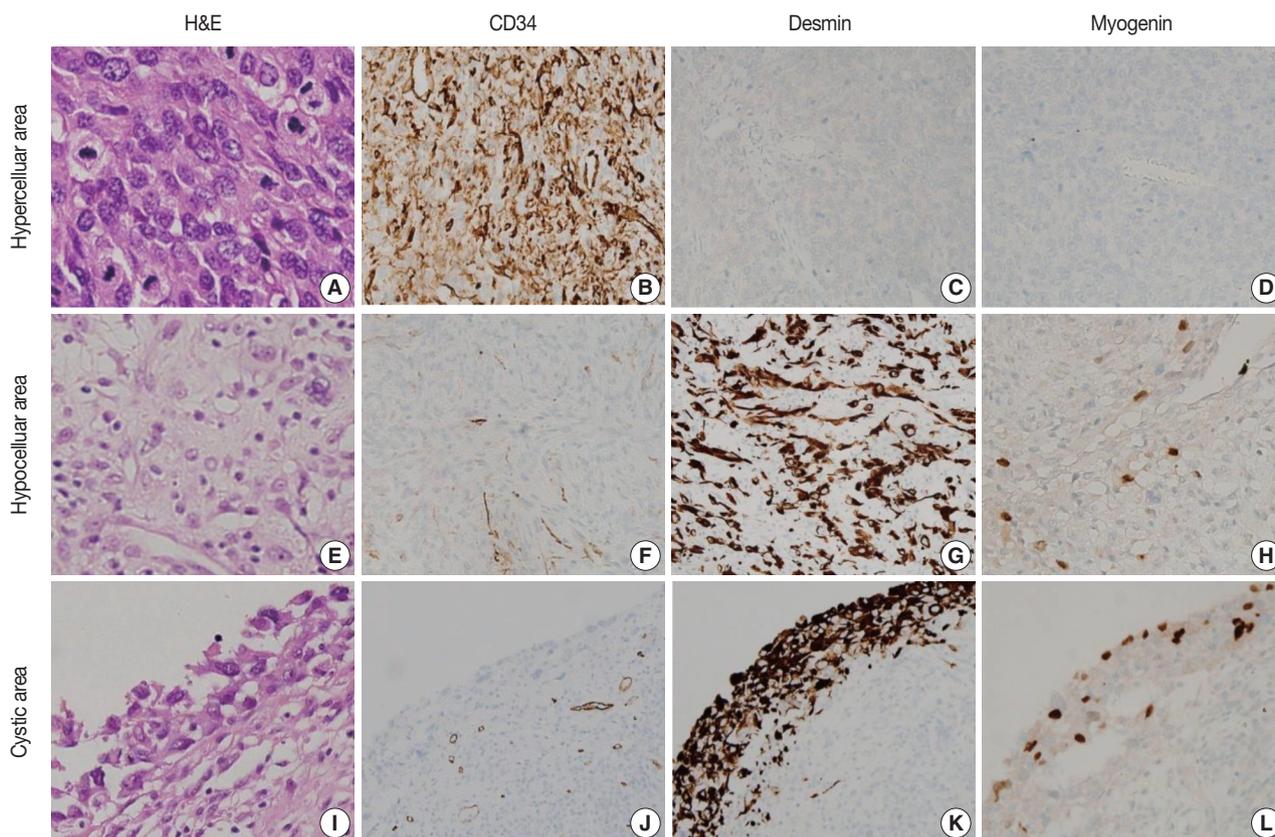
Fig. 3. Morphologic and immunohistochemical findings. (A) The hypercellular area is composed of short spindle or epithelioid cells with prominent nucleoli and high mitotic activity (63/10 highpower fields) and shows immunoreactivity for CD34 (B) and immunonegativity for desmin (C) and myogenin (D). (E) The hypocellular area is composed of plump epithelioid cells and shows immunoreactivity for CD34 (F) and strong immunopositivity for desmin (G) and myogenin (H). (I) The cystic component is composed of pleomorphic rhabdoid cells and shows focal immunoreactivity for CD34 (J) and strong immunopositivity for desmin (K) and myogenin (L).

and has a storiform growth pattern. Cells are monomorphic and spindly with scant eosinophilic cytoplasm. It usually has no significant pleomorphism and rare histiocytes.[5] DFSP is less deeply located than SFT and usually involves the dermis.[12]

Barthelmess *et al.*[13] identified recurrent somatic fusions of two genes, NGFI-A binding protein 2 (*NAB2*) and *STAT6*, located at 12q13, as presumable tumor-initiating events in SFT. Although the authors raised the possibility that specific *NAB2-STAT6* fusion variants may be associated with higher risk of aggressive behavior,[13] there are no distinct molecular features that differentiate benign from malignant tumors.

Surgical excision has been the standard treatment option for both benign and MSFTs, but late recurrences have been observed.[14] Radiotherapy is often used to improve local control, and chemotherapy is used for lesion that cannot be completely excised.[15] However, the benefits of these adjuvant chemoradiation therapies remain unproven. In conclusion, we present a rare case of MSFT with rhabdomyosarcomatous differentiation. This case

report expands our knowledge of the histologic features of MSFT.

Conflicts of Interest

No potential conflict of interest relevant to this article was reported.

REFERENCES

1. Collini P, Negri T, Barisella M, *et al.* High-grade sarcomatous overgrowth in solitary fibrous tumors: a clinicopathologic study of 10 cases. Am J Surg Pathol 2012; 36: 1202-15.

2. Rajeev R, Patel M, Jayakrishnan TT, *et al.* Retroperitoneal solitary fibrous tumor: surgery as first line therapy. Clin Sarcoma Res 2015; 5: 19.

3. Demicco EG, Park MS, Araujo DM, *et al.* Solitary fibrous tumor: a clinicopathological study of 110 cases and proposed risk assess-

ment model. Mod Pathol 2012; 25: 1298-306.

4. Robinson LA. Solitary fibrous tumor of the pleura. Cancer Control 2006; 13: 264-9.

5. Fletcher CD, Unni KK, Mertens F. World Health Organization classification of tumours of pathology and genetics tumours of soft tissue and bone. Lyon: IARC Press, 2002.

6. Thway K, Hayes A, Ieremia E, Fisher C. Heterologous osteosarcomatous and rhabdomyosarcomatous elements in dedifferentiated solitary fibrous tumor: further support for the concept of dedifferentiation in solitary fibrous tumor. Ann Diagn Pathol 2013; 17: 457-63.

7. Wetzel W, Alexander R. Myxoid liposarcoma: an ultrastructural study of two cases. Am J Clin Pathol 1979; 72: 521-8.

8. Yokoi T, Tsuzuki T, Yatabe Y, et al. Solitary fibrous tumour: significance of p53 and CD34 immunoreactivity in its malignant transformation. Histopathology 1998; 32: 423-32.

9. Bishop JA, Rekhtman N, Chun J, Wakely PE Jr, Ali SZ. Malignant solitary fibrous tumor: cytopathologic findings and differential diagnosis. Cancer Cytopathol 2010; 118: 83-9.

10. Miguchi M, Takakura Y, Egi H, et al. Malignant peripheral nerve sheath tumor arising from the greater omentum: case report. World J Surg Oncol 2011; 9: 33.

11. Zhang HY, Feng Y, Zhang Z, Gao G, Zhao JS. Synovial sarcoma of the buttocks presenting with a non-healing wound and rapid progression after local resection: a case report. World J Surg Oncol 2012; 10: 125.

12. Chang D, de Oliveira CR, Saito CF. Malignant solitary fibrous tumour of the extremities. Acta Ortop Bras 2010; 18: 107-9.

13. Barthelmeß S, Geddert H, Boltze C, et al. Solitary fibrous tumors/hemangiopericytomas with different variants of the NAB2-STAT6 gene fusion are characterized by specific histomorphology and distinct clinicopathological features. Am J Pathol 2014; 184: 1209-18.

14. Baldi GG, Stacchiotti S, Mauro V, et al. Solitary fibrous tumor of all sites: outcome of late recurrences in 14 patients. Clin Sarcoma Res 2013; 3: 4.

15. de Perrot M, Kurt AM, Robert JH, Borisch B, Spiliopoulos A. Clinical behavior of solitary fibrous tumors of the pleura. Ann Thorac Surg 1999; 67: 1456-9.

■ CASE STUDY ■

Mucinous Carcinoma with Extensive Signet Ring Cell Differentiation: A Case Report

Hye Min Kim · Eun Kyung Kim
Ja Seung Koo

Department of Pathology, Yonsei University
College of Medicine, Seoul, Korea

Corresponding Author
Ja Seung Koo, MD
Department of Pathology, Severance Hospital,
Yonsei University College of Medicine, 50 Yonsei-ro,
Seodaemun-gu, Seoul 03722, Korea
Tel: +82-2-2228-1772
Fax: +82-2-362-0860
E-mail: kjs1976@yuhs.ac

Breast cancers that present with mucin include mucinous carcinoma and carcinoma with signet ring cell differentiation. The former shows extracellular mucin and the latter shows abundant intracellular mucin. Here, we report a case of breast cancer showing both extracellular mucin and extensive signet ring cell differentiation due to abundant intracellular mucin. Unlike mucinous carcinoma, this case had the features of high-grade nuclear pleomorphism, high mitotic index, estrogen receptor negativity, progesterone receptor negativity, human epidermal growth factor receptor-2 positivity, and ductal type with positivity for E-cadherin. In a case with signet ring cell differentiation, differential diagnosis with metastatic signet ring cell carcinoma of the stomach and colon is essential. In this case, the presence of accompanied ductal carcinoma *in situ* component and mammaglobin and gross cystic disease fluid protein-15 positivity were findings that suggested the breast as the origin.

Key Words: Breast; Mucinous carcinoma; Signet ring cell

According to the World Health Organization (WHO) classification, breast cancers that could show mucinous differentiation include mucinous carcinoma and carcinoma with signet ring cell differentiation.[1] Both tumors have a common feature in that they contain or secrete mucin; however, mucinous carcinoma exhibits tumor cells floating in the extracellular mucin,[2] whereas in carcinoma with signet ring cell differentiation, the tumor nucleus is pushed into a corner by abundant intracellular mucin.[3] Carcinoma with signet ring cell differentiation is reportedly difficult to define as a distinct entity, since prominent signet ring cell differentiation can appear in invasive lobular carcinoma, invasive carcinoma of no special type, and other special types in common.[4] Mucinous carcinoma usually shows estrogen receptor (ER) and progesterone receptor (PR) positivity and human epidermal growth factor receptor-2 (HER-2) negativity with relatively good prognosis,[5,6] while carcinoma with signet ring cell differentiation frequently expresses ER and PR,[7] with an uncertain prognosis.[8]

Here, we report a case of breast cancer secreting prominent extracellular mucin and showing distinct signet ring cell differentiation due to abundant intracellular mucin.

CASE REPORT

A 64-year-old woman presented with nipple discharge from right breast for 3 months. On physical examination, a palpable mass was noted in the right breast without other remarkable findings. She had no remarkable medical history or familial history. Diagnostic mammogram revealed a 5.4-cm-sized mass with microcalcification in the palpable area in the right upper medial portion of the breast. In magnification view, the parenchymal distortion measured about 6.3 cm in maximal diameter including grouped coarse heterogeneous calcification. In diagnostic ultrasound, a 3-cm-sized heterogeneous area including calcification in the inner part was observed 3 cm from the nipple in the right upper medial 2 o'clock direction and five core needle biopsies were performed. The pathologic diagnosis of biopsy was ductal carcinoma *in situ* (DCIS) with a suspicious area of invasion showing mucinous differentiation. Breast magnetic resonance imaging showed right nipple retraction without pathologic lymph node, and skeletal metastasis was not observed in whole body bone scan. The patient underwent total mastectomy and sentinel lymph node dissection of the right breast.

The surgical specimen was sent to the Department of Pathol-

ogy. On gross examination, the cut surface revealed a gelatinous gray white mass (2.2 × 2.0 cm). On histologic examination, the tumor with expanding margin was observed in the low-power view (Fig. 1A). The tumor cell clusters were floating in the mucin pool and the cell density was higher in the periphery than in the center (Fig. 1A). In the high-power view, the tumor cell cluster floating in the mucin pool showed nuclear atypia suitable for nuclear grade 3 and the mitotic count was 14 in 10 high power fields. Many tumor cells were seen as signet ring cells with the tumor nucleus pushed into a corner by abundant intracellular mucin (Fig. 1B). DCIS was observed in the periphery of the expanding invasive nodule, comprising 60% of invasive tumor area (Fig. 1C). The DCIS component showed a significantly high nuclear grade and signet ring cell differentiation, but extracellular mucin was not observed (Fig. 1D). Serial immunohistochemical staining results showed that tumor cells were negative for ER (Fig. 1E) and PR (Fig. 1F) and positive for HER-2 (3+) (Fig. 1G), with a Ki-67 labeling index of about 30%. In addition, tumor cells were positive for mammaglobin (Fig. 1H), gross cystic disease fluid protein-15 (GCDFP-15) (Fig. 1I), E-cadherin, and MUC-1, and tumor mucin was positive for Alcian blue and mucicarmine. A total of 12 axillary lymph nodes were evaluated, but no metastasis was noted. The patient has been followed on an outpatient basis after surgery and to date, there is no evidence of recurrence or metastasis.

DISCUSSION

Representative breast cancers that secrete mucin are mucinous carcinoma and carcinoma with signet ring cell differentiation according to WHO classification.[1] In mucinous carcinoma, mucin appears as extracellular mucin,[2] whereas in carcinoma with signet ring cell differentiation, mucin is shown as abundant intracellular mucin.[3] However, the case reported here had the typical findings of both extracellular mucin and extensive signet ring cell differentiation due to abundant intracellular mucin. In addition, this case was different from typical mucinous carcinoma due to the existence of the following features: (1) high-
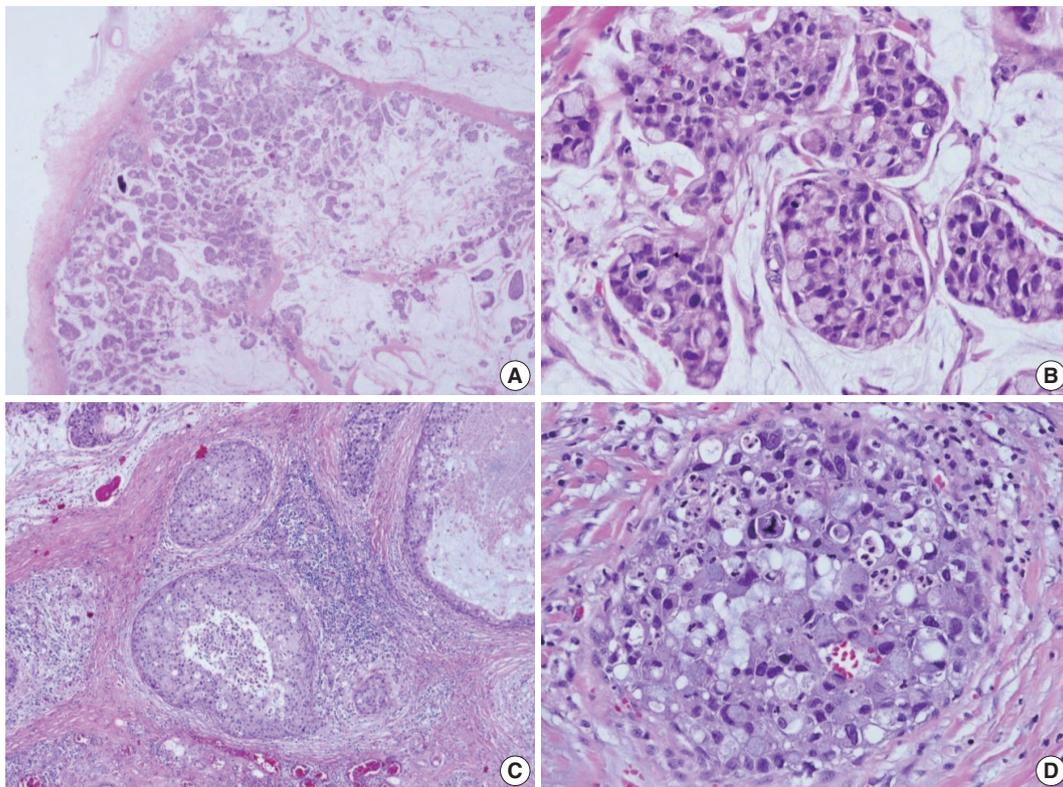

Fig. 1. Histologic features and biomarker status in mucinous carcinoma with extensive signet ring cell differentiation. (A) In the low-power view, a tumor with an expanding margin is observed. Tumor cell clusters floating in the mucin pool are shown and the cell density is higher in the periphery than in the center. (B) In the high-power view, tumor cell cluster floating in the mucin pool shows dysplasia suitable for the nuclear grade 3. Many tumor cells are seen as signet ring cell with the nucleus pushed into the corner by abundant intracellular mucin. (C) Ductal carcinoma *in situ* (DCIS) is observed in the periphery of the expanding invasive nodule. (D) The DCIS component shows significantly high nuclear grade and signet ring cell differentiation. *(Continued to the next page)*
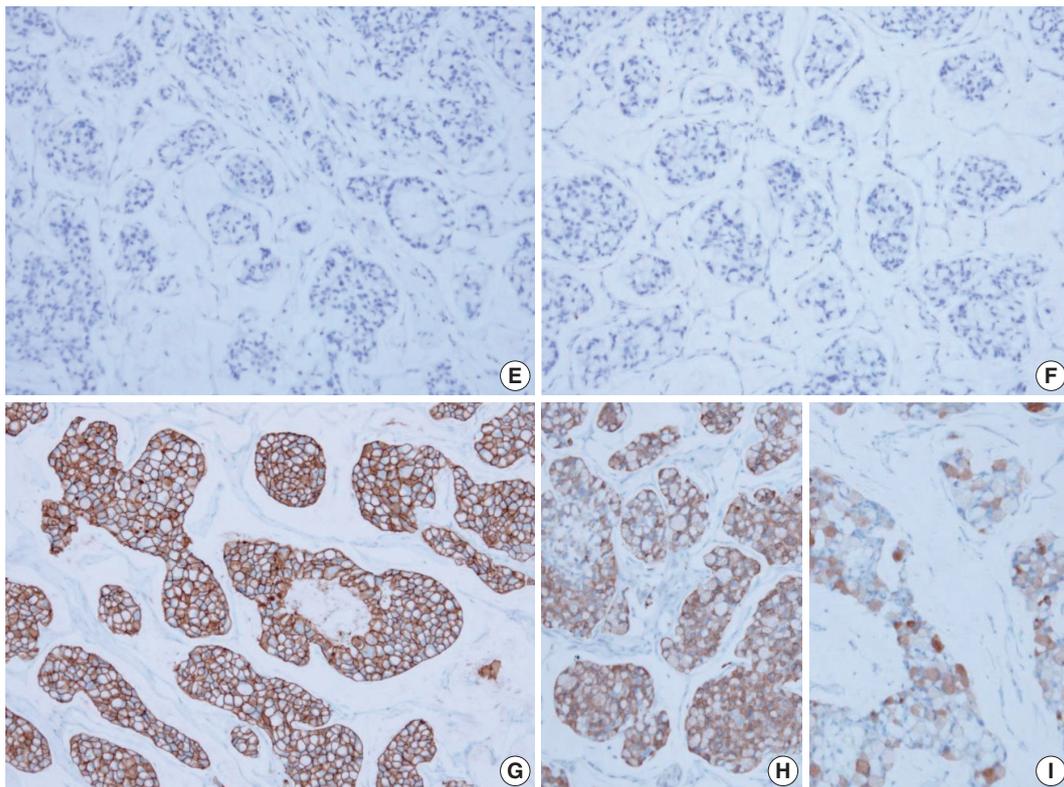
Fig. 1. *(Continued from the previous page)* Mucinous carcinoma cells are negative for estrogen receptor (E) and progesterone receptor (F) and positive for human epidermal growth factor receptor-2 (3+) (G). Mucinous carcinoma cells are positive for mammaglobin (H) and gross cystic disease fluid protein-15 (I).

grade nuclear pleomorphism, (2) high mitotic index, and (3) ER negativity, PR negativity, and HER-2 positivity. Carcinoma with signet ring cell differentiation has been reported to appear mainly in lobular carcinoma.[9] However, we suggest that this case is ductal type due to the positivity of E-cadherin. In the case of carcinoma with signet ring cell differentiation, hormone receptors are reported to be positive;[7] however, in this case, there was a difference in that the ER and PR immunohistochemical staining results were negative. In previous studies of carcinoma with signet ring cell differentiation, some reported that mucinous carcinoma is accompanied by signet ring cell component, which is a similar finding with this case. However, the proportion of signet ring cell component in mucinous carcinoma was reported to be 8%–17%, which shows significant difference with this case in the amount of signet ring cell component.[4] Previously published case reports that are most similar to this case include the report by Leung *et al.*,[10] which showed very similar histologic feature with this case. Furthermore, Kuroda *et al.*[11] reported a case of invasive ductal carcinoma of breast with signet ring cell and mucinous carcinoma components, which is a similar finding to that in this report. To the best of our knowledge, the case reported

here is the first case reported in Korea.

In such a case with signet ring cell differentiation, the most important differential diagnosis is metastatic signet ring cell carcinoma. In signet ring cell carcinoma of the stomach and colon extracellular mucin and signet ring cell differentiation due to abundant intracellular mucin are frequently observed. The presence of accompanied DCIS component and mammaglobin and GCDFP-15 positivity in this case suggest breast as the origin. The immunohistochemical markers widely used to help differentiate between signet ring cell carcinoma of the stomach and colon and signet ring cell carcinoma of the breast are CDX2, cytokeratin 20, MUC-1, and ER.[12]

The case reported here shows both extracellular mucin and extensive signet ring cell differentiation due to abundant intracellular mucin. Notably, this finding does not appear in separate regions in the tumor, but as a pattern of floating signet ring cell in a mucin pool. Therefore, we speculate that this finding is not a result of a mixed form of mucinous carcinoma and carcinoma with signet ring cell differentiation, but rather is signet ring cell differentiation in mucinous carcinoma cells. We report this case because it has the features of high-grade nuclear pleomorphism,

high mitotic index, ER negativity, PR negativity, and HER-2 positivity, which differ from typical mucinous carcinoma.

Conflicts of Interest

No potential conflict of interest relevant to this article was reported.

REFERENCES

1. Lakhani SR, Ellis IO, Schnitt SJ, Tan PH, Vijver MJ. WHO classification of tumours of the breast. 4th ed. Lyon: International Agency for Research on Cancer, 2012.

2. Coady AT, Shousha S, Dawson PM, Moss M, James KR, Bull TB. Mucinous carcinoma of the breast: further characterization of its three subtypes. Histopathology 1989; 15: 617-26.

3. Hull MT, Seo IS, Battersby JS, Csicsko JF. Signet-ring cell carcinoma of the breast: a clinicopathologic study of 24 cases. Am J Clin Pathol 1980; 73: 31-5.

4. Bartosch C, Mendes N, Rios E, et al. Morphological features and mucin expression profile of breast carcinomas with signet-ring cell differentiation. Pathol Res Pract 2015; 211: 588-95.

5. Barkley CR, Ligibel JA, Wong JS, Lipsitz S, Smith BL, Golshan M. Mucinous breast carcinoma: a large contemporary series. Am J Surg 2008; 196: 549-51.

6. Lacroix-Triki M, Suarez PH, MacKay A, et al. Mucinous carcinoma of the breast is genomically distinct from invasive ductal carcinomas of no special type. J Pathol 2010; 222: 282-98.

7. O'Connell FP, Wang HH, Odze RD. Utility of immunohistochemistry in distinguishing primary adenocarcinomas from metastatic breast carcinomas in the gastrointestinal tract. Arch Pathol Lab Med 2005; 129: 338-47.

8. Frost AR, Terahata S, Yeh IT, Siegel RS, Overmoyer B, Silverberg SG. The significance of signet ring cells in infiltrating lobular carcinoma of the breast. Arch Pathol Lab Med 1995; 119: 64-8.

9. Raju U, Ma CK, Shaw A. Signet ring variant of lobular carcinoma of the breast: a clinicopathologic and immunohistochemical study. Mod Pathol 1993; 6: 516-20.

10. Leung KM, Yeoh GP, Chan JK, Cheung PS, Chan KW. Ductal type signet ring cell carcinoma of breast with growth pattern of pure mucinous carcinoma. Pathology 2011; 43: 282-4.

11. Kuroda N, Fujishima N, Ohara M, Hirouchi T, Mizuno K, Lee GH. Invasive ductal carcinoma of the breast with signet-ring cell and mucinous carcinoma components: diagnostic utility of immunocytochemistry of signet-ring cells in aspiration cytology materials. Diagn Cytopathol 2007; 35: 171-3.

12. Chu PG, Weiss LM. Immunohistochemical characterization of signet-ring cell carcinomas of the stomach, breast, and colon. Am J Clin Pathol 2004; 121: 884-92.

Mucinous Cystadenoma of the Testis: A Case Report with Immunohistochemical Findings

Gilhyang Kim[1] · Dohee Kwon[1]
Hee Young Na[1] · Sehui Kim[1]
Kyung Chul Moon[1,2]

[1]Department of Pathology, [2]Kidney Research Institute, Medical Research Center, Seoul National University College of Medicine, Seoul, Korea

Corresponding Author
Kyung Chul Moon, MD
Department of Pathology, Kidney Research Institute, Medical Research Center, Seoul National University College of Medicine, 103 Daehak-ro, Jongno-gu, Seoul 03080, Korea
Tel: +82-2-740-8380
Fax: +82-2-743-5530
E-mail: blue7270@snu.ac.kr

Mucinous cystadenoma of the testis is a very rare tumor. Herein, we report a case of mucinous cystadenoma arising in the testis of a 61-year-old man, along with a literature review. Computed tomography showed a 2.5-cm-sized poorly enhancing cystic mass. Grossly, the tumor was a unilocular cystic mass filled with mucinous material and confined to the testicular parenchyma. Histologically, the cyst had a fibrotic wall lined by mucinous columnar epithelium without atypia. Immunohistochemical staining was positive for cytokeratin 20 and CDX2, as well as focally positive for cytokeratin 7. The pathologic diagnosis was mucinous cystadenoma.

Key Words: Testis; Cystadenoma, mucinous; Immunohistochemistry

Testicular/paratesticular tumors resembling mucinous or serous ovarian tumors are rare; between the two subtypes, mucinous neoplasms are less commonly reported than serous neoplasms.[1-7] To our knowledge, there have been approximately 24 case reports of mucinous neoplasms of the testis or paratestis, and only four cases of "testicular mucinous cystadenoma" were found in the English-language literature (Table 1).[1,2,8-11] In Korea, two cases of mucinous cystadenomas of the paratestis or spermatic cord have been reported.[4,7] However, there has been no published report of testicular mucinous cystadenoma in Korea. Here, we report a case of mucinous cystadenoma in the parenchyma of a testis.

CASE REPORT

A 61-year-old Korean man presented with a painless right testicular mass. Serum tumor markers including β-human chorionic gonadotrophin, α-fetoprotein, and lactate dehydrogenase were within normal limits. Urine cytology was negative for malignant cells. Computed tomography (Fig. 1A) and ultrasound (Fig. 1B) imaging showed a 2.5-cm-sized poorly enhancing cystic mass at the right testis. Radical orchiectomy was performed.

Pathological examination demonstrated that the cystic mass was confined within the testicular parenchyma, with a size of $2.5 \times 2.4 \times 1.7$ cm. On macroscopic examination, the mass had a unilocular cavity filled with mucinous materials (Fig. 1C). The cyst wall was composed of thick fibrous tissue. There was no solid or papillary growth or calcification in the cyst.

Microscopically, the cyst was surrounded by a thick fibrous wall and was filled with mucinous material (Fig. 2A–C). The cyst had a single layer of columnar mucinous epithelial cells without nuclear atypia (Fig. 2D). Stromal mucin spillage was found around the tumor with inflammatory cell infiltration (Fig. 2E). The inflammatory cells were composed of lymphocytes, plasma cells, and histiocytes (Fig. 2F). There was no hemorrhage, necrosis, or calcification. Teratomatous elements, such as cartilage, bone, or other mesenchymal teratomatous compo-

Table 1. Cases of primary testicular mucinous cystadenoma

Age (yr)	Side	Maximum diameter (cm)	Immunohistochemistry	Follow-up	Reference
61	Rt	2.5	CK7 (f+), CK20 (+), CDX2 (+), PAX8 (–), Calretinin (–), D2-40 (–), WT-1 (–)	NDR 13 days	Current case
43	Rt	4.6	ND	NDR 2.5 yr	Shimbo et al.[2]
35	Rt	9.0	AFP (–), CA 19-9 (–), MUC2 (+), MUC5AC (–)	NDR 8 mo	Nokubi et al.[9]
55	Rt	4.0	CK7 (+), CK20 (+), MUC2 (+), MUC5AC (+)	NDR 5 mo	Naito et al.[10]
39	Rt	2.0	CK7 (–), CK20 (+), CA125 (–), Chromogranin (f+), Synaptophysin (–)	NDR 1 yr	Alasio et al.[11]

Rt, right; CK7, cytokeratin 7; f, focal; +, positive; CK20, cytokeratin 20; –, negative; NDR, no disease recurrence; ND, not none; AFP, α-fetoprotein; CA 19-9, carbohydrate antigen 19-9; CA125, carbohydrate antigen 125.
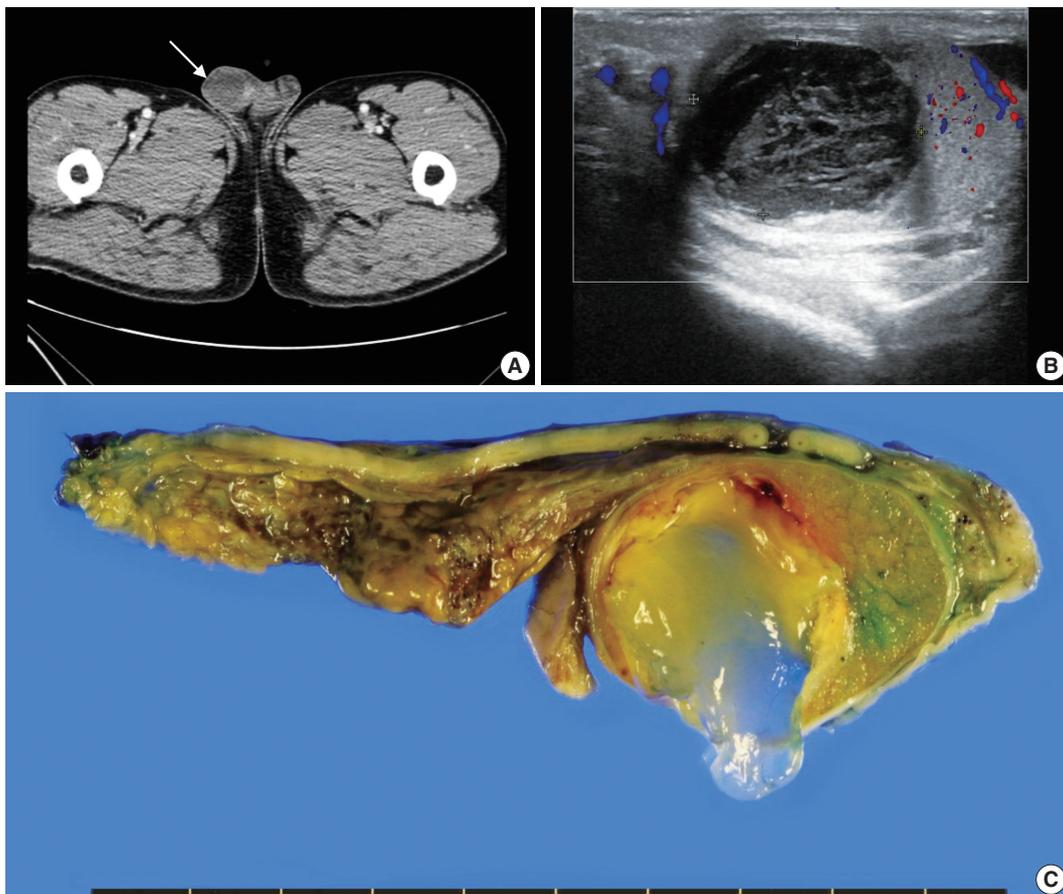

Fig. 1. Representative images of radiologic and macroscopic findings of a right testicular mass. Computed tomography (A) and ultrasound imaging (B) present a cystic mass (arrow in A) suspected to have a tumorous condition. (C) Surgical specimen reveals a mass with a unilocular cyst filled with mucinous materials.

nents, were not found. Squamous epithelium and intratubular germ cell neoplasia were also absent. Mitotic figures were not observed. Microscopically, the tumor was limited to the testicular parenchyma without involvement of the tunica albuginea.

Immunohistochemically, the lining epithelial cells were positive for cytokeratin 20 (CK20) (Fig. 3A) and CDX2 (Fig. 3C), as well as focally positive for cytokeratin 7 (CK7) (Fig. 3B). The cells were negative for PAX-8 (Fig. 3D), D2-40, WT-1, and cytokeratin 5/6 (CK5/6). Calretinin was weakly positive in cytoplasm.

This study was approved by the Institutional Review Board (IRB) of Seoul National University Hospital.

DISCUSSION

Mucinous neoplasms of the testis or paratestis are rare and
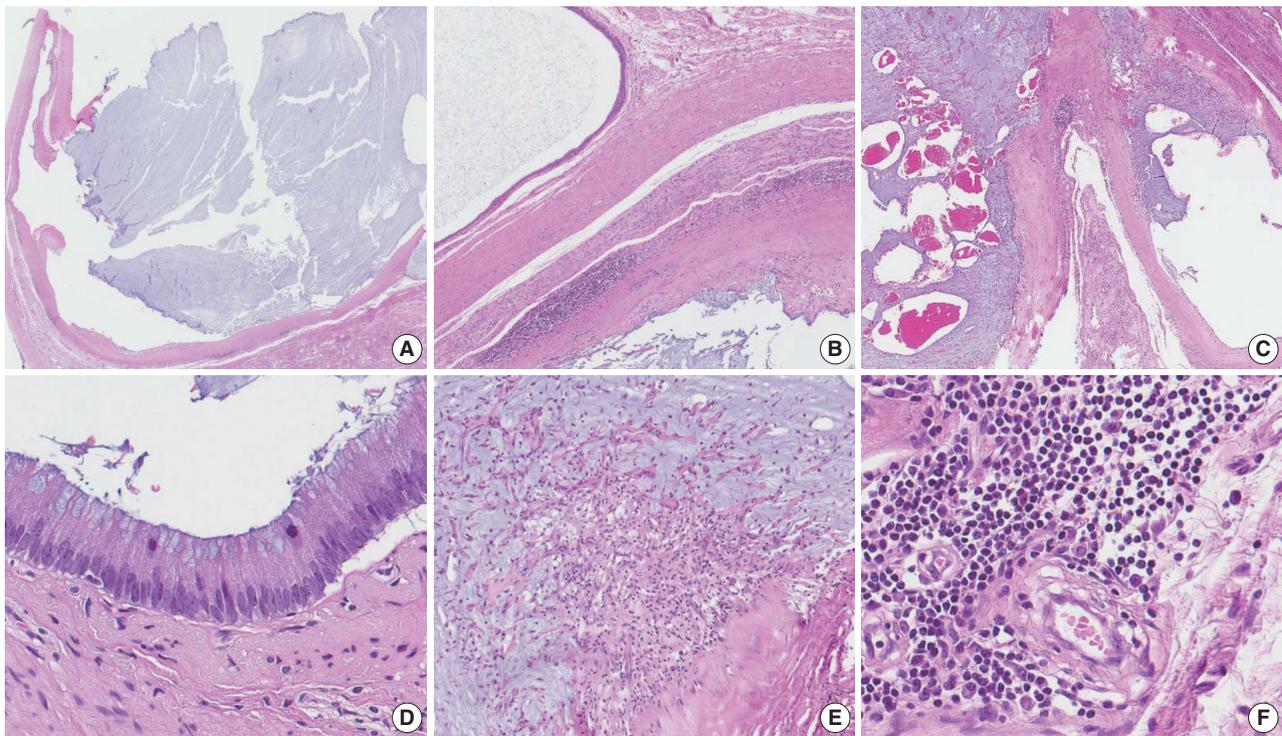
Fig. 2. Microscopic findings of the mucinous cystadenoma of the testis. (A) The tumor has a uniloculated cyst with an expanding growth pattern. (B) The cyst is surrounded by a thick fibrous capsule, and there are some inflammatory cells around the tumor. (C) The cyst is filled with mucinous material. (D) The wall of the cavity is lined by a single layer of columnar mucinous epithelium, and the lining cells show no cytologic atypia. (E) Mucin extravasation into the stroma and some inflammatory cell infiltration are observed. (F) The inflammatory cells are composed of lymphocytes, plasma cells, and histiocytes.

not well described in the medical literature.[8,12] The first reported case of mucinous neoplasm was mucinous cystadenoma in the paratestis of an 11-year-old boy by Kellert in 1959.[1] To date, most reported testicular/paratesticular ovarian-type surface epithelial neoplasms have been of the "serous" subtype,[5,13,14] and "intratesticular" neoplasms have rarely been reported.[12] Previous papers reported approximately 24 cases of mucinous neoplasms of the testis or paratestis; among these, only four reports described "testicular mucinous cystadenoma" excluding the present case.[1,2,8,9] In the Korean literature, three cases of serous borderline tumors of the testis/paratestis and two cases of paratesticular mucinous cystadenomas were found, but there has been no report of any "mucinous cystadenoma of the testicular parenchyma" to date.[3-7]

The histologic features of mucinous cystadenomas of the testis resemble those of common ovarian mucinous cystadenomas.[1,2] That is, the cyst is typically composed of mucinous epithelium with tall, columnar endocervical-like cells lacking nuclear atypia.[15] However, there are several histologic differences between testicular mucinous cystadenomas and ovarian mucinous cystadenomas. Testicular mucinous cystadenomas are generally not as large as

ovarian tumors, purportedly because the testicular tumors are found by patients earlier than their ovarian counterparts due to the sites at which the tumors arise. Testicular tumors are more often unilocular and more frequently exhibit mucus extravasation associated with fibrosis or calcification than ovarian tumors, possibly because of trauma due to their superficial location.[15]

The origin of testicular mucinous neoplasms has not yet been clarified; thus, several hypotheses have been suggested. Ulbright and Young[15] supported the theory that the tumors arise from metaplasia of the mesothelium of the visceral tunica vaginalis. Another theory, suggested by Shimbo *et al.*,[2] is that inflammation results in mesothelial introduction into the testicle and mucinous metaplasia. The theory that the tumors arise from the remnants of the Müllerian ducts persisting in the male appendix, testis, or extratesticular scrotal contents is considered the most reasonable by some researchers.[8,16] Others have postulated the possibility of one-sided teratoma cell differentiation.[9,15,17]

Differential diagnoses include testicular mucinous borderline neoplasms/carcinomas, germ cell tumors, mesotheliomas, and metastatic mucinous tumors.[15] In comparison with mucinous borderline tumors or mucinous carcinomas, mucinous cystade-
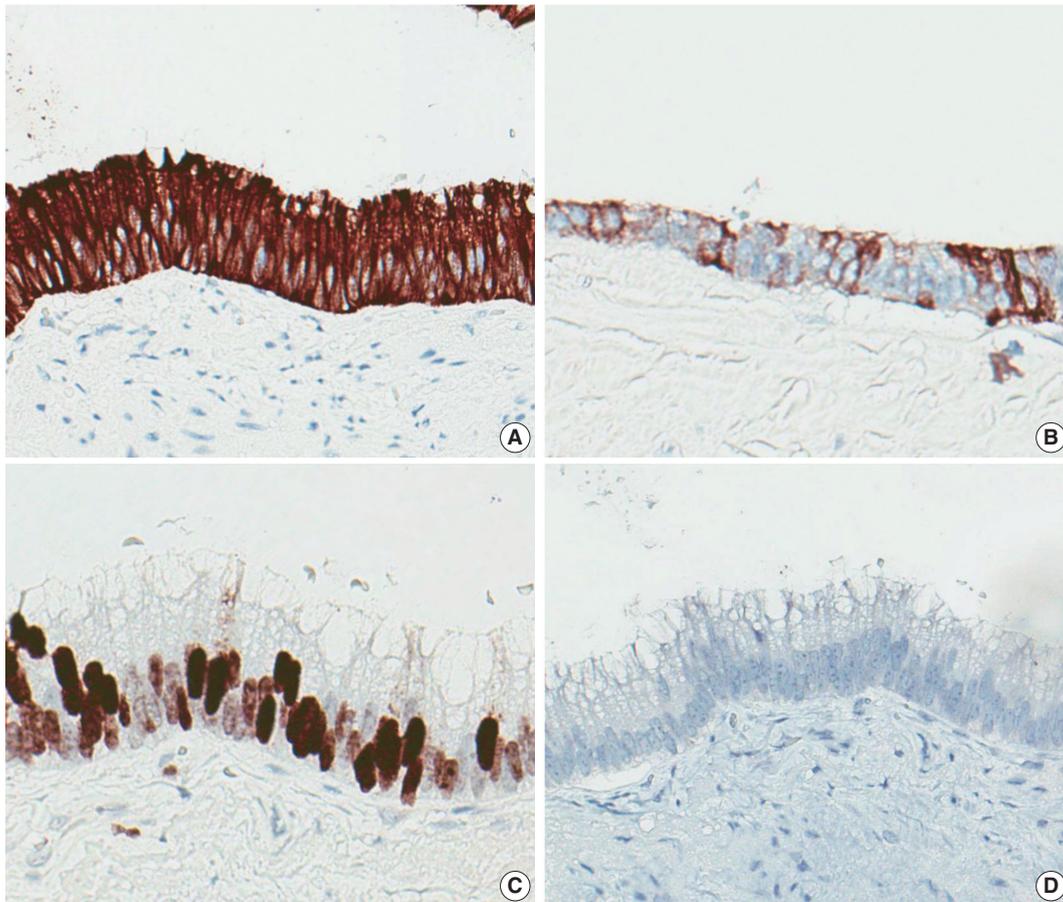
Fig. 3. Immunohistochemical staining results. The lining cells are positive for cytokeratin 20 (A), focally positive for cytokeratin 7 (B), positive for CDX2 (C), and negative for PAX8 (D).

nomas lack the atypia of tumor cells.[8,15] Testicular mucinous carcinomas or borderline neoplasms have been reported more frequently than testicular mucinous cystadenomas. To date, seven mucinous borderline neoplasms and four mucinous carcinomas have been reported.[1,8] It is also important to rule out germ cell tumors, for example, teratomas with prominent mucinous components. Teratomas are known to occur in patients with a median age of 23–29 years. Teratomas almost always have components other than mucinous epithelial lined cysts, and 90% of those tumors occurring in adults are accompanied by intratubular germ cell neoplasia of unclassified type.[15] Unlike testicular mucinous cystadenomas, mesotheliomas exhibit positivity for calretinin, which is known to be expressed in mesothelial cells.[10] Pathologists must consider metastatic mucinous tumors. The appropriate immunohistochemical staining, cytologic atypia, and history of mucinous carcinoma are critical for determining the origin of the tumor.

The immunohistochemical profile of the tumor has not been specified until now.[8] However, in several reports, testicular muci-

nous neoplasms have shown immunostaining that is positive for both CK7 and CK20 or positive for CK20 and negative for CK7.[8] The present case showed positive staining for CK20 and focal positive staining for CK7, a result similar to previous studies. Additionally, the present case also showed positive staining for CDX2 and negative staining for PAX8, D2-40, and CK5/6. Calretinin immunostaining was weak only in the cytoplasm. CDX2 is known to be useful in distinguishing primary ovarian mucinous tumors from metastases of lower gastrointestinal tract origin.[18] There has been only one case report of CDX2 expression in testicular or paratesticular mucinous neoplasms, revealing CDX2-positive and PAX8-negative staining.[4] Together with the results of this report, testicular or paratesticular mucinous tumors may express CDX2. Immunohistochemical results for calretinin, CK5/6, D2-40, and PAX8 suggest that testicular mucinous cystadenoma does not originate from mesothelium or Müllerian duct remnants, while the results support the possibility of monodermal teratoma differentiation.

Although only a small number of testicular mucinous cyst-

adenomas have been reported, these reported cases have shown good prognosis, similar to the prognosis of ovarian mucinous cystadenomas.[1]

In conclusion, mucinous cystadenoma of the testis is an extremely rare benign tumor and likely expresses CDX2.

Conflicts of Interest

No potential conflict of interest relevant to this article was reported.

REFERENCES

1. Elliott JE, Klein JR, Drachenberg DE. Primary testicular mucinous neoplasms: case report and literature review. Can Urol Assoc J 2010; 4: E112-5.

2. Shimbo M, Araki K, Kaibuchi T, Kuramochi H, Mori I. Mucinous cystadenoma of the testis. J Urol 2004; 172: 146-7.

3. Park KM, Cho NB, Song KY. A serous papillary cystadenoma of low malignant potential in paratesticular tissue. Korean J Pathol 1996; 30: 463-5.

4. Kim JY, Lee YT, Kang HJ, Lee CH. Primary mucinous cystadenoma of the spermatic cord within the inguinal canal. Diagn Pathol 2012; 7: 139.

5. Park MI, Kim HS, Suh KS, Kang DY. Paratesticular papillary serous tumor of low malignant potential: a case report. Korean J Pathol 2004; 38: 427-9.

6. Park HJ, Park SW, Chon WH, Jung SG, Park NC. A serous papillary cystadenoma of borderline malignancy in testis. Korean J Androl 2007; 25: 36-8.

7. Weon HC, Kim IS, Jang CS, Hong SJ, Lee MS. Papillary mucinous cystadenoma, paratesticular: a case report. Korean J Urol 1986; 27: 359-60.

8. Celdran JO, Rodriguez CS, Valverde FM, Compiano LO. Primary mucinous cystadenocarcinoma of the testis: an extremely rare ovarian-type surface epithelial carcinoma. J Cancer Res Ther 2015; 11: 647.

9. Nokubi M, Kawai T, Mitsu S, Ishikawa S, Morinaga S. Mucinous cystadenoma of the testis. Pathol Int 2002; 52: 648-52.

10. Naito S, Yamazumi K, Yakata Y, *et al*. Immunohistochemical examination of mucinous cystadenoma of the testis. Pathol Int 2004; 54: 355-9.

11. Alasio TM, Borin J, Taylor K, Bar-Chama N, Unger PD. Intratesticular mucinous cystadenoma: immunohistochemical comparison with ovarian and colonic tissue. Arch Pathol Lab Med 2005; 129: 399-402.

12. Burger T, Schildhaus HU, Inniger R, *et al*. Ovarian-type epithelial tumours of the testis: immunohistochemical and molecular analysis of two serous borderline tumours of the testis. Diagn Pathol 2015; 10: 118.

13. Olla L, Di Naro N, Puliga G, Tolu GA. Intraparenchymal serous papillary cystadenoma of the testis: a case report. Pathologica 2013; 105: 15-7.

14. Remmele W, Kaiserling E, Zerban U, *et al*. Serous papillary cystic tumor of borderline malignancy with focal carcinoma arising in testis: case report with immunohistochemical and ultrastructural observations. Hum Pathol 1992; 23: 75-9.

15. Ulbright TM, Young RH. Primary mucinous tumors of the testis and paratestis: a report of nine cases. Am J Surg Pathol 2003; 27: 1221-8.

16. Amin MB. Selected other problematic testicular and paratesticular lesions: rete testis neoplasms and pseudotumors, mesothelial lesions and secondary tumors. Mod Pathol 2005; 18 Suppl 2: S131-45.

17. Young RH, Scully RE. Testicular and paratesticular tumors and tumor-like lesions of ovarian common epithelial and mullerian types: a report of four cases and review of the literature. Am J Clin Pathol 1986; 86: 146-52.

18. Vang R, Gown AM, Wu LS, *et al*. Immunohistochemical expression of CDX2 in primary ovarian mucinous tumors and metastatic mucinous carcinomas involving the ovary: comparison with CK20 and correlation with coordinate expression of CK7. Mod Pathol 2006; 19: 1421-8.

Heterotopic Ossification in the Gallbladder

Jihyun Ahn · Sunyoung Kim · Kangseung Kim[1] · Seogjoon Kim[2]

Departments of Pathology, [1]General Surgery, and [2]Radiology, Dongkang Medical Center, Ulsan, Korea

Heterotopic ossification is a common pathologic process in cases of atherosclerotic plaques, traumatic injury, severe burns, some carcinomas, and benign neoplasms.[1] However, heterotopic ossification is extremely rare in the gallbladder. Less than 10 cases have been reported in the literature to date.[2-8] While the pathogenesis of heterotopic ossification of the gallbladder is unclear, it may clinically lead to the misinterpretation of cholelithiasis, etc. Herein, we report a case of heterotopic ossification in the gallbladder epithelium.

CASE REPORT

A 26-year-old man visited our hospital for abdominal pain of several days duration. Laboratory data showed positivity for hepatitis B surface antigen and hepatitis B e antigen, negativity for hepatitis B surface antibody and hepatitis B e antibody, and increased hepatitis B virus DNA. Alanine transaminase was slightly increased (65 U/L), but aspartate transaminase, bilirubin, alkaline phosphatase, and γ-glutamyl transpeptidase were within normal range. An ultrasound revealed diffuse wall thickening of the gallbladder with a 1.0 cm-sized gallstone and chronic liver disease (Fig. 1). Computed tomography demonstrated a collapsed gallbladder with mild wall thickening. The patient underwent laparoscopic cholecystectomy. During the operation, a 1.0 cm-sized, black stone was noted in the gallbladder. On gross examination, the gallbladder measured $6.7 \times 3.3 \times 2.0$ cm in size. The mucosal surface was greenish, velvety with focal whitish streaks at the body, about 0.6×0.6 cm in dimension; in addition, the wall was thickened, measuring up to 1.0 cm. Microscopically, the gallbladder wall was thickened with Rokitansky-Aschoff sinuses and infiltrated by polymorphous inflammatory cells. The mucosa was slightly atrophic with focal mature lamellar bone. Osteoblastic rimming or bone marrow components were absent (Fig. 2).

DISCUSSION

Heterotopic ossification (bone metaplasia) in the gastrointestinal tract is rare.[9] Most reported cases were associated with benign and malignant epithelial neoplasms. In the gallbladder, stromal osseous metaplasia has been described in metastatic adenocarcinoma.[10] However, bone metaplasia in benign gallbladder is extremely rare. In 1957, Indyk and Shipton[2] described heterotopic bone formation in the gallbladder accompanied by cholelithiasis. Since then, six cases have been reported in the English literature,[2-8] of which four cases were associated with cholelithiasis and two cases showed spicules of bone in the cholesterol polyps.[3,4] Rege and Vargas[5] reported intramuscular fasciitis-like proliferation and bony metaplasia in the gallbladder of a 7-year-old boy with sickle cell disease. They proposed the term cholecystitis ossificans to describe their case; furthermore, they suggested that the mucosal insult by repetition predisposed the gallbladder to dystrophic calcification and/or fasciitis, subsequently creating a favorable microenvironment for bone formation.[5] This mechanism is further corroborated by reports of heterotopic ossification in other sites of chronic injury, such as atherosclerotic plaques, traumatic injury, and severe burns.[1] However, it is still early to conclude that stones induce heterotopic ossification in the gallbladder.

Three other cases showed heterotopic ossification without accompanied cholelithiasis. Chen[6] described a case of polypoid intramucosal lesions composed of bone lined by flattened gall-

Corresponding Author
Jihyun Ahn, MD
Department of Pathology, Dongkang Medical Center, 239 Taehwa-ro, Jung-gu, Ulsan
44455, Korea
Tel: +82-52-241-1375, Fax: +82-52-241-1366, E-mail: jvcjh@hanmail.net

bladder mucosa, designated as osteoma of the gallbladder. Yosepovich *et al.*[7] and Nelson and Kahn[8] also described heterotopic bones occupying gallbladder wall or mucosa, respectively.

Fig. 1. Radiologic finding. Ultrasound shows diffuse wall thickening of the gallbladder with a 1 cm-sized gallstone.
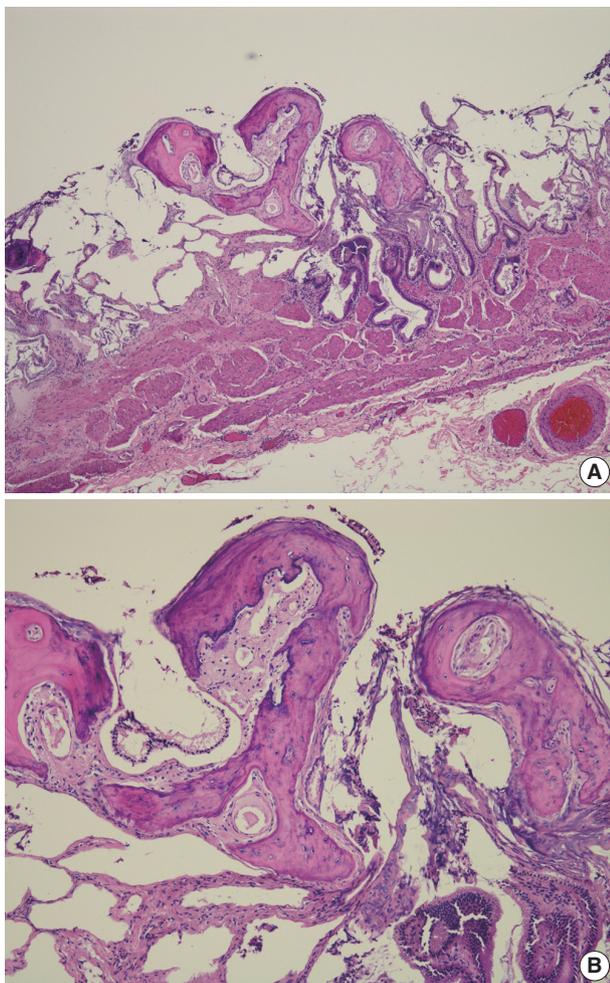

Fig. 2. Pathologic findings. (A, B) Microscopic findings show autolytic mucosa with focal mature bone.

The former was composed of mature lamellar bone with osteoblastic rimming and bone marrow components, while osteoblastic rimming or bone marrow was absent in the latter.[7,8] Our case was similar to the latter except for the occurrence of the stone. Clinicians should be aware of heterotopic ossification since it can clinically mimic stones and lead to altered treatments and patient outcome.

To our knowledge, this is the first report of heterotopic ossification in the gallbladder in Korean patients. The pathogenesis and clinical significance of heterotopic ossification remain to be elucidated.

Conflicts of Interest

No potential conflict of interest relevant to this article was reported.

REFERENCES

1. Ramirez DM, Ramirez MR, Reginato AM, Medici D. Molecular and cellular mechanisms of heterotopic ossification. Histol Histopathol 2014; 29: 1281-5.

2. Indyk JS, Shipton EA. Heterotopic bone formation in the gall-bladder. Med J Aust 1957; 44: 9-11.

3. Ortiz-Hidalgo C, Baquera-Heredia J. Osseous metaplasia in polypoid cholesterosis. Am J Surg Pathol 2000; 24: 895.

4. Lin MY, Shikle JF. To pick a 'bone' with the gallbladder. South Med J 2009; 102: 773-4.

5. Rege TA, Vargas SO. Cholecystitis and cholelithiasis associated with an intramural fasciitis-like proliferation and osseous metaplasia. Pediatr Dev Pathol 2011; 14: 80-3.

6. Chen KT. Osteomas of the gallbladder. Arch Pathol Lab Med 1994; 118: 755-6.

7. Yosepovich A, Nass D, Zagatsky M, Kopolovic J. Chronic cholecystitis with bone metaplasia: a case report. Pathol Res Pract 2002; 198: 765-6.

8. Nelson JJ, Kahn AG. A case of bone metaplasia of the gallbladder epithelium. South Med J 2009; 102: 322-4.

9. Haque S, Eisen RN, West AB. Heterotopic bone formation in the gastrointestinal tract. Arch Pathol Lab Med 1996; 120: 666-70.

10. Cavazza A, De Marco L, Asioli S, Pastore L, Gardini G. Stromal osseous metaplasia in metastatic adenocarcinoma of the gallbladder. Tumori 1999; 85: 133-4.

Mucosal Schwann Cell Hamartoma in Colorectal Mucosa: A Rare Benign Lesion That Resembles Gastrointestinal Neuroma

Jiheun Han · Yosep Chong · Tae-Jung Kim · Eun Jung Lee · Chang Suk Kang

Department of Hospital Pathology, College of Medicine, The Catholic University of Korea, Seoul, Korea

The term mucosal Schwann cell hamartoma (MSCH) was first proposed by Gibson and Hornick in 2009[1] to describe a group of neuronal polyps purely composed of S-100–positive Schwann cells, in an attempt to distinguish from true "neuromas" and "neurofibromas." To our knowledge, only 10 cases have been reported in the literature since it was first described (Table 1). MSCH is currently thought to have no association with any inherited disorder. Herein, we describe a case of MSCH and discuss the morphologic and immunohistochemical features with a differential diagnosis in the gastrointestinal (GI) tract.

CASE REPORT

A 2-mm-sized rectal polyp was found in a follow-up colonoscopy of a 49-year-old male who has no significant family history of other neuronal lesions or inherited syndromes but had a tubular adenoma resected 2 years prior (Fig. 1A). On microscopic examination, the rectal polyp showed a poorly circumscribed proliferation of spindle cells in the lamina propria, separating the crypt architecture (Fig. 1B). The cells were uniformly elongated, with tapered nuclei and abundant eosinophilic cytoplasm with indistinct cell borders. Nuclear atypia, pleomorphism, or mitosis was not observed (Fig. 1C). On immunohistochemical staining, the cells displayed a strong and diffuse positivity for S-100 in both the nucleus and cytoplasm (Ventana, Roche, Tucson, AZ, USA) (Fig. 1D). In comparison, the cells did not have im-

munoreactivity for c-Kit, CD34, glial fibrillary acidic protein, epithelial membrane antigen (EMA), smooth muscle actin, or neurofilament protein (NFP). Because the spindle cells did not form a discrete mass but rather an interspersed proliferation between normal structures, the lesion was diagnosed as MSCH.

DISCUSSION

A diagnosis of MSCH should be made after exclusion of other lesions that resemble spindle cell proliferation and other neuronal tumors. Gastrointestinal stromal tumors, which are the most common spindle cell tumor in the GI tract, can be easily excluded by the characteristic immunoreactivity of c-Kit.

Colorectal neurofibromas are another important differential diagnosis of MSCH because they are also composed of Schwann cells, fibroblasts, perineural cells, and NFP-positive axons and usually form a vague tumor without discrete demarcation. However, they are often associated with neurofibromatosis type 1 (NF1), which is usually accompanied by multiple cutaneous neurofibromas. Colorectal lesion as a primary clinical presentation without skin manifestation is also exceedingly rare.[1]

Mucosal neuromas appear as an ill-defined mass and are composed of hyperplastic nerve fibers arranged in an irregularly ramifying manner.[1] In contrast to our case, mucosal neuromas have perineurial capsules, which are often EMA-positive. They are almost always multiple and a part of the multiple endocrine neoplasia syndrome type IIb (MEN2B), of which the most important component is a medullary thyroid carcinoma.

GI ganglioneuromas are most common in colorectal neuronal lesions and reveal hypercellular stroma composed of mainly S-100–positive Schwann cells. They differ from MSCH in that they are mixed with variable numbers of neuron-specific enolase–

Corresponding Author
Chang Suk Kang, MD, PhD
Department of Hospital Pathology, Yeouido St. Mary's Hospital, College of Medicine,
The Catholic University of Korea, 10 63-ro, Yeongdeungpo-gu, Seoul 07345, Korea
Tel: +82-2-3779-1312, Fax: +82-2-2258-1628, E-mail: cskang@catholic.ac.kr

positive ganglion cells.[1,2] Solitary polypoid ganglioneuromas are not associated with systemic manifestations;[3] however, ganglioneuromatous polyposis and diffuse ganglioneuromatosis are associated with Cowden syndrome, Juvenile polyposis syndrome, MEN2B (particularly with diffuse ganglioneuromatosis), and NF1.[4]

Table 1. Features of Schwann cell hamartoma repoerted in colorectum

Reference	Year	No. of cases	Location	Age (yr)	Sex	Symptom	Endoscopic finding
Gibson and Hornick[1]	2009	26	Predominantly in rectosigmoid colon	Mean 62 (46–88)	M:F= 10:16	Asymptomatic (most common), diarrhea, lower GI bleeding	Sessile polyp, 1–6 mm (mean, 2.5 mm)
Pasquini *et al.*[6]	2009	1	Rectosigmoid colon	60	F	Occult blood in the stool	Sessile polyp, 5 mm
Rocco *et al.*[5]	2011	1	Sigmoid colon	67	F	Asymptomatic	Sessile polyp, 3 mm
Sagami *et al.*[7]	2012	1	Sigmoid colon	40	M	Occult blood in the stool	Many small whitish nodules in mucosa
Bae *et al.*[3]	2013	1	Descending colon	41	F	Asymptomatic	Polyp, 8 mm
Neis *et al.*[4]	2013	1	Sigmoid colon	59	M	Underlying ulcerative colitis	Polyp, 3 mm
Ferro de Beca *et al.*[8]	2014	1	Sigmoid colon	72	M	Asymptomatic	Polyp, 5 mm
Klair *et al.*[2]	2014	1	Rectum	78	F	Abdominal pain and intermittent tenesmus	Polyp, 7 mm along with rectal erythema and inflammation
Kanar *et al.*[9]	2015	1	Sigmoid colon	67	M	Asymptomatic	Polyp, 6 mm
Bae *et al.*[10]	2015	1	Rectum	20	M	Abdominal discomfort and loose stools	Polyp, 4 mm and scattered tiny polyp-like mucosal elevation
Present case	2015	1	Rectum	49	M	Asymptomatic	Tiny polyp-like mucosal elevation, 2 mm

M, male; F, female; GI, gastrointestinal.
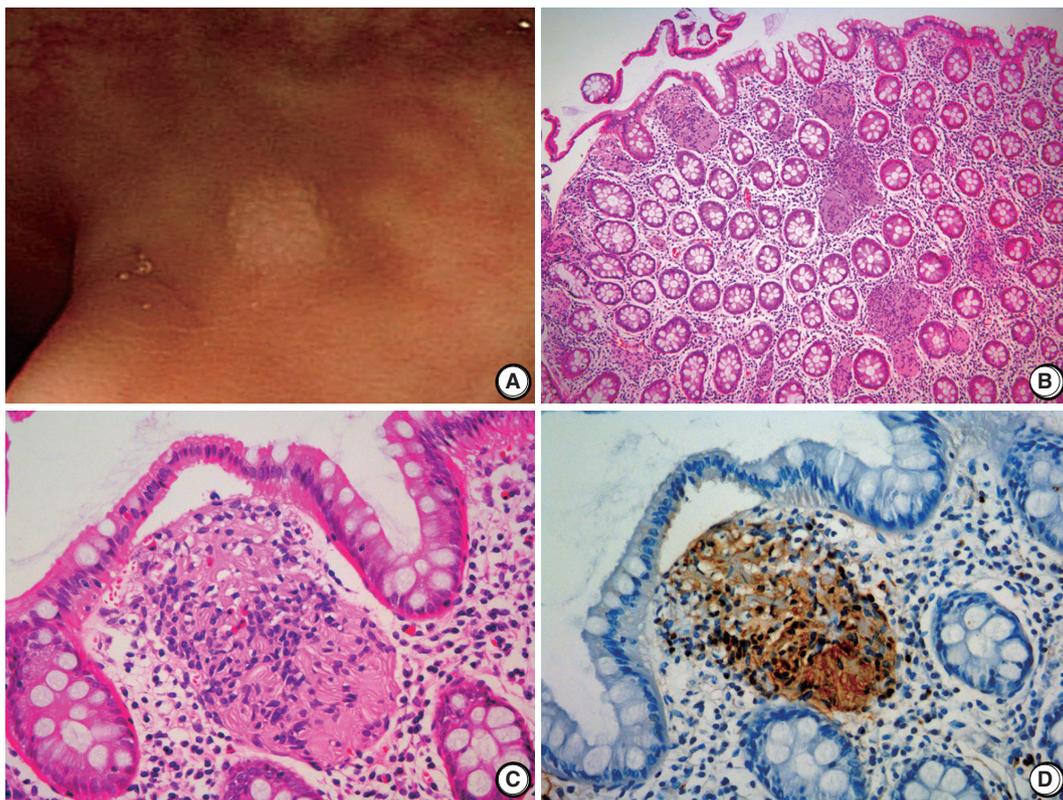
Fig. 1. Schwann cell hamartoma of rectal mucosa. (A) Colonoscopy shows a 2-mm sized tiny polyp-like mucosal elevation without erosion or ulceration. (B, C) Hematoxylin and eosin shows scattered proliferation of bland spindle cells in the lamina propria. (D) Immunohistochemical staining for S-100 displays a positivity of both nucleus and cytoplasm.

GI schwannomas are composed of bland spindle cells arranged in vague fascicles. Unlike their counterparts from the central nervous system and peripheral soft tissue, the nuclear palisading, so-called Verocay bodies, are absent, which can be similar to MSCH. However, they have characteristic peripheral lymphoid cuffs and form more demarcated tumors than do MSCH.[4,5]

Mucosal perineuromas are usually solitary lesions and are characterized by a whorled growth pattern of bland spindle cells that expand the lamina propria,[5] which are morphologically very similar to MSCH. Unlike MSCH, they have colonic epithelium with serrated architecture and express perineural markers such as EMA, whereas they are negative for S-100 protein.[2]

Finally, inflammatory fibroid polyps (Vanek's tumor) can be confused with MSCH. They are composed of stellate or spindle-shaped, bland stromal cells that are arranged in an onion skin-like pattern around blood vessels and mucosal glands.[5] They have inflammatory infiltrates dominated by eosinophils, which are not observed in MSCH. Additionally, they are not immunoreactive for S-100 and are extremely rare in the colon.

MSCH is a rare benign lesion, and cases with clinical features are summarized in Table 1. Cases are primarily detected as small polyps that range from 1 to 8 mm (mean, 5 mm) and are predominantly located in the rectosigmoid colon. Patients are typically asymptomatic, and none of the patient cases were associated with an inherited syndrome. The clinical features of this case are similar to those summarized in Table 1.

In summary, MSCH is a rare lesion that can be found incidentally during routine colonoscopy. Although there is currently no indication that MSCH is related to inherited syndromes or malignancies, it is important for pathologists to include it in the differential diagnosis of S-100–positive spindle cell proliferative lesions for accurate diagnosis and to prevent aggressive or unnecessary treatments.

Conflicts of Interest

No potential conflict of interest relevant to this article was reported.

REFERENCES

1. Gibson JA, Hornick JL. Mucosal Schwann cell "hamartoma": clinicopathologic study of 26 neural colorectal polyps distinct from neurofibromas and mucosal neuromas. Am J Surg Pathol 2009; 33: 781-7.

2. Klair JS, Girotra M, Agarwal A, Aduli F. Mucosal Schwann cell hamartoma: just benign or more? Int J Colorectal Dis 2014; 29: 1597-8.

3. Bae MN, Lee JE, Bae SM, et al. Mucosal Schwann-cell hamartoma diagnosed by using an endoscopic snare polypectomy. Ann Coloproctol 2013; 29: 130-4.

4. Neis B, Hart P, Chandran V, Kane S. Mucosal schwann cell hamartoma of the colon in a patient with ulcerative colitis. Gastroenterol Hepatol (N Y) 2013; 9: 183-5.

5. Rocco EG, Iannuzzi F, Dell'Era A, et al. Schwann cell hamartoma: case report. BMC Gastroenterol 2011; 11: 68.

6. Pasquini P, Baiocchini A, Falasca L, et al. Mucosal Schwann cell "Hamartoma": a new entity? World J Gastroenterol 2009; 15: 2287-9.

7. Sagami S, Fukumoto A, Amano M, et al. A case of mucosal Schwann cell hamartoma. Nihon Shokakibyo Gakkai Zasshi 2012; 109: 1776-83.

8. Ferro de Beça F, Lopes J, Maçoas F, Carneiro F, Lopes JM. Tactoid body features in a Schwann cell hamartoma of colonic mucosa. Int J Surg Pathol 2014; 22: 438-41.

9. Kanar O, Nakshabendi R, Berry AC. Colonic mucosal Schwann cell hamartoma on incidental screening colonoscopy. J Gastrointestin Liver Dis 2015; 24: 411.

10. Bae JM, Lee JY, Cho J, Lim SA, Kang GH. Synchronous mucosal Schwann-cell hamartomas in a young adult suggestive of mucosal Schwann-cell harmatomatosis: a case report. BMC Gastroenterol 2015; 15: 128.

![JPTM - Journal of Pathology and Translational Medicine logo with QR code]